

8818

NASA Technical Memorandum 87225

Low-Cycle Thermal Fatigue

(NASA-TM-87225) LOW-CYCLE THERMAL FATIGUE
(NASA) 114 p HC A06/MF A01 CSCI 20K

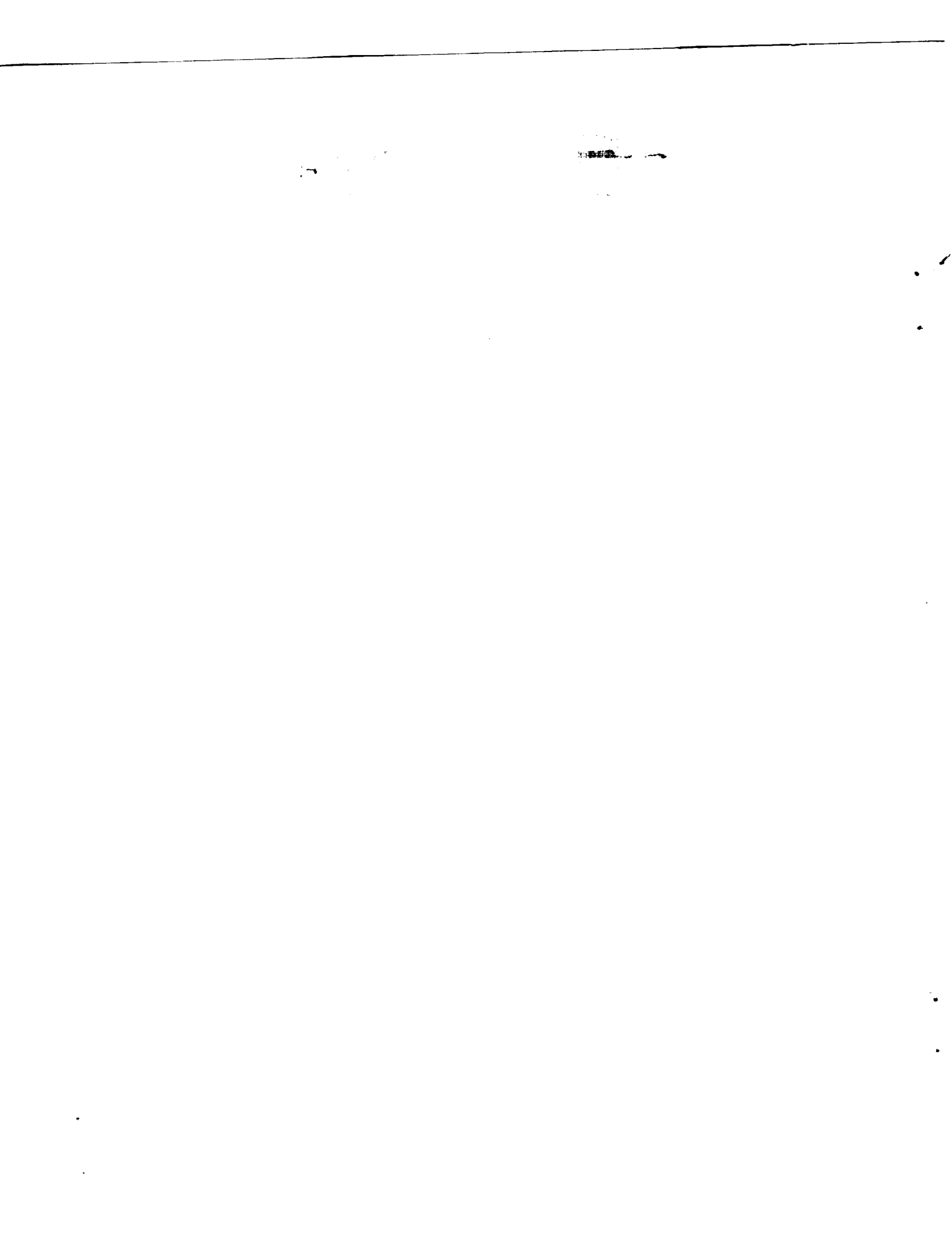
N86-26651

Unclas
G3/39 43421

Gary R. Halford
Lewis Research Center
Cleveland, Ohio

February 1986

NASA



CONTENTS

	Page
INTRODUCTION	1
NOMENCLATURE	4
HISTORICAL PERSPECTIVE	5
THERMAL AND THEMOMECHANICAL FATIGUE--UNBALANCED DEFORMATION AND CRACKING PROCESSES	7
A. CYCLIC IMBALANCES IN BULK BEHAVIOR	8
1. Cyclic Stress-Strain Response	8
a. Temperature-Dependence of Strength and Mean Stress Development	8
b. Ratchetting	9
c. Multiaxial Stress-Strain States	9
d. Metallurgical Instabilities	10
2. Cyclic Crack Initiation	10
a. Temperature-Dependent Fatigue Resistance	11
1. Stress (Elastic Strain)	12
2. Inelastic Strain	12
3. Total Strain	12
4. Damage Parameters	12
5. Strainrange Partitioning	13
b. Mean Stress Effect on Life	13
1. Elastic Cycling	13
2. Inelastic Cycling	15
c. Ratchetting (exhaustion of ductility)	16
d. Multiaxial Factors	17
e. Metallurgical Instabilities and Mechanisms	17
3. Cyclic Crack Propagation	19
a. Temperature Dependent Propagation Rates	20
b. Unbalanced Aspects	20
B. LOCALIZED BEHAVIOR	21
1. Environmental Effects	21
2. Inhomogeneous Constituents of Material	22
a. Surface Oxides and Coatings	22
b. Internal Particles, Fibrous Elements, and Interfaces	23
THERMAL FATIGUE RESISTANCE	24
A. TEST METHODS AND EQUIPMENT	24
B. TRENDS IN BEHAVIOR	26
1. Crack Initiation	26
2. Crack Propagation	27

THERMOMECHANICAL FATIGUE (TMF)	28
A. EXPERIMENTAL PROCEDURES	28
B. TRENDS IN BEHAVIOR	29
1. Crack Initiation	29
2. Crack Propagation	31
BITHERMAL FATIGUE	32
A. RATIONALE FOR BITHERMAL FATIGUE.	32
B. BITHERMAL FATIGUE RESULTS	34
ISOTHERMAL LIFE PREDICTION MODELS	36
PREDICTION OF TMF LIVES USING IDEALIZED ISOTHERMAL CHARACTERISTICS	38
A. CONSTANT COFFIN-MANSON FAILURE CRITERION	40
1. TMF Life Prediction for Time-Independent Constitutive Behavior	40
a. Total Strain Range Criterion	41
b. Ostergren Approach	42
2. TMF Life Prediction for Time-Dependent Constitutive Behavior	43
a. Total Strain Range Criterion	43
b. Ostergren Approach	43
B. CONSTANT TOTAL STRAIN RANGE FAILURE CRITERION	45
C. CONSTANT OSTERGREN FAILURE CRITERION	45
1. Time-Independent Constitutive Behavior	45
2. Time-Dependent Constitutive Behavior	46
3. TMF Life Prediction for Time-Independent and Time-Dependent Cases	46
a. Ostergren Approach	46
b. Manson-Coffin Failure Criterion	46
c. Total Strain Range Criterion	47
D. INTERPRETATION OF ANALYSES	47
THERMAL FATIGUE LIFE PREDICTIONS OF ENGINEERING STRUCTURAL COMPONENTS	48
A. HEAT EXCHANGER INLET NOZZLE	49
B. TURBINE ROTOR	50
C. HIGH PRESSURE TURBINE BLADE	50
D. COMBUSTOR LINER	51

DO's AND DON'Ts IN DESIGN AGAINST THERMAL FATIGUE 52

 A. THE THERMAL FORCING FUNCITON 52

 B. GEOMETRY OF STRUCTURAL COMPONENTS AND THERMAL/PHYSICAL PROPERTIES . . 53

 C. MATERIAL MECHANICAL RESPONSE CHARACTERISTICS 55

REFERENCES 56

TABLES

LOW-CYCLE THERMAL FATIGUE

Gary R. Halford
National Aeronautics and Space Administration
Lewis Research Center
Cleveland, Ohio 44135

INTRODUCTION

Low-cycle thermal fatigue (LCTF) is one of the dominant failure modes in high temperature structural components. In fact, the problem is intensifying in aeronautical gas turbine blades and vanes as greater emphasis is placed on internal cooling of hollow airfoils to permit higher gas temperatures. The resultant thermal gradients at thin leading and trailing edges become greater, and the propensity for thermal fatigue cracking increases. As greater performance is demanded of gas turbines, operating temperatures increase, rotational speeds increase, thermal transients intensify, and durability suffers. As a case in point, the United States Space Shuttle Main Engine utilizes turbo-machinery that extracts over seven hundred horsepower per turbine blade. Yet, the blade airfoil is only about the size of a thumb. Their durability is measured in just thousands of seconds of operation during which time low-cycle thermal fatigue cracks initiate and grow to readily detectable proportions.

Pressure vessel and piping components in the electric power industry also must be designed to resist thermal fatigue cracking. This is done at great expense, because the consequences of suffering low-cycle thermal fatigue cracking would be many times more expensive than the cost of initial analyses. Structural safety, particularly when high pressure steam and radioactive substances are involved, is of paramount importance. It demands that structural integrity be maintained even under the most severely imaginable circumstances. Thermal fatigue cracking problems also abound in a multitude of less sophisticated but equally important high-temperature hardware.

The cost of all thermal fatigue failures, and of the prevention of those that might have occurred, is quite high. Costs of replacement parts alone are estimated at several billion dollars/yr in the United States (ref. 1). In addition, valuable natural resources are being lost in terms of nonrecyclable strategic materials such as cobalt, chromium, and nickel. In the aeronautical gas turbine engine industry, which maintains an enviably high positive balance of international payments for the United States, hot section component maintenance costs in 1990 are expected to exceed two billion dollars/yr (ref. 2). Since a sizable fraction of the maintenance is thermal fatigue cracking related, there is a strong economic driver for better understanding of the failure processes of thermal fatigue. Emphasis is on developing more thermal fatigue resistant alloys, and utilizing these and existing materials as efficiently and effectively as their inherent durability characteristics permits. The very heart of current efforts directed toward low-cycle thermal fatigue is concentrating on being able to understand and to relate isothermal and thermal low-cycle fatigue. The task would be reasonably straightforward if the cyclic deformation mechanisms were independent of temperature, and the thermal cycling history did not alter the metallurgical state of the material either internally or at its exposed free surfaces. For the most part, however, none of these conditions exist and hence the problem becomes complicated. If there are mechanisms that are activated during thermal cycling and not during isothermal

fatigue, then not only is the problem complicated, it becomes physically impossible to predict low-cycle thermal fatigue response solely from an isothermal basis. Correlations and engineering approximations have therefore become a necessary ingredient to the problem's solution. This has been the approach used in the prediction of low-cycle thermal fatigue in the past, and will likely remain as such for a number of years to come. While most approaches proposed to-date are empirical, considerable qualitative insights have been achieved. Emphasis is being placed now on making them more quantitative.

Two of the simplest and most common engineering approximations for projecting isothermal behavior into nonisothermal cycling conditions are: (1) to assume that the isothermal fatigue resistance at the maximum temperature is representative of the thermal cycling fatigue resistance, or (2) to assume that the lowest isothermal fatigue resistance within the range of temperatures of thermal cycling is the one to use in estimating the thermal fatigue resistance. Other occasionally assumed criterion are the use of an algebraic average or integrated equivalent temperature between the two extreme temperatures. None of these assumptions are based upon a sound understanding of the mechanisms of low-cycle thermal fatigue damage accumulation. An in-depth discussion of these and alternative approaches will be presented in a later section. First, however, it is advisable to present a brief description of the thermal fatigue process.

Fatigue in metals is the consequence of repeated reversals of inelastic deformation. It is now well established that solids must be able to be deformed by nonrecoverable inelastic deformation in order to be prone to progressive failure by the mechanism known as fatigue. This mechanism is a direct consequence of repeated cyclic inelastic deformation. When the deformation is highly localized and is detectable only at the microscopic scale, many thousands or even millions of cycles must be applied to initiate a crack and propagate it to macroscopic proportions. If the cyclic inelastic deformation is greater and distributed more homogeneously on the macroscopic scale, the lifetime may be but a few cycles or as many as tens of thousands of cycles to failure. This is the regime of low-cycle fatigue. While low-cycle fatigue can result from repeated large strains at constant temperature conditions, the technologically more important condition called thermal fatigue is more often than not the source of the deformation that imparts low-cycle endurance in high temperature structures. In the case of thermal fatigue, the cyclic deformation is imposed as the result of the constrained differential thermal expansion within a solid caused by temperature gradients induced during alternate heating and cooling. Thermal fatigue is typically a low-cycle fatigue problem (approximately less than 10^4 cycles to failure) owing principally to the low frequency of thermal cycling of most engineering structures. For example, aeronautical gas turbine engines experience one major thermal fatigue cycle per flight, i.e., start-up, idle, acceleration, cruise, deceleration, idle and shut-down. No more than a few flights per day are scheduled, so the rate of cycling is less than about 1000/yr. This is in the low cycle fatigue regime even if the engines are operated for 10 yr or more.

Mechanical components of engineering structures that operate at elevated temperatures undergo their major temperature change at the beginning and end of each usage. Rapid temperature changes produce high thermal gradients and thus high thermal stresses and strains. The cyclic loading conditions induced by temperature gradients are essentially deformation limited loadings. Hence, the laboratory studies of thermal fatigue (or more appropriately - thermal

strain fatigue) are generally limited to strain-controlled low-cycle fatigue tests. Until recently, the thermal fatigue resistance of materials was assessed by conducting isothermal low-cycle fatigue tests at the expected maximum temperature of the thermal fatigue cycle. Long time operation at the steady state elevated temperature of the structural component was simulated by imposition of hold periods at the peak tensile or compressive strain within the isothermal cycle. Thus long time exposure effects brought about by oxidation, hot corrosion, and creep could be assessed in the relatively simple laboratory simulation experiments.

As a consequence, an extremely large isothermal data base has grown over the years that supports a design philosophy that embodies the same simplistic assumptions. As computer-controlled testing equipment and techniques have evolved, the capability to perform well-controlled, thermomechanical fatigue* experiments, however, has begun to manifest itself. Comparison of thermomechanical fatigue results with isothermal results has sometimes revealed alarming discrepancies, particularly wherein thermomechanical fatigue resistance is significantly lower than would have been expected based upon isothermal fatigue resistance. A following section deals with results reported in the literature.

*Thermomechanical fatigue is the terminology adopted for mechanical fatigue that has a superimposed uniformly varying temperature cycle. The two cycles have the same period, but the temperature and the mechanical strain can be programmed to otherwise vary independently of one another. Thermal fatigue, on the other hand, is associated with no external mechanical constraint; the stresses and strains are self imposed due to differential thermal expansion brought about by the temperature gradients.

NOMENCLATURE

ϵ	axial strain (dimensionless)
$\Delta\epsilon$	total strain range
$\Delta\epsilon_{el}$	elastic strain range
$\Delta\epsilon_{in}$	inelastic strain range
$\dot{\epsilon}_{in}$	inelastic strain rate
σ	axial stress
$\Delta\sigma$	stress range
σ_T	peak tensile stress in cycle
ν	frequency of cycle
E	modulus of elasticity
ΔW_T	tensile hysteresis energy
N_f	cycles to fatigue failure (crack initiation)
T	temperature
α	} exponents
β	
γ	
δ	
n	
m	} coefficients
A	
B	
F	
G	
K	

HISTORICAL PERSPECTIVE

A state-of-the-art review of low-cycle thermal fatigue is incomplete without the obligatory references to the early works that provided the foundation for evolution of the field. Discussion of these references will be kept brief by mentioning only the major activities that were carried out by the foresighted, dedicated researchers of three and four decades ago. While a smattering of isolated work had been carried out prior to 1950, most of the substantial, directed research efforts began in the late 1940s and early 1950s. The world economy, particularly in the United States, had recovered sufficiently from World War II to finance these activities. Thermal fatigue cracking was attracting attention in several unrelated industries, and thus the problem was attacked independently by the pioneering researchers.

In the railroad industry, thermal fatigue cracking, or heat checking, of railway car wheel rims during braking prompted the University of Illinois Engineering Experiment Station to mount research efforts to better understand the parameters involved. Professor Harry Wetenkamp and co-workers published some of their early work in June of 1950 (ref. 3).

In the area of atomic power that was beginning to arouse interest, concerns were given to the potentially severe thermal fatigue problems created by large temperature excursions in plant components as power levels were brought up and down. Working through the Knolls Atomic Power Laboratory and the Research and Development Center of the General Electric Company, Dr. Louis F. Coffin, Jr. assembled thermal fatigue machines that could impose large temperature variations on axial low-cycle fatigue specimens (ref. 4). The specimens were instrumented with extensometers that could detect the sizeable plastic strains that were suffered by samples of the austenitic stainless steel being evaluated. Coffin's classic paper (ref. 5) summarizing these extensive results was published in 1954.

While the above work was going on, the aeronautical gas turbine engine was slowly evolving as a viable propulsion system, and the former NACA Aircraft Engine Research Laboratory (NASA Lewis Research Center) was deeply involved in research to improve performance, efficiency and durability of turbine components. Some of the early turbine components (combustors, disks, blades, guide vanes, etc.) survived less than a hundred hours of operation before failing by creep and thermal fatigue cracking mechanisms. These problems attracted the attention of a number of the Research Center's staff, including S.S. Manson. He has since devoted a substantial portion of his research career to a better understanding of thermal fatigue, and to developing numerous life prediction methods for the aerospace industry as well as others. His concepts of Strain Invariance, 1966 (ref. 6), for thermally driven problems, the method of Universal Slopes, 1965 (ref. 7); the 10 percent Rule, 1967 (ref. 8); Modified Time and Cycle Fraction Approach to Creep-Fatigue Analysis, 1971 (ref. 9); and the Strainrange Partitioning Method, 1971 (ref. 10), have seen extensive use throughout the world. Applications have ranged from the design of gas turbine engine combustor liners, nuclear pressure vessel and piping components, to the United States Space Shuttle Main Engine. His extensive articles in Machine Design Magazine in the early 1960s provided the basis for his classic book on Thermal Stress and Low Cycle Fatigue published in 1966 (ref. 11). In a review paper entitled "Thermal Fatigue" published in 1974 by R.J. E. Glenny of the Royal Aircraft Establishment of England (ref. 12), credit is given to a number of NACA/NASA researchers for some of the earliest, best-documented examples of thermal fatigue cracking in gas turbine engine blading. Results had been

reported for tests on J47 and J33 turbine engines. It was this environment that encouraged Dr. David A. Spera of the NASA-Lewis Laboratories to pursue thermal fatigue problems in his Ph.D. studies as well as in his daily work at the Laboratories. In a conference on Thermal Fatigue of Materials and Components organized by Drs. Spera and Mowbray (of the General Electric Company) under the auspices of the American Society for Testing and Materials in 1976, Dr. Spera introduced the conference with a paper entitled "What is Thermal Fatigue?" (ref. 13). In that paper, he cited some of the very early researches into thermal fatigue cracking.

The University of Alabama's Bureau of Engineering Research has been a source of thermal fatigue research beginning in the 1950s with support from the Oak Ridge National Laboratories (ORNL) of Oak Ridge, Tennessee. The practical problems of thermal fatigue cracking in atomic power plant components drove this research. Dr. Harry Majors, Jr., prepared a summary of the literature on thermal fatigue as of 1956 (ref. 14). At Alabama, Professor Eugene E. Carden spearheaded thermal fatigue efforts and was one of the first along with Dr. R.W. Swindeman (ref. 15) of ORNL to perform well controlled thermomechanical fatigue tests in which axial specimens are thermally cycled under servo-controlled strain conditions.

Outside the United States, research on thermal and low-cycle fatigue emerged a little slower following the war. Nevertheless, the Japanese, working through their universities, and in particular, through Kyoto University and the late Professor Shuji Taira, played a catch-up game and were soon publishing numerous papers on the subject of thermal and low-cycle fatigue.

In addition to the valuable thermomechanical fatigue data that was generated, emphasis was placed on techniques for estimating thermal fatigue life based upon isothermal fatigue results. Because of the introduction of creep in the thermal cycles, Professor Taira and his students (ref. 16) were the first to apply the concept of summing creep damage due to time fractions during cyclic loading tests. This work was reported in 1962. They relied upon the Robinson (ref. 170) time fraction rule proposed in 1952 for variable stress creep rupture loading conditions. Significant refinements were made to this approach a few years later by Spera [18] and by Manson, Spera, and Halford (ref. 19). The time- and cycle-fraction rule for creep-fatigue life prediction is a cornerstone of the ASME Boiler and Pressure Vessel Code Case N-47-22 for nuclear component design [19].

In the United Kingdom, papers concerning high temperature low-cycle fatigue began to appear in the late 1950s and early 1960s. Early low-cycle fatigue research reports were published by P.P. Benham [20-22], while a student at London University and later as a Lecturer at the Imperial College of London. Meanwhile, at the National Gas Turbine Establishment, Glenny and co-workers (refs. 23 and 24) were developing the fluidized bed technique for thermal fatigue testing of candidate turbine blade and vane materials. Repeated thermal shock experiments were performed with ceramics, cermets, and metals. The fluidized bed technique proved to be highly effective providing extremely high heat transfer rates from the hot and cold beds to the test sample (in the shape of a tapered disk) that was alternately transferred from one to the other. Similar tests beds were subsequently built and used extensively in the United States (ref. 25). To overcome problems associated with the inherent coupling of thermal cycling and mechanical cycling in fluidized bed testing, Forrest and Penfold (ref. 26) at the National Physical Laboratories in Teddington developed

a thermal cycling bending machine. With the machine, mechanical strain cycling and thermal cycling could be imposed independently of one another. The technique did not spread extensively, since it was at about the same time that servo-controlled machines were being developed for high-temperature axial strain controlled testing. The latter provided a much better system for simulating thermal fatigue since stresses, strains, and temperatures could be measured directly, and any two of the three could conceivably be independently programmed as a function of time. Hence, better controlled and more easily interpreted tests could then be performed.

Results of Russian thermal fatigue research didn't start appearing as translations in the Western Hemisphere until the very early 1960s. Among the more prolific authors were S.V. Serensen, R.M. Schneiderovitch, G.S. Pisarenko, P.I. Kotov, Ya. B. Fridman, L.B. Getsov, and T.F. Balandin, G.N. Tret'yachenko, and A.F. Malygin.

Despite the technological importance of thermal fatigue, there have been few published reviews of the literature in this area. Most reviews were performed very early in the development of the field, and today serve only as historical documents. Attempts to summarize current thermal fatigue research and to assess the state-of-the-art are notably lacking. It is the intent of the present survey of the field to begin to fill this void.

Among the early summaries or bibliographies are those by Thielsch in 1952 (ref. 27), Majors in 1956 (ref. 14), Miller in 1959 (ref. 28), Glennly (ref. 29) and Yen (ref. 30) in 1961, Akimov and Sklyarov (ref. 31) (Russian experimental work up to 1962), Gusenkov and Kotov (ref. 32) (Russian work up to 1983), and Carden (ref. 33) and Baron (ref. 34) in 1964. Manson's book on Thermal Stress and Low-Cycle Fatigue in 1966 (ref. 11) and Spera's Doctoral Thesis in 1968 (ref. 18) covered the work in the field up to and including the 1960s. A literal explosion of thermal fatigue research occurred in the 1970's and has spread into the 1980s. Several factors were responsible, including the availability of more appropriate thermomechanical fatigue testing equipment, increased demands from designers for more accurate representations of thermal fatigue resistance, the use of finite element structural analyses, and an added awareness that isothermal fatigue representations of thermal fatigue were no longer adequate in many cases.

Another way that work in a particular field gets summarized is through Conferences and Symposia on the subject. In the area of thermal fatigue, the more notable such conferences and books are those listed under references 35 to 61.

THERMAL AND THERMOMECHANICAL FATIGUE - UNBALANCED DEFORMATION AND CRACKING PROCESSES

A strong distinction is made herein between the terms "thermal fatigue" and "thermomechanical fatigue". The former is associated with self-imposed constrained thermal expansion in solids undergoing cyclic temperature gradients. Superimposed mechanical loadings may also be involved. In contrast, "thermomechanical fatigue" will be used to indicate variable temperature fatigue in which the mechanical strain is imposed only by externally applied loads. Temperature gradients are intentionally avoided in thermomechanical fatigue experiments. Thermomechanical fatigue is an experimental simplification of thermal fatigue. It permits experiments to be conducted for which a

test volume of material is subjected to uniformly (with respect to gauge length) varying (with respect to time) temperature, stress, and strain. Thus, all of the macro-phenomenological variables can be measured and/or controlled; a luxury not affordable with thermal fatigue cycling.

Thermal fatigue is viewed as a repetition of unbalanced processes i.e., the tensile and compressive halves of the cycle are dissimilar. These lead to cyclic crack initiation and crack propagation lives that differ, usually on the low side, from more balanced isothermal fatigue cycling. It is thus not surprising that poor prediction of thermal fatigue life often results when isothermal information is used as a predictive baseline.

In this paper, we will discuss the various mechanisms of thermal fatigue and point out how these differ from isothermal fatigue mechanisms. Numerous examples will be used to illustrate the unbalanced/balanced viewpoint that distinguishes the difference between thermal fatigue and isothermal fatigue. Unbalanced mechanisms (i.e., mechanisms that are different in the to- and-from portions of a stress-strain fatigue cycle) are manifested in cyclic stress-strain response, cyclic crack initiation, cyclic crack propagation, and final fracture. Each of these will be expanded upon in the main body of the text. Suffice it to say herein, that thermal fatigue cycling is the antithesis of balanced cycling. In discussing unbalanced mechanisms, it is convenient to distinguish between bulk behavior and localized surface or interfacial behavior. These will be discussed separately.

A. CYCLIC IMBALANCES IN BULK BEHAVIOR

1. Cyclic Stress-Strain Response.

a. Temperature - Dependence of Strength and Mean Stress Development

The stress-strain response of a solid is generally regarded as a characteristic of bulk properties. There are at least three distinct aspects of stress-strain behavior that are important to our discussion of unbalanced cyclic mechanisms. These are elastic, plastic, and creep responses.

(1) Elastic - Even the elastic stress-strain response of solids is a function of temperature since the modulus of elasticity is invariably a decreasing, and frequently nonlinear function of increasing temperature. Thus, an elastic thermomechanical cycle exhibits a nonlinear response with the solid being stiffer at the cold end of the temperature cycle and more compliant at the high temperature end. This response is illustrated in figure 1 for an in-phase thermomechanical cycle wherein the elastic stress-strain response exhibits concave-downward (negative) curvature. The cycle shown is completely reversed in terms of strain (and hence balanced in only this one respect), but is not reversed (and hence unbalanced) with respect to the stress response. A lower tensile than compressive stress is evident which is a direct result of the difference in the values of the elastic moduli at the extreme temperatures. The degree of stress imbalance is a direct function of the temperature range and the overall temperature level.

(2) Plastic - If we now consider large enough, and rapidly applied, thermomechanical strains to induce time-independent plasticity, we will encounter additional nonlinearity and an unbalanced tensile versus compressive stress response. Typically, yield strength decreases with increasing temperature and hence, the high temperature end of the TMF cycle will have the lowest stress

response. There will also be a slight shift in the mean elastic and plastic strains, even though the total strain is completely reversed. These shifts, however, are of little or no engineering significance and will be ignored herein. The important imbalance is in the stress response and a mean stress develops, as shown in figure 2.

(3) Creep - Thermomechanical cycling at low straining rates and at maximum temperatures in the creep regime results in a further unbalance in the peak stress responses. Because creep further reduces strength (i.e., stress response), the peak stress of the maximum temperature is lower in a low strain rate thermomechanical test than in a rapid one. The peak stress response at the lowest temperature of the cycle will be essentially independent of strain rate. Hence, the highest temperature half of the thermomechanical cycle becomes more and more unbalanced relative to the cooler half as the cycling rate decreases, or as the maximum temperature of the cycle increases. A typical mechanical stress-strain hysteresis loop is shown in figure 3 for conditions involving significant time-dependent creep strains.

How to deal with the stress imbalances (i.e., mean stresses) noted above will be discussed in the cyclic crack initiation and propagation sections that follow. Note that the extent of the mean stress increased in going from the elastic to the plastic, then on to the creep conditions in figures 1 to 3. Despite the increase in the magnitude of the mean stress, there are reasons to believe (that will be developed later in the paper) that the mean stress plays no role in the expected lives of any of the three cycles depicted.

b. Ratchetting

Ratchet strains are unidirectional inelastic deformation that are incrementally accumulated on each cycle of loading, and are frequently associated with the thermal fatigue process. Thermal strain ratchetting is a classical nonlinear material response characteristic of thermally cycled structures. It is another imbalance of thermal fatigue that results directly from the unsymmetric hysteresis loop response of thermally cycled materials. Ratchet strains may be composed of either time-independent plasticity or time-dependent creep. Figure 4 illustrates thermal fatigue hysteresis loops with compressive creep ratchetting. This is the general appearance of a hysteresis loop at the inner wall of a thermally cycled tube (alternate hot and cold fluids carried by the pressurized tube).

c. Multiaxial Stress-Strain States.

Multiaxial fatigue concepts are extremely important since thermal fatigue invariably involves some degree of biaxial loading. Multiaxiality is also another source for imbalances in thermal fatigue loadings especially when both thermal and mechanical loading are involved. As the free surface of a structural component is suddenly subjected to external heating, the surface material wants to expand equally in all directions within the plane of the surface. Depending upon the geometry of the component, an equibiaxial compressive component of stress and strain will be superimposed with a uniaxial compressive component. The extremes are a flat plate heated near its center as shown in figure 5(a) (producing an equibiaxial stress-strain field) and a thin edge of a wedge also heated near its center, see figure 5(b), (producing an essential uniaxial stress-strain state). Since numerous structural components subjected to thermal fatigue loadings are also loaded mechanically, the opportunity

arises for nonproportional loadings, and hence high degrees of imbalance in the mechanical stress-strain hysteresis loop. An example of the complex nature of such loadings is given in figure 6 taken from reference 62. Nonproportional loading in this case simply means that the state of stress and strain at any point in the cycle is different from the other points, i.e., the hysteresis loop is not balanced. The phasing between temperature and state of stress and strain becomes an important factor in non-proportional loading associated with thermal fatigue. Little is known experimentally, at the moment, about the extent of these effects on cyclic stress-strain response and upon cyclic crack initiation and propagation. Cyclic constitutive modeling efforts are being devoted to isothermal, non-proportional loading (refs. 63 and 64), and nonisothermal, proportional loading (ref. 65 and 66).

d. Metallurgical Instabilities

The microstructural features of engineering alloys are complex, and are frequently achieved through intentional thermal and mechanical processing techniques to impart desired mechanical and physical characteristics. Polycrystalline grains sizes and orientation, work hardening, precipitates, etc. are examples of dominant microstructure features of importance in fatigue. Even in isothermal fatigue, these features can change and the change is reflected in cyclic flow resistance, i.e., change in the mechanical hysteresis loop. The material becomes a constantly changing entity with ensuing difficulties in interpreting fatigue resistance. The problem is compounded in thermal fatigue loading, since the cyclic deformation and the cyclic temperature became an extension of the thermal and mechanical processing that had gone on earlier. While only certain alloys will undergo large and unstable (rapidly changing) property changes, all materials will experience a microstructure change in thermal fatigue that is different than would be expected from isothermal experience. For a thermal fatigue cycle that varies between low temperatures (no creep attainable) and a high enough temperature for creep, thermal recovery (annealing), precipitation of second phase particles, etc. to take place; a unique combination of deformation mechanisms will shift the tensile and compressive response from what would be expected from isothermal behavior alone. During the high temperature portion of the cycle, the material will be deformed by plasticity and creep, but these deformations will be applied to material just having undergone a half cycle of cold working. The small amount of cold working will make the material a little stronger in the tensile half of the cycle than it would have been had only high temperature deformation taken place instead. Thus the tensile flow stress response will be a little greater than otherwise. Similarly when the cold working deformation occurs in compression on the next half cycle, the material has just been subjected to high temperature creep and plasticity, thus not imparting as much cold work as would have occurred otherwise during a low temperature cycle. Hence, the compressive stress response is not as great as it would have been in an isothermal low temperature cycle. It is seen from the above simple example that thermal cycling can introduce additional degrees of imbalance to the stress response than would be predicted based upon isothermal considerations only. Additional thermal cycling imbalances come into play when dealing with fatigue crack initiation, as will be discussed later.

2. Cyclic Crack Initiation

Cyclic crack initiation concepts in fatigue have been used to advantage in engineering design ever since the phenomenon of fatigue was first recognized

over a century ago. Crack initiation is considered to be a singular event. Details of how the event evolves are considered to be irrelevant. A unified precise definition of the event has evaded researchers over the years with the result that a broad range of definitions have been used and considerable confusion has resulted. For example, in the past in the area of isothermal low-cycle fatigue testing, failure into two pieces (or strong indications of impending failure, such as load drop-off in strain controlled tests) of the relatively small (1 cm) diameter specimens was usually considered as the initiation event. With the advent of in situ SEM equipment and surface replication techniques, the crack initiation event can be pegged at a much smaller crack size. The lower the cyclic lifetime of a given material, the smaller the fraction of total life consumed in generating a crack which is much smaller than the specimen dimension. Stated alternately, cracks emerge sooner in low-cycle fatigue than in high cycle fatigue. In the case of recent high temperature low-cycle fatigue results reported by Moreno, et al. (ref. 67) for a cast nickel-base superalloy, surface crack lengths of 0.030 in. "initiated" as early as 0.1 to 0.6 of the total separation life for specimens with surface crack lengths at separation of about 0.40 to 0.50 in.

A discussion of the definition of the cyclic crack initiation event is pertinent to the problem of thermal fatigue because the stress-strain-temperature fields in a structural component are decreasing functions of the distance into the surface of solid. Hence, the driving forces to propagate a thermal fatigue crack are usually decreasing as the crack grows. Thus, details leading up to the "initiation" event can become important, since they can differ considerably between isothermal or thermomechanical loading and thermal loading. For isothermal or thermomechanical testing of axial loaded specimens, as the crack grows inward, it grows into a more and more severe stress-strain field (temperature would not be varying) as cross-sectional area is reduced by the presence of the crack. As a means of addressing this problem, researchers such as Moreno, et al. (ref. 67) are defining the initiation event to be at a small enough crack dimension that differences between the crack driving forces are minimized in isothermal or thermomechanical fatigue and thermal fatigue. However, if the initiation size is defined to be smaller than the crack dimensions that can be handled accurately by existing cyclic crack growth (fracture mechanics) concepts, then a difficult-to-handle gap in life exists between the well defined initiation and well defined propagation stages.

While the crack initiation event is clearly tied to the conditions at the free surface of the specimen, considerable research (refs. 7, 68 and 69) has been devoted in the area of isothermal low-cycle fatigue to correlation of the initiation event with bulk material properties such as stiffness, strength, and ductility. Because of the engineering success of these correlations, we will treat the initiation event in connection with bulk material behavior.

The aforementioned unbalanced features of thermal fatigue can have significant influence on the crack initiation event, regardless of its lack of precise definition. These will be discussed briefly in the following section after we first examine the effect of temperature level on criteria for fatigue crack initiation.

a. Temperature-Dependent Fatigue Resistance

Just as monotonic tensile and creep properties depend upon temperature, so does fatigue "strength". Here, the term strength refers to a parameter (or

criterion) used to correlate fatigue life. Common parameters are stress range (or elastic strain range = stress range/elastic modulus), inelastic strain range, total strain range, hysteresis energy, products of stress and strains parameters, and products of these parameters with time factors such a frequency, strain rate, etc. The temperature variation of fatigue resistance is of extraordinary importance to thermal and thermomechanical fatigue since a spectrum of exposure temperatures are involved in each loading cycle. How to analytically deal with variable fatigue resistance as a cycle is traversed is one of the critical keys to being able to predict thermal fatigue life from isothermal information.

i. Stress (Elastic Strain) - Figure 7 depicts how the fatigue strength of an alloy varies with test temperature. With but few exceptions, stress range versus cyclic life curves decrease as a material weakens under higher and higher temperatures. Normalizing the stress range with respect to the modulus of elasticity (which also decreases with temperature) to obtain elastic strain range frequently results in fatigue curves that are relatively insensitive to temperature at levels below the creep and oxidation regimes. ASME Code Case N-47-22 takes advantage of this observation for the austenitic stainless steel, AISI Type 316. (ref. 19). This is shown in figure 8 at life levels in the range of 10^4 to 10^6 cycles to failure (the elastic regime) for temperatures between 38 and 483 °C. At temperatures within the creep range, the stress range (or elastic strain range versus life) curve drops with increasing temperature.

ii. Inelastic Strain - In the low-cycle fatigue region, inelastic strain range is commonly used as the life correlating variable. It is not as easy to generalize the temperature variation of inelastic strain range fatigue resistance. However, predictive correlations have been established over the years [7,68,69] which indicate that the tensile ductility and inelastic strain range resistance are coupled. That is, if ductility changes with temperature in a certain pattern, the inelastic strain range fatigue resistance will follow the same pattern. The correlations hold only up to a certain temperature region, beyond which different correlations come into play. At temperatures in the creep range, the Strainrange Partitioning life relations can be estimated using tensile and creep rupture ductilities (ref. 69).

Since thermal fatigue is encountered primarily as a low-cycle fatigue problem, it is necessary to consider the temperature variations in low-cycle fatigue resistance, and hence inelastic strain range resistance.

iii. Total Strain - As discussed above, both the elastic and inelastic strain range fatigue curves vary with temperature; consequently the sum of the two, the total strain range, also varies with temperatures, but in a more complex manner than do the individual components. Interestingly, the only way that the total strain range fatigue resistance can be temperature independent is for both components to be temperature independent as well. The most common behavior is for the total strain range versus life curve to be a decreasing function of temperature, as was shown in figure 8.

iv. Damage Parameters - Numerous fatigue parameters have been proposed over the years (refs. 70 to 72) that are made up of products of the individual variables; stress range, strain range, peak tensile stress, time, frequency, ratio of tensile going and compressive going times and frequencies, etc. One such parameter is that proposed by Ostergren (ref. 71). It takes

the form of the product of the peak tensile stress and the inelastic strain range. This product is proportional to the tensile hysteresis energy. Certain materials and conditions may require the additional multiplication of a frequency term that may be either the total cycle frequency or a combination of tensile going and compressive going frequencies. Only a few data sets have been analyzed using this parameter and it is difficult to generalize as to the extent of its variation with respect to temperature level. Variations most assuredly would take place over the temperature range of most thermal fatigue cycles, and hence procedures would have to be developed to deal with the variation.

v. Strainrange Partitioning - The Strainrange Partitioning method (ref. 10) for treating high temperature creep fatigue cycling utilizes inelastic strain range versus life input data. Rather than working with the total inelastic strain range alone, the method relies on partitioning the inelastic strain range into recognizably different forms of inelastic strains, i.e., time-independent plasticity and time-dependent creep. Either can occur in either tension or compression, and hence four extreme cases of inelastic strain range can be envisioned: tensile and compressive plasticity (PP), tensile and compressive creep (CC), tensile creep and compressive plasticity (CP), and tensile plasticity and compressive creep (PC). In general, it is expected that the low-cycle fatigue life relations based upon each of the four cycle types will be temperature dependent. Note that the cycles involving creep, CC, CP, and PC are not defined, nor is there a need to define them, for temperatures below the creep range. For some engineering alloys, it has been found (ref. 73) that the four life relations are insensitive to temperature over the range of engineering interest. While the life relations may not vary with temperature, the degree of partitioning of creep and plasticity will be a distinctive function of temperature, as well as a function of the time within a cycle. Prospects of having temperature insensitive life relations should simplify the analysis and life prediction of a thermal fatigue cycle. Even if the isothermal life relations were temperature independent, other factors of a thermal cycle, not captured in isothermal testing, may come into play and alter the predicted thermal fatigue life.

b. Mean Stress Effect on Life

In an earlier section it was shown that significantly large mean stresses can develop under thermal cycling. Their effect on cyclic crack initiation will now be discussed.

1. Elastic Cycling - Concerns for mean stress effects on life originated in the high cycle fatigue life regime wherein inelastic deformation was negligibly small. Numerous mean stress theories emerged (ref. 62) as different mean stress effects were documented for a variety of materials and testing techniques. The formation of Morrow (ref. 74) is selected as being representative of the trends found for elastic mean stress effects.

$$\sigma_a = (\sigma_f' - \sigma_m) (N_f)^b \quad (1)$$

where σ_a , σ_f' , and σ_m are the stress amplitude, a material constant relating to the fatigue strength level, and the mean stress, respectively; N_f is the number of cycles to crack initiation, and b is another material constant indicative of the slope of the basic fatigue curve in a log-log plot, i.e., Basquin's exponent. The equation reflects the observation that for a given

stress amplitude (or range), a tensile (positive) mean stress reduces N_f and a compressive mean stress increases N_f . As derived in reference 75, Morrow's equation can be recast in the following form,

$$(N_{fm})^b = (N_{f0})^b - V_\sigma \quad (2)$$

where N_{fm} and N_{f0} are the crack initiation lives respectively for a cycle with and without a mean stress, and V_σ is the ratio of the mean stress to the alternating stress. The question arises as to whether the recast Morrow formulation is directly applicable to the thermal cycle of figure 1. The following rationale is developed to support the argument that the Morrow formulation must be modified and be expressed in terms of mean elastic strain, rather than mean stress, to become applicable for elastic thermal fatigue cycles. Circumstances can be envisioned (i.e., cycles involving inelastic strain), however, wherein further modification will be required. For now, we shall examine the simpler elastic case.

Consider the situation of a material whose elastic strain range versus crack initiation life curve is independent of temperature over the range from T_1 to T_2 , as discussed in an earlier section. For this case, completely reversed stress (or strain) cycles at T_1 and T_2 would appear as in figure 9 for case A and B, respectively. Both cycles have exactly the same strain range, and because the modulus of elasticity, E , is lower at the higher temperature, the stress range is lower. A life of $N_f = 10^5$ cycles to crack initiation is assumed arbitrarily. Note that the ratio, V , of the mean to the amplitude is zero in both cases for both stress and strain.

Now consider thermomechanical strain cycling between T_1 and T_2 . We can simplify the cycle for ease of discussion by transforming it into a bithermal cycle in which the temperature is changed during each half cycle at the origin (zero stress and strain) before straining is resumed. In other words, the tensile deformation is imposed and removed at T_1 or T_2 and the compressive deformation is imposed and removed at T_2 or T_1 , respectively. The resultant cycles are shown in Cases A/B and B/A for in-phase and out-of-phase cycles, respectively. Since the strain ranges are the same as had been imposed in cases A and B, it is obvious that an algebraic compressive mean stress develops in A/B while a tensile mean stress is present in B/A. Does the compressive mean stress of A/B prolong the life or the tensile mean stress of B/A reduce the life relative to $N_f = 10^5$? It is highly unlikely that the lives in either case would differ from 10^5 , since nothing mechanical is being done to the material that is any different than done in portions of cases A and B. We are taking opposite halves of two balanced cycles, each have the same initiation life of 10^5 cycles, and putting them together into a single cycle. The only reason that an algebraic mean stress developed is because the material wanted it that way as its elastic modulus changed with temperature. By considering elastic strains rather than stress in this situation, we realize that the mean elastic strain term is zero, and hence the V ratio for the elastic strain is zero. This would correspond well with the logic that tells us that the cyclic life would not be altered. Thus, for elastic thermal cycling it appears reasonable to interpret the Morrow mean stress equation in terms of mean elastic strains.

In general,

$$V_{\epsilon_{el}} = \frac{\epsilon_{el)max} + \epsilon_{el)min}}{\epsilon_{el)max} - \epsilon_{el)min}} \quad (3)$$

and since, $\epsilon_{el} = \sigma/E$,

$$V_{\epsilon_{el}} = \frac{\sigma_{max}/E_1 + \sigma_{min}/E_2}{\sigma_{max}/E_1 - \sigma_{min}/E_2} \quad (4)$$

or

$$V_{\epsilon_{el}} = \frac{1 + R_{\sigma} (E_1/E_2)}{1 - R_{\sigma} (E_1/E_2)} \quad (5)$$

where, $R_{\sigma} = \sigma_{min}/\sigma_{max}$

For this general case, E_1 corresponds to the modulus at the maximum stress and E_2 to the minimum stress. Equation (5) degenerates properly for an isothermal cycle wherein $E_1 = E_2$ and hence $V_{\epsilon_{el}} = V_{\sigma}$. Thus, for

isothermal fatigue, there need be no distinction between V ratios for elastic strain and stress.

11. Inelastic Cycling (plasticity and/or creep) - When inelastic strains are present in a thermal cycle, mean stresses may also be encountered, as illustrated in figures 2 and 3. Following the example of figure 9, we can consider two stress-strain hysteresis loops shown in figure 10 with equal strain ranges at temperatures T_1 and T_2 ($T_1 > T_2$). It is assumed that the strain rate is high enough so that only time-independent plasticity occurs at the high temperature, T_1 . It can be reasoned that some material must surely exist (for example, the AISI Type 316SS of ref. 73) for which the cyclic crack initiation lives would be the same for these two conditions. Imposing the condition of equal lives is needed to make the reasoning process tractable. Taking the tensile half of high temperature CASE C, and combining it with the compressive half of low temperature CASE D yields the in-phase bithermal cycle, CASE C/D with a compressive mean stress. Similarly, CASE D/C exhibits a tensile mean stress nominally equal in magnitude to the compressive mean stress of CASE C/D. Again, the question arises as to whether the algebraic mean stresses impart a beneficial, detrimental, or negligible influence on the crack initiation lives for the combined bithermal cycles. Continuing with the same logic used in conjunction with figure 9, it is argued that the lives for CASES C/D and D/C should be the same and equal to CASE C or D. If indeed the mean stress, or mean elastic strain, is deduced to impart no effect on crack initiation life, then it would be highly desirable to modify equation (5) to account for this behavior. To do so, let's reexamine the development of equation (5).

If one were to consider the peak tensile and compressive stresses in figure 9 to be at the point of impending yield, those stresses could then be considered as the respective "yield" or flow strengths at the two temperatures,

T_1 and T_2 . Thus, if instead of examining the mean elastic strains per se, one were to multiply the ratio of the observed minimum to maximum stresses by the absolute value of the inverse ratio of the respective flow stresses, one would have an effective ratio of -1 . This ratio produces an effective V ratio of zero, and implication that there should be no effect on crack initiation life in this case. The general expression for the effective V ratio for use with Morrow's modified mean stress-life relation, equation (2), is as follows,

$$V_{\text{effective}} = \frac{1 + R_{\sigma} / R_y}{1 - R_{\sigma} / R_y} \quad (6)$$

where,

R_y = the absolute value of the compressive flow strength/tensile flow strength at their respective temperatures and strain rates.

Hence, if the peak tensile and compressive stresses in a thermal cycle are equal to respective isothermal flow strengths at the two extreme temperatures, then the value of $R_{\sigma} / R_y = -1$, and $V_{\text{effective}} = 0$; as desired. Note that the flow strengths of interest in equation (6) are the flow strengths measured at the same strain rates and at the same inelastic strains as are encountered in the thermal cycle.

We now have a more general expression for the effective mean stress to amplitude ratio for use with all forms of fatigue cycling, whether it be isothermal, thermomechanical, elastic or inelastic.

Another approach to the mean stress-strain problem was suggested by Halford and Nachtigall (ref. 75) when dealing with the influence of creep and plasticity on the development of mean stresses in isothermal creep-fatigue cycles. They argued that mean stress (or mean elastic strains) effects on low-cycle fatigue life would be absent if the inelastic strains within a cycle were above a certain level. A level of ten percent of the value of the elastic strain range was suggested, based upon existing mean stress relaxation results, as a transition strain range. Above this level, the mean stress (elastic strain) effects would diminish to zero, while below, they would begin to exert their full influence. An arbitrarily selected transition region was proposed such that,

$$V_{\text{effective}} = V_{\sigma} \exp[-70(\Delta\epsilon_{in}/\Delta\epsilon_e)]^2 \quad (7)$$

To-date, there is no direct experimental verification of the above proposals for dealing with mean stress effects on thermal fatigue lives. A partial explanation for this is that it is experimentally difficult to isolate mean stress effects from other unbalanced thermal effects that are invariably present.

c. Ratchetting (exhaustion of ductility)

An earlier section introduced the phenomenon of thermal ratchetting as one of the numerous imbalances in the thermal fatigue problem. Its influence on thermal fatigue crack initiation life has not been studied extensively.

The simplest approach has been to adopt the classical linear exhaustion of ductility concept and recognize that the ductility being exhausted may be either time-dependent creep or time-independent plasticity, or combinations of the two. Manson (ref. 76), in 1960, prepared an excellent discourse on how to deal with thermal ratchetting problems. Authoritative experimental studies designed to isolate the effects on life of this highly unbalanced aspect of thermal cycling are nonexistent. Isothermal ratchetting experiments may be helpful, but they can not capture the full influence of thermal ratchetting on thermal fatigue crack initiation life. In thermal fatigue, the ratchetting could be by creep mechanisms activated on material that is exposed every other half cycle to low temperature plastic deformation damage. The resultant combined deformation mechanisms could differ considerably from isothermal mechanisms of ratchetting damage. This appears to be a fruitful area for future fatigue research.

d. Multiaxial Factors

As noted earlier, the combination of biaxial stress-strain fields and thermomechanical fatigue is a common occurrence in components subjected to high-temperature service (ref. 62). Yet, well-controlled, thermomechanical, biaxial low-cycle fatigue tests results are nonexistent for non-proportional loading. Exciting research possibilities exist based upon some of the few isothermal, high- and low-temperature results reported by various investigators (refs. 77 to 80). For example, fatigue cracks may be initiated and grow via a shear mode at low temperatures, but shift to a maximum principal stress criteria at high temperatures (ref. 78). Opportunities exist in this field for researchers equipped with the proper equipment to run these complex controlled experiments.

e. Metallurgical Instabilities and Mechanisms

It is well known that stress and strain together with exposure to environment such as high temperature and reactive gases can produce unusual metallurgical instabilities. Strain aging is one such phenomenon. Some materials, subjected both to strain and high temperature, develop precipitates that alter the deformation and strength characteristics of the material. Examples of how metallurgical instabilities and other microstructural mechanisms can affect thermal-fatigue are presented in the following paragraphs.

While investigating isothermal creep-fatigue interactions in the wrought cobalt-base superalloy L-605, at 1400 °F, Manson, et al. (ref. 9) observed a strong strain-aging effect. Rather than exhibiting conventional creep induced weakening as the cyclic strain rate was lowered, an opposite behavior was manifested. Reducing the strain rate allowed greater time at temperature for a solid state metallurgical reaction to occur. Carbon, initially in solution with the matrix, precipitated forming an $M_{23}C_6$ type carbide. The precipitation would not have occurred had it not been for the nucleation sites provided by dislocations that were created by the cyclically imposed inelastic strains. As the carbides increased in number and size while cycling progressed, the cyclic stress-strain response of the alloy changed dramatically. The alloy was thus changing its cyclic flow resistance, and its resistance to fatigue failure. The amount of change depended upon several factors - the amount of deformation imposed, the duration of exposure, and the temperature. Hence, the fatigue resistance became dependent upon the imposed cyclic history. The implication to thermal damage analysis is that the fatigue life at a prescribed

load (strain) level is no longer a unique quantity dictated by the magnitude of the loading. Instead, details of prior loadings can alter the fatigue life relation. For example, consider two high temperature levels for fatigue loadings. One is at low temperature giving rise to prolific dislocation generation, but no thermal activation or carbide precipitation, and producing a life, N_1 . The other is at a high temperature where dislocations and precipitation nuclei are formed. As the material is cycled between these temperatures, the high temperature strain age hardening effect is now felt at the low temperature. The ensuing alternate mixture of deformation mechanisms will set up a different crack initiation condition than existed for the two separate isothermal conditions. It is reasonable to assume that the thermal fatigue life would be different from either isothermal life.

Another example of loading history effect on altering fatigue resistance at high temperatures is one encountered by Leverant, et al. (ref. 81) while studying the effects of surface protection coatings on thermomechanical fatigue behavior. TMF cycling can introduce mechanisms of damage not encountered during isothermal fatigue. A case in point is found in the results of TMF experiments conducted in support of the development of surface protection coatings. While at high temperatures, coatings provided the required oxidation protection and are fatigue resistant because they are also quite ductile. However, depending upon composition, they may be exceptionally brittle at low temperatures. If thermal cycling is imposed such that the coating is subjected to tensile strains at low temperatures, a brittle coating readily cracks. This, in turn, causes the substrate alloy to crack prematurely, and thus compromises its cyclic durability compared to isothermal high temperature fatigue. Isothermal testing at high temperatures would not uncover this failure mechanism. Furthermore, if the temperature-strain phasing in the TMF cycle is altered, the low temperature could be applied while the coating stresses and strains are compressive. Under these conditions, the low temperature brittleness of the coating is not as influential in governing the crack initiation, and the cyclic life is greater. An example of this behavior is shown in figure 11 for a CoCrAlY (13A1) coated, cast superalloy (ref. 11). The reverse trend of having the out-of-phase more damaging than in-phase for coated material compared to bare is a direct result of different cracking mechanisms. As is evident from these contrasting conditions, the mechanisms of cracking and the crack initiation life will be dependent upon details of the material, of the TMF cycle phasing, the overall temperature level, and upon the magnitude of the thermal variation, ΔT .

The phasing of temperature and strain cycling during thermal fatigue can produce unusual combinations of microstructural mechanisms. In a recent study of thermomechanical fatigue behavior of the nickel-base superalloy, MAR M-200, Bill, et al. (ref. 82) observed significant differences in thermal fatigue resistance depending upon whether in-phase or out-of-phase cycling was imposed. See figure 12. During in-phase cycling, the peak tensile stresses and strains occur at the same time as the peak temperature. Early appearing cracks fill with oxide while being held open by the tensile stress. This situation is not experienced in the out-of-phase cycling for which compressive stresses close any cracks at the high temperature, greatly retarding oxidation within the cracks. Out-of-phase cycling was found to be considerably less damaging than in-phase. Furthermore, the two phasings result in different modes of internal cracking at the ubiquitous carbides. In-phase cycling produced carbide-matrix interfacial cracking, while out-of-phase cycling caused the carbides themselves to fracture. More thorough interpretation and comparison of the deformation

and cracking mechanisms are contained in reference 82. It is significant to note that both in-phase and out-of-phase cycling produced lives considerably less than isothermal cycling at the peak temperature.

3. Cyclic Crack Propagation

The total fatigue life can be divided into two stages; crack initiation and propagation. As discussed in Subsection 2 above, the initiation stage can be considered an event that may contain a sizeable portion of microcrack growth and even some macrocrack propagation. For present purposes, the propagation stage will be taken as that portion of the fatigue life that can be accurately and conveniently described by fracture mechanics principals. That is, the crack is of sufficient size that it can be detected, measured, and described reliably; and it develops a crack tip stress-strain field that can be described by stress intensity equations of fracture mechanics.

A dichotomy exists, however, when trying to predict TMF lives using fracture mechanics concepts. The first point to recognize is that TMF is almost invariably associated with low-cycle fatigue, which in turn is most frequently associated with large scale plastic straining. The second point, which tends to be at odds with the first, is that fracture mechanics is not, as yet, at a level of engineering development to deal simply and routinely with large scale plastic deformation. Fracture mechanics is even less capable of routinely handling cyclic inelastic deformation, and even less capable still for treating variable temperature coupled with cyclic inelastic straining. Never-the-less, linear elastic fracture mechanics has been applied to cyclic crack propagation in the large strain regime, and with engineering acceptable results (ref. 83 to 86). In addition, there is considerable activity to develop non-linear fracture mechanics for application to both isothermal and thermomechanical high-temperature, low-cycle, creep-fatigue cracking problems (ref. 87 to 90). Whether descriptive mathematical models are available or not, the propagation stage of fatigue is an important portion of the thermal fatigue life of many engineering components. Design philosophy in recent years is tending toward greater emphasis on predicting fatigue life on the basis of the crack propagation portion. Any extra life due to an initiation stage is simply an additional benefit that may be present, but is not relied upon to achieve the desired design life. This is not appreciably different from the crack initiation design philosophy in that any extra life due to a macro-propagation stage is an additional life benefit that is not counted upon to achieve the crack initiation life design goal.

In applying crack propagation concepts to the life prediction of TMF cycling, similar imbalances as encountered in isothermal fatigue are found to be present. For thermal strain driven problems, mean stresses and loads will develop, there will be imbalances in the deformation mechanisms at the temperature extremes of the cycle, crack closure will occur at a different point within the cycle than it would have in isothermal loading, thermal ratchetting occurs, etc. To complicate matters, isothermal crack propagation resistance can become a sensitive function of temperature if based on stress intensity parameters, such as K_{max} and ΔK . Examples of results from the literature are presented in a following section.

a. Temperature Dependent Propagation Rates

Some of the earliest crack propagation experiments conducted under well-controlled thermomechanical conditions were those reported by Rau, Gemma, and Leverant (ref. 83) of Pratt and Whitney Aircraft in 1973 for three cast super-alloys used in gas turbine vanes and blades. Isothermal crack propagation results for the alloy B1900 + Hf (PWA 1455) were also obtained and showed an order of magnitude increase in cyclic crack propagation rate in going from a test temperature of 427 to 983 °C. Factoring the temperature dependence of the isothermal growth rates into a rational prediction of TMF growth rates has as yet to be accomplished. Their out-of-phase TMF crack growth rates are greater than the highest isothermal rates, although the TMF cycling was over a slightly different range of temperature (316 to 927 °C) making a direct comparison difficult. Nevertheless, it appears that TMF cycling introduces life reducing factors above and beyond those found in isothermal cycling. An interesting aspect of their results is that the highest isothermal growth rates were at the highest temperature, yet in the out-of-phase TMF cycling, the tensile stresses and strains are applied not at the highest temperature where rates are high, but rather at the lowest temperature where the isothermal growth rates are an order of magnitude or more lower. Apparently, the alternate exposure to high temperature deformation and oxidation at the crack tip can significantly reduce subsequent crack resistance at lower temperatures.

b. Unbalanced Aspects

The TMF crack growth results (ref. 83) for the PWA 45 coated cobalt-base alloy, MAR-M-509 (PWA647), showed a significant dependence upon the phasing. Out-of-phase TMF crack growth rates were greater by about an order-of-magnitude than in-phase rates. The authors explained this behavior on the basis that, a) the high temperature during crack closure in compression produced more inelastic deformation at the crack tip, thus producing more damage, and b) the crack tip was sharpened more by the high temperature deformation than it would have been at a lower temperature. Both features of this explanation are of an unbalanced nature compared to isothermal crack growth behavior. Phasing of the loading and the temperature can produce a significant affect on the degree of load (crack tip) imbalance in the mechanisms of inelastic deformation, the amount of deformation, the local stresses, the amount of time and position within a cycle of when a crack is open or closed, the extent of oxidation of the crack faces and crack tip, and the local ratchetting.

TMF Ratchetting results were also reported by Rau, et al. (ref. 83) for the cobalt-base alloy MAR-M-509 (PWA-647). Even though the overall specimen ratchet strain/cycle was very small (one series of tests involved a 0.000035 creep ratchet strain/cycle), the crack propagation rates increased by as much as an order of magnitude. Such large increases were observed despite the fact that the primary crack was shielded by the numerous parallel secondary cracks at the specimen surface. Multiple cracking sites are frequently observed in TMF, and their presence obviously increases the complexity of life analysis by means of fracture mechanics principles. Additional TMF ratchetting results have been reported by Gemma, Ashland, and Mascsi (ref. 91) in 1981.

Very recent TMF crack growth results presented by Marchand and Pelloux (ref. 86) for Inconel X-750 indicate that the effect of phasing of load and temperature on grow rates can be rationalized by the introduction of an effective closure stress. Growth rates exceeding an order-of-magnitude difference

due to phasing and mean loading conditions were collapsed into a single band of behavior with a band width of two on growth rates.

Okayaki and Koizumi (ref. 92) have successfully applied the cyclic J-integral concept to their TMF crack propagation results on three high temperature steels, 12Cr-Mo-V-W, cast Cr-Mo steel, and 304 stainless. Only slight differences in growth rates between in-phase and out-of-phase experiments remained when the results were correlated with the cyclic range of the J-integral. Vast amounts of research that are beyond the scope of this chapter have been devoted to the modeling of isothermal fracture mechanics for mean loading effects, crack closure, etc. The intent of this section is simply to point out the added imbalances that can be present during thermal or thermomechanical fatigue crack propagation that are not present during isothermal cycling.

B. LOCALIZED BEHAVIOR

The actual mechanistic processes of fatigue crack nucleation and growth are highly localized ones that commence with the very first cycle of fatigue. Cyclic crystallographic slip begins to occur within localized bands in favorably oriented grains. The local deformation and cracking mechanisms, together with localization of applied stress and strain at discontinuities, combine to enhance the heterogeneous nature of the problem. Once a crack forms and begins to be the driver (along with the applied loading) of the stress-strain field around the crack, the high stresses and strains become localized in the immediate vicinity of the crack tip. In view of the localized aspects of fatigue, it is at first surprising that bulk material properties have been successfully correlated with fatigue resistance. On closer examination, however, it must be realized that the total fatigue life is the integrated effect of a multitude of local events. The integration masks the individuality of each event.

Localization with respect to thermal and thermomechanical fatigue can be described best in terms of the major contributors: environmental influences and inhomogeneity of material constituents. These may impact at either external or internal surfaces or interfaces. Environmental impact is felt at externally exposed surfaces such as, (1) the virgin surface of the material, (2) newly exposed crack faces, and (3) the crack tip. Material inhomogeneity produces localization at internal interfaces.

1. Environmental Effects

The most common form of environmental degradation in high temperature fatigue is surface oxidation in which metallic elements from the surface layer combine with atmospheric oxygen to form metal oxides. Under static isothermal conditions, the oxide thickness grows in time at an exponentially decaying rate. The oxides are less dense than the substrate material, and expand as they form. Crack wedging due to the crack filling with oxide and expanding the crack open is an aspect of crack growth that hastens fatigue failure at high temperatures. In the case of thermal cycling, the presence of oxides (which form in the crack at high temperatures) in the lower temperature portion of a TMF cycle alter the crack growth behavior compared to lower temperature isothermal cycling wherein no oxides are present. Oxidation of crack faces likely contributes to differences between in- and out-of-phase TMF crack propagation rates. For in-phase experiments, the crack is held open while at the peak temperatures, and greater oxidation can take place; while for out-of-phase

cycling, the crack is held tightly closed during the period when oxidation could occur. Hence, thicker oxide layers form on the crack faces in the in-phase compared to the out-of-phase tests. The thicker oxides enhance the wedging action as the crack is loaded into compression. Enhanced cyclic crack growth rates will result from this unbalanced mechanism when it is the dominant mechanism. Other mechanisms, however, have an opportunity to become overriding in an in-phase TMF cycle. These include, but are not restricted to, (1) blunting of the crack tip due to localized high-temperature tensile creep, and (2) reduced elastic strain energy at the crack tip to drive the crack. If the cracks are progressing slowly, the oxidation process could also be depleting desirable strengthening elements from the alloy just in front of the crack, thus promoting faster crack growth. This would continue until a dynamic equilibrium was reached between rate of oxidation and rate of crack extension. Basic research along these lines has been reported by Liu [93] for isothermal crack growth conditions.

2. Inhomogeneous Constituents of Material

a. Surface Oxides and Coatings

The environment can also significantly influence crack initiation lives by the growth of surface oxides. These tend to grow fastest at intersections of grain boundaries with the free surface. The chemical potential is substantially greater at such discontinuities in the crystalline structure. As oxidation takes place, the grain boundaries are attacked, regions on either side of the boundary are depleted of strengthening elements, and the oxides wedge the boundaries open. When this action is combined with imposed mechanical deformation and a temperature variation, the oxidized boundaries are even more prone to cracking. Another factor also comes into play. The thermal expansion coefficients of the oxides and the matrix alloy are unequal. Thus additional cyclic strains are induced in both the oxides and the matrix. Since the oxides have less ductility, are thinner, and can support less load, they tend to crack first. Once cracked, the oxides channel the cracking, constraining it to continue on into the matrix. Thus again hastening the initiation and crack growth processes. The imbalances of a TMF cycle aid in the extent to which the oxides aggravate the crack initiation and propagation problem. An example is discussed in an earlier section in connection with an intentionally applied brittle ceramic protective surface coating. Out-of-phase TMF cycling can result in drastically reduced crack initiation lives. The problems associated with protective surface coatings are similar to those for naturally formed surface oxides layers.

Naturally forming oxides are usually not as adherent as the specially designed surface coatings. It is therefore not unusual in thermal cycling environments to have natural oxides spall from the substrate, thus exposing nascent surfaces that can then reinitiate the high oxidation rates of virgin material. The net result of repeating the processes of oxidation followed by spallation is to significantly increase the oxidation recession rate and the overall weight loss of the material. While engineered surface protection coatings are more tenacious than surface oxides, spallation is possible. In fact, the major failure mechanism for thick thermal barrier coatings (TBC) has been found to be one of buckling in compression and separating from the substrate as the coating bows out and away from the surface. These fascinating results have been reported and analyzed in detail by Miller, et al. (refs. 94 and 95).

Strangman and co-workers (refs. 81, 96 and 97) have developed a thorough mechanics analysis of equilibrium and compatibility of surface protection coatings and substrates for thermal fatigue conditions. Working principally with the coefficients of thermal expansion, elastic moduli and yield strains of the coating and substrate, variously phased thermomechanical cycles have been examined. Figure 13 illustrates the resultant strain - temperature phasings that develop in the coatings and substrate as various types of TMF cycles are applied. The influence of the differential between coefficients of thermal expansion is clear from the figure. Their results emphasize the benefit of research to develop coatings with compatible mechanical and physical properties in addition to having desirable chemical/metallurgical properties needed for oxidation protection.

b. Internal Particles, Fiberous Elements, and Interfaces

Just as the interface between coatings or oxides and a physically dissimilar substrate created a need for extra consideration under thermal cycling conditions, so do any of the other forms of mechanical and physical inhomogeneities in engineering materials. Metallic materials designed for high temperature service (and hence, thermal fatigue) invariably are complex in their microstructural features. The γ' , second-phase particles in cast nickel-base superalloys, the oxide particles in ODS (oxide dispersion strengthened) alloys, the carbides in precipitation hardened steels, and even the high strength, high stiffness fibers imbedded in ductile metals of metal matrix composites all contribute to additional differential thermal expansion strains during thermal cycling. Obviously, the signs of the strains depend upon the relative values of coefficient of thermal expansion, and upon whether heating or cooling is taking place. As with coatings and oxide layers that are typically more brittle at low temperatures, tensile strains imposed on the inhomogeneities while in a brittle temperature regime can cause premature crack initiation that can propagate into the matrix, if the interface is coherent. If there is no bond between the inhomogeneity and the matrix, the fracturing of the brittle element will not be as disastrous to the matrix. The interfaces mentioned above further contribute to the localization of the fatigue deformation and cracking processes. Because the properties of the materials on either side of the interface can change with temperature, the introduction of thermal or thermo-mechanical fatigue can result in an even greater degree of imbalance of the fatigue mechanisms than present in homogeneous materials.

Among the engineered materials that are not susceptible to these additional internal thermal strains are the metal matrix composites. Several modes of premature damage are possible because of the significantly large differential between the coefficients of thermal expansion of the matrix and the strong-stiff fibers [98]. The matrix may undergo large internal inelastic deformations, potentially leading to internal crack initiation. Fiber/Matrix debonding is also common, and gross macroscopic ratchetting deformation of the composite has been reported. To understand what is happening during thermal cycling of composites requires the use of sophisticated three-dimensional elasto-plastic-creep analyses. Such analyses are beyond the scope of this chapter.

THERMAL FATIGUE RESISTANCE

The thermal fatigue resistance of materials has been measured by numerous laboratory test techniques. Each utilizes an external heating and cooling source that can rapidly heat and cool localized areas of samples. Typically, the sample sports a sharp edge that is designed to be the initiation site for cracks. Just as is the case for thermal fatigue loadings of components in service, the specimen edge heats and cools more rapidly than the bulk, thus inducing thermal stress and mechanical strain gradients. The principal test methods and equipment used over the past few decades are surveyed in the following section.

A. TEST METHODS AND EQUIPMENT

The various thermal fatigue test methods utilize five basic means for transferring heat to and from the specimen. These can be categorized as follows: (1) hot gas flow, (2) fluidized bed, (3) radiation, (4) resistance heating, and (5) radio frequency induction. A summary of the various high temperature fatigue testing techniques was prepared by Hirschberg (ref. 99) in 1982.

Alternate impingement of hot combustion gases from a high velocity nozzle and cold compressed air is probably the first and most common form of thermal fatigue testing. Automated equipment was designed and built by the Allison Division of General Motors in the early 1950s (ref. 100) to test such alloys as A-286, Discalloy 24, and L-605. All of the aeropropulsion engine manufacturers, and related industries, have used this technique extensively over the intervening years. It is still in common usage.

In the late 1950s, Glenny (ref. 23), of the National Gas Turbine Establishment in the U.K., developed a new technique wherein small tapered disk specimens were alternately immersed in hot and cold fluidized beds. The "fluid" was silica particles levitated by large volumes of low-velocity air. The beds were heated by resistance windings around the circumference. As the particles came in contact with the specimen, heat was conducted at a rather rapid rate. In fact, quite high heat transfer coefficients could be obtained by the technique. It has been used extensively by other researchers such as Mowbray and Woodford (ref. 101), and Bizon and Spera (ref. 102) in an attempt to identify alloys with the greatest thermal fatigue resistance. Both Mowbray and Woodford (ref. 101) and Bizon, et al. (ref. 103) have performed extensive thermal and structural analyses of fluidized bed test specimens to better understand the stress-strain-temperature-time response of the material at the crack initiation location.

The third major technique for imparting rapid heating to a surface is via radiation from high intensity quartz lamps (and cooling by compressed air). Among the users of this technique has been Pratt and Whitney Aircraft in the study of gas turbine combustor liners. They designed and built a rig that was turned over to the Lewis Research Center in 1985. The McDonnell-Douglas Company took advantage of this technique in the 1960s when activities intensified on the development of a United States supersonic aircraft. The problem being addressed was the skin heating effect due to high speed flight in the atmosphere. Another radiation type of thermal fatigue heating technique is being employed by the Rocketdyne Division of Rockwell International under

contract to the NASA Lewis. The technique is used in an attempt to simulate the extremely high rates of heat transfer found in liquid oxygen/hydrogen space propulsion systems.

Direct resistance heating, i.e., the passage of high electric current through a metallic specimen, has been used primarily for isothermal and thermo-mechanical fatigue testing. One of the first users of this technique was L.F. Coffin, Jr. (ref. 5). Kamachi, et al. (ref. 104) have taken advantage of the technique in their recent studies of the thermal fatigue resistance of stainless steels.

High frequency (RF) and low frequency (AF) induction heating techniques have been used only sparingly as a source of heating for thermal fatigue experiments (i.e., temperature gradients imposed on specimens). In Germany, as early as 1955, R~deker (ref. 105) was applying this technique in his thermal fatigue studies of hot-working tools. This heating technique is now quite common in most high-temperature, low-cycle fatigue laboratories for use in isothermal and TMF studies.

A particularly thorough documentation of the various techniques in use up to about 1961 has been presented by Glennly (ref. 29). Pertinent details from 45 references to thermal fatigue testing are summarized in a table prepared in reference 12.

Various thermal fatigue testing techniques have evolved as means for simulating component service conditions. How well a simple laboratory thermal fatigue test duplicates the complex thermal, mechanical, and environmental conditions in a structure has not been known until quite recently. With the development of finite element structural analysis capability and cyclic constitutive equations, both the structure and the specimen can be thoroughly analyzed and compared on a more rational basis. The results of structural analyses of the Glennly disk specimen and the NASA Lewis Illinois of Technology Research Institute wedge specimen have been published in references 101 and 103, respectively. These results are available for direct comparison with similar detailed analyses of structural components subjected to realistic service conditions. Direct comparison, however, is quite difficult, because of the large number of parameters involved. A few of the parameters could be held constant, but many of the others would not be, thus making comparisons questionable.

It is generally recognized that thermal fatigue results are as varied as the techniques to measure thermal fatigue resistance. There is no standard for thermal fatigue testing, and there likely never will be. Because there are so many variables associated with thermal cycles, there is no single representative cycle for all materials and conditions. There is a growing dissatisfaction with this approach for assessing the thermal fatigue resistance of structural components. Thermal fatigue test results are approximate indicators of whether a material might survive in a given service situation. Test results serve as a means of ranking the relative thermal fatigue resistance of different materials.

What is obviously needed is an appropriate theory for dealing with thermal cycling and mechanical loading. Such a theory would be the link between thermal fatigue testing and thermal fatigue loadings in service components. The material constants, geometry, environment, and thermal characteristics could be

fitted to the laboratory thermal fatigue results, then applied to the structural components. Attributes of thermal fatigue theories will be discussed in subsequent sections.

B. TRENDS IN BEHAVIOR

Thermal fatigue test lives are most frequently reported as the number of cycles to initiate a crack of some stated size (ref. 101), although some studies have reported rates of cyclic crack growth as well (ref. 101 and 106).

1. Crack Initiation

One of the most extensive programs documenting the relative thermal fatigue resistance of engineering alloys was supported by the NASA Lewis and carried out at the Illinois Institute of Technology Research Institute (IITRI) using their fluidized bed test facility. Alloys studied have ranged from wrought Udimet 700 to advanced directionally solidified superalloys with sophisticated surface protection coatings. Single-edge and double-edge wedge specimens, as shown in figure 14 have been tested. The outstanding feature of this testing system is the capability of testing as many as 18 specimens simultaneously. Testing was interrupted on a regular schedule and the specimen edges were visually examined at 30X magnification for thermal fatigue cracks. Results have been reported in a number of different publications, (ref. 102, 107 to 111). An example of the comparative thermal fatigue results for 26 alloys and conditions (ref. 102) are shown in figure 15. The results are dramatic. The superiority of directionally solidified (DS) alloys over their polycrystalline counterparts, and the benefits of coatings are clearly illustrated. Crack initiation lives ranged from 12 to 12 000 cycles for the same external thermal environment of 1088 to 316 °C with 3 min exposure times in each bed.

Over 100 alloys and alloy plus coating combinations have been studied in this facility since it first came on line in the late 1960s. The facility is also versatile enough to permit the testing of rather small component parts such as turbine blades from the Space Shuttle Main Engine (ref. 112) and automotive gas turbine integrally bladed disks (ref. 113).

A large portion of the thermal fatigue data generated by aerospace industries has likely not been published in the open literature because of the proprietary status assigned to such information. Only a few examples of the vast amount of the published results on thermal fatigue crack initiation have been pointed out herein. The reader is directed to the numerous conference proceedings on thermal fatigue (refs. 35 to 61) to locate thermal fatigue results for specific materials, temperatures, and end applications. Not all thermal fatigue problems are associated with what are thought of as structural load bearing members. A prime example is the thermal fatigue cracking problem encountered in the soldered joints of leadless chip carriers in miniaturized electronic components (refs. 114 to 117). Temperature ranges of only 100 °C can cause local strains in the solder to exceed several percent. The differential thermal expansion between the chip material and the carrier material is responsible for the problem. The problem is further compounded by the low strength of the solder. This permits it to absorb the majority of the differential expansion, and hence concentrates the local strain to very high levels.

Fortunately, the solders are quite ductile and offer high cycle strain resistance. Nevertheless, failure lives are shorter than desired, and research efforts are underway (ref. 117) to better understand the nature of the failures and hence propose solutions.

2. Crack Propagation

Only limited cyclic crack propagation results have been reported in the literature for thermal fatigue cycling. Considerable difficulties are encountered in gathering such information, since in situ crack size measurements are not possible for most specimen geometries and heating techniques. Consequently, specimens must be removed from the test facility after cooling to room temperature. Even after the specimen has been prepared for crack size measurements, the only accurate dimensional measurement is the crack length along a free surface. Crack depths or cracked areas must be determined based upon an assumed shape for the crack front. The crack measurement procedure is time consuming and limits the number of such measurements that are convenient during a thermal fatigue test.

Not only are the measurements time-consuming, but their intrinsic value is questionable. The rate of crack growth depends highly upon the specific geometry, the specific cyclic thermal environment, the rate of heat flow to and from the crack region, the material and its coating, etc. Thermal fatigue cracks grow through regions of variable temperatures, variable stresses and strains, and even variable material composition and grain size (for cast specimens). These factors, while quite important to the analysis and thermal fatigue life prediction of components, becloud the interpretation of results. Hence, it is not recommended that crack growth data be generated under thermal fatigue conditions if generalized crack growth resistance information is being sought. Thermal fatigue crack growth information, however, is invaluable in assessing the accuracy of crack propagation life prediction methods when applied to simulated service cracking of components. In other words, thermal fatigue crack growth results are valuable primarily for establishing qualitative behavioral trends and for verifying theories.

In 1973, Mowbray and Woodford [101] reported results of a thorough study of the thermal fatigue crack growth rates of two cast superalloys, FSX 414 (cobalt-base) and Rene 77 (nickel-base). Tapered disk specimens of the Glenn type were cycled between two fluidized beds. One bed was maintained at a constant low temperature of 24 °C, while the high temperature bed was held at any one of five temperatures between 820 and 1020 °C. Immersion times in the hot bed were controlled at fixed values ranging from 1 to 60 min. The problems of multiple crack initiation and crack stress fields interacting was avoided by notching the periphery to initiate early, dominant cracks at well defined locations. Macroscopic surface crack lengths (1 to 8 mm) were measured optically at X30 on both faces of the tapered disks. Curves for crack length versus applied cycles were quite linear, despite the numerous nonlinear aspects of the problem. Typical examples of crack growth are shown in figure 16 for the two alloys studied.

Spera, Calfo and Bizon (ref. 106) reported crack growth results for thermal fatigue tests of simulated turbine blades. Cracked area versus applied cycles data were presented. Areas were calculated from surface crack length measurements and the assumption that the crack front was a straight line. This was probably a good assumption considering the thin geometry of the leading

edge of the airfoil where all of the cracks initiated. Again, a remarkably linear crack (area) growth curve was observed for the four conditions investigated. Figure 17 shows these results. It is interesting to note that the coated blade (curve B) had a crack initiation life nearly twice that of the blade with no coating (curve A), indicating that the coating is serving its intended environmental protection function quite well in the case. Once the coating had cracked into the substrate, however, the rate of crack growth equaled that of the uncoated blade.

The thermal fatigue crack growth information presented herein is an example of the limited type of data that have been reported. Thermal fatigue related conferences (refs. 35 to 61) contain a few papers dealing with crack propagation.

Interest is waning in the thermal fatigue test as a means of studying the thermal fatigue resistance of materials. In its place is the considerably more basic and sophisticated thermomechanical fatigue test. This testing technique is discussed in the next section.

THERMOMECHANICAL FATIGUE (TMF)

A. EXPERIMENTAL PROCEDURES

Thermomechanical fatigue (TMF) is the term used to describe fatigue in which temperature is varied throughout a cycle in a well controlled manner, and the temperature gradients within a specimen test section are held near zero. The mechanical strains and the temperature can be controlled independently of one another if desired. Typically, these two variables are programmed to follow prescribed patterns with respect to time, and with a fixed phase relation. In-phase TMF cycling is the condition in which the maximum tensile strain occurs at the same instant as the peak temperature, and the maximum compressive strain occurs at the minimum temperature. Out-of-phase (180°) TMF is the opposite condition with tension cold and compression hot. Intermediate phasings have also been employed (refs. 81 and 118) in attempts to simulate a particular thermal fatigue cycle experienced by a component part in service. The most sophisticated of these intermediately phased cycles is the so-called "faithful cycle". Here, a smooth, axially loaded laboratory test sample is subjected to a strain-time and temperature-time history that faithfully reproduces the cycle calculated for a critical location of a component part in service. Such cycles can become rather complex and can involve extremely long hold periods at maximum, or near maximum temperature. However, the in-phase and out-of-phase TMF cycles are more valuable from the point of view of measuring generic material characteristics.

TMF testing techniques have become a common form of high temperature fatigue evaluation, and are rapidly replacing the less sophisticated thermal fatigue testing approaches.

The first TMF experiments were performed and reported by L.F. Coffin, Jr. in the early 1950s. While lacking the benefits of accurate high temperature extensometry and closed loop servocontroller technology, the apparatus permitted a study of the strain-temperature phasing effects that had not been possible previously. Strain ranges could be varied while keeping the temperature extremes fixed, or at a fixed strain range, the temperature extremes could be

varied. This degree of freedom in controlling the variables allowed Dr. Coffin to isolate the independent variables and gain a much better appreciation of the cause and effect relationships governing variable temperature low-cycle fatigue.

Slowly, improvements in extensometry, load cells, heating and cooling techniques, electrohydraulics, servocontrollers, programmers, recorders, and now computers have allowed researchers in the field to conduct TMF experiments on a routine basis (ref. 118).

A variety of experimental procedures have been employed to conduct TMF tests. Closed-loop, electrohydraulic, servocontrolled, axially loaded machines are now used exclusively. The heating techniques are usually induction or direct resistance, with a few experiments being conducted with quartz lamp furnaces. Specimens are either of uniform gage length, in which case, an axial extensometer is used, or have an hourglass configuration that is used with diametral extensometry. Direct resistance heating is inappropriate for uniform gage length specimens because of the temperature gradient that develops along the gage length as heat is lost through the grips.

In performing a TMF test, the thermal strains (due to thermal expansion) of the specimen and the "apparent" strains caused by expansions within the components of the extensometer can be considerably greater than the mechanical strains experienced by the specimen. One of the first problems to be overcome in TMF testing, is to cancel the extraneous strains from the total extensometer output, so that only the specimen mechanical strain remains. Typically, a specimen is thermally cycled through the desired temperature-time history, while the specimen is held at zero load (stress). The extensometer output is then recorded and incorporated into a computer program that later subtracts this synchronized signal from the total extensometer output as the specimen is thermally and mechanically strained. The resultant output is the mechanical strain experienced by the specimen. Further details of these techniques can be found in reference 118.

The TMF crack growth measurements reported by Rau, Gemma, and Leverant (ref. 83) and Gemma, Langer, and Leverant (ref. 84) have used the basic thermal cycling and straining techniques reported by Hopkins (ref. 118). Similar techniques have been employed by Marchand and Pelloux (ref. 86).

B. TRENDS IN BEHAVIOR

1. Crack Initiation

An extensive TMF crack initiation data base has been generated since the first experiments were conducted by Coffin (ref. 5) over 30 yr ago. At latest count, nearly 40 alloys have been studied with a total of 93 different TMF conditions. These results are much too extensive to include herein, but a brief summary tabulation is included to illustrate the diversity of TMF behavior that has been observed for a wide variety of alloys. In some of the studies, isothermal creep-fatigue results were also determined for direct comparison with the TMF behavior.

In summarizing the TMF and isothermal data trends in table I, a coding system has been adopted from the work of Kuwabara, Nitta and Kitamura (ref. 119). The coding is illustrated in figure 18. When in-phase TMF cycles

produce crack initiation lives that are less than equivalent out-of-phase TMF cycles, the letter "I" is listed. If the reverse is true, the letter "O" is listed. If the in-phase and out-of-phase life curves are parallel or converge at low lives, the letter designations remain "I" or "O". Should the life curves converge at long lives, (a less common occurrence), a prime is added to the letter. And, if the in-phase and out-of-phase life curves are nearly equal, the letter "E" is employed. Finally a notation is made as to whether an isothermal life curve determined at the maximum temperature of the TMF cycle is above (A), nearly equal to (N) or below (B) the corresponding TMF life curve.

The coding has been applied to fatigue behavior based on either total strain range or inelastic strain range, or both, if data were originally presented to permit both being determined. Also, comparisons between isothermal and TMF lives are made for both in-phase and out-of-phase TMF cycles. In cases where no measurements were made, or data were not reported, a question mark is listed in the table.

Despite the enormous volume of data, few of the investigators conducted enough tests to permit complete entries in table I. The most thorough results were reported by Kuwabara, Nitta and Kitamura (ref. 119), and Sheffler and Doble (ref. 146). Frequently, the isothermal results were ill-conditioned for direct comparison with the TMF data. For example, TMF tests invariably have a component of creep strain in the high temperature half of the cycle, i.e., CP for in-phase and PC for out-of-phase TMF cycling. Yet, the isothermal results generated for comparison invariably did not contain the same extent of CP or PC strains for a proper direct comparison. The judgments appearing in table I are based upon the raw data presented in the cited references, and reflect no attempt to compare the isothermal and TMF behavior via an evaluated life prediction model.

Nevertheless, there are some interesting observations to be gleaned from table I. First, and most importantly, is the fact that almost every conceivable behavior combination has been observed. Let us now examine specific trends:

When comparing in-phase TMF and isothermal fatigue results on the basis of total strain range, we find that over half of the reported results are categorized by the designation "N". That is, the isothermal and TMF life results are nearly equal. In 40 percent of the cases, the TMF lives are below the isothermal lives and in only three instances (7 percent) were the TMF lives greater than isothermal lives, thus dispelling the notion that isothermal fatigue tests at the maximum TMF cycle temperature provide a conservative estimate of TMF life. Out-of-phase results differ from the in-phase, in that almost three-fourths of the data sets have nearly equal TMF and isothermal lives, leaving only 20 percent of the data sets having TMF lives greater than isothermal.

For comparisons based upon the inelastic strain range, the above percentages change. The major change involves a greater percentage of TMF results having lives less than the isothermal lives at the peak TMF temperature. Specifically, 55 percent of the in-phase and 44 percent of the out-of-phase results have TMF lives less than isothermal lives. In only one instance (Inconel 718, out-of-phase, (ref. 119) was it observed that TMF lives were

greater than comparable isothermal lives. Again, it is clear that isothermal fatigue resistance at the peak temperature does not provide a conservative estimate of TMF life.

Finally, the relative positions of the in-phase and out-of-phase strain range versus fatigue life curves have been categorized, and designations of O, E, I, and I' have been used. Out-of-phase lives are less than in-phase lives in 33 percent (total strain range basis) and 24 percent (inelastic strain range basis) of the cases, whereas in-phase lives are less than out-of-phase lives in 40 percent (total strain range basis) and 66 percent (inelastic strain range basis) of the cases. Whether one phasing or the other is lower is highly dependent upon the alloy, temperature levels, and cycle times.

2. Crack Propagation

One of the first TMF crack growth studies to be reported in the literature was that of Rau, Gemma and Leverant (ref. 83) in 1972. These studies were followed by those reported in 1976 by Gemma, Langer and Leverant (ref. 84). The materials were advanced cobalt- and nickel-base superalloys that were seeing service in aeronautical gas turbine engines. Crack growth rates were correlated with the range of the strain intensity factor using elastic fracture mechanics principles. Cyclic crack propagation rates were found to be nearly an order-of-magnitude greater for out-of-phase TMF cycles than for in-phase cycles. Accelerated crack growth of coated specimens occurred when the peak tensile strain were imposed when the coating was at a temperature range where it was relatively brittle. The high growth rates for out-of-phase cycling are even greater than the isothermal rates at the same temperature as the peak tensile strain (lowest TMF cycle temperature for out-of-phase cycles). Tensile ratchetting strains promoted multiple crack initiation in the coating, and subsequent increases in cyclic crack growth rates.

In tests on directional solidified MAR-M 200 with varying crystallographic orientations relative to the loading axis, it was found that the crack growth rates for all orientations could be correlated by normalizing the strain intensity factor by the elastic modulus in the direction of loading. Only out-of-phase thermomechanical loading was employed. Since these pioneering studies, several others have been published. Most have concluded that TMF crack growth rates are faster than isothermal growth rates measured at the peak temperature of the TMF cycles (refs. 81, 83 to 85, 91). With the exception of the results of Marchand and Pelloux (ref. 86) for INCONEL X-750, and Kuwabara, Nitta and Kitamura (ref. 119) for 304 stainless steel, out-of-phase TMF crack growth rates were considerably greater than in-phase TMF growth rates. Koizumi and Okazaki (ref. 147) have found nearly identical crack growth rates for TMF and peak temperature isothermal tests for a 12Cr-Mo-V-W steel.

In 1974, Taira, Fujino and Maruyama (ref. 148) reported results for a 0.16 percent carbon steel which were obtained from TMF cycles at three temperature levels; 100 to 300 °C, 300 to 500 °C, and 400 to 600 °C. The out-of-phase crack growth rates were only slightly affected by the temperature levels, but the in-phase TMF growth rates increased dramatically as the peak temperature increased. As a consequence, in-phase growth rates were higher than out-of-phase at only the two highest temperature levels. At the lowest temperatures, out-of-phase growth rates were highest. These results are reproduced in figure 19.

In summary of this section, it is appropriate to quote from Marchand and Pelloux (ref. 86):

"From the TMF crack growth data available in the open literature, it can be seen that there is no generalization to be made concerning the severity of damage associated with in-phase and out-of-phase cycling, and that there is no hard and fast rule for relating TMF data to isothermal testing."

BITHERMAL FATIGUE

At our present state of technological development, we are forced to rely heavily on our extensive and reasonably well-understood isothermal fatigue knowledge and data bases for the design of components subjected to thermal fatigue loadings. The considerable gap between isothermal and thermomechanical fatigue technology can be bridged by an approach that retains the simplicity and ease of interpretation of isothermal fatigue testing, yet captures the first order effects of the more complex thermomechanical cycling. The approach is called bithermal fatigue. The experimental procedures involve tensile and compressive halves of a cycle being imposed isothermally at two significantly different temperatures. The higher temperature is chosen to be in the time-dependent creep and oxidation-prone regime of the material, and the lower temperature in the regime wherein time dependencies are minimized due to lack of thermal activation.

A. RATIONALE FOR BITHERMAL FATIGUE

Figure 20 provides a schematic illustration of the temperature versus strain relationship for the bithermal cycles employed in studies to date. Both in-phase (wherein all of the tensile inelastic strain is imposed at the highest temperature) and out-of-phase (wherein the converse is true) bithermal cycles are illustrated. In the figure, the bithermal cycles are compared to conventional thermomechanical cycles. Resultant stress versus mechanical strain hysteresis loops are illustrated in figure 21. Note that the thermal free expansion strains are not included in the strains shown in this figure. While bithermal cycling in the past has been used to introduce time-dependent creep strains at the high temperature, and time-dependent plastic strains at the low temperature (i.e., a CP or PC type Strainrange Partitioning cycles), it can be used to introduce plastic strains only at both temperatures. This latter condition is extremely difficult to achieve with conventional thermomechanical cycling, since thermal cycling a specimen usually cannot be accomplished with a high enough rate to preclude the introduction of creep. In the bithermal testing technique, the specimen is held at zero stress during the temperature excursions, and hence no mechanical deformation (other than any creep recovery) takes place. Once at the high temperatures, the deformation can be imposed at high enough rates to preclude creep. Such PP bithermal experiments should help to isolate time-independent from time-dependent damage mechanisms.

Among the important effects of thermomechanical loading that are naturally encompassed by bithermal fatigue experiments are: (a) influence of alternate high and low temperatures on the cyclic stress-strain and cyclic creep response

characteristics; (b) possibility of introducing both high temperature and low temperature deformation mechanisms within the same cycle, but limiting the number of active mechanisms at high temperature by proper choice of the temperature level, stress level, and hold time; and (c) thermal free expansion mismatch straining between surface oxides and the substrate (or coatings and substrate). Much of the relative simplicity of testing and interpretation of isothermal results, however, is retained by the bithermal testing procedures.

Many of the troublesome experimental aspects of TMF cycling can be overcome readily by bithermal testing. During TMF cycling, precisely controlled temperature and strain histories must be synchronized or the mechanical hysteresis loop becomes highly distorted. Distortion of this loop hampers measurement and interpretation of the stresses and strains. This problem is minimized by use of bithermal cycling, since temperature is held constant during the application of mechanical strain. Obviously, the temperature must be accurately controlled at a constant value or the hysteresis loop will distort in this case as well. However, constant temperature control is easier to achieve than is accurate variable temperature and strain both in magnitude and phase relationship. For in-phase or out-of-phase TMF cycles, the peak temperatures and strains must occur simultaneously and repeatedly. If this is not accurately controlled, the mechanical hysteresis loop distorts and accurate interpretation of results is difficult. Still another experimental disadvantage of TMF cycling that can be overcome by the bithermal procedure has to do with the uniformity of the temperature profile along the axial gage section of a specimen (when utilizing an axial extensometer) during heating and cooling. It is difficult to maintain a uniform temperature profile while also changing the temperature, since the gradients tend to increase as the cycling becomes more rapid. Should a thermal gradient develop along the gage length in a TMF test, the hysteresis loop will again experience distortion with subsequent difficulties in interpretation. For bithermal experiments, no mechanical strain changes are imposed during heating or cooling, and temperature gradients can readily be ignored during the temperature transition period at zero stress. Finally, bithermal cycles can be run and thermal strains can be subtracted from the extensometer signal in a simple manner, not requiring nearly as high an accuracy as for TMF cycling. Because the thermal strain of both the specimen and the extensometer can be considerably larger than the mechanical strain, it is common practice to first document this component of the strain signal (by thermally cycling the specimens under zero load control) and then subtracting it from the total strain signal. The difference is the mechanical strain. Once the difference signal is obtained, it can be amplified to provide an accurate mechanical strain signal. For a TMF test, the subtraction process becomes critical and the accuracy of the mechanical strain signal depends upon the accuracy of the total signal and the apparent thermal signal. The accuracy of the thermal signal and the accuracy of its subtraction from the total signal is relatively unimportant to the bithermal cycle. If the subtraction process is perfect and complete, the resultant mechanical hysteresis loops will appear as in figure 21. On the other hand, if the subtraction is imperfect, the only effect is to have the upper (tensile) and lower (compressive) halves of the hysteresis loop displaced horizontally by the amount of the error. This error does not affect the accuracy of the mechanical strain signal.

Interestingly enough, the bithermal testing technique was not originally proposed as an alternative to thermomechanical fatigue testing. Instead, it was used in the evaluation of the isothermal Strainrange Partitioning (SRP) characteristics of alloys. Hence, numerous bithermal fatigue tests were per-

formed on a variety of alloys, but comparative thermomechanical fatigue tests were seldom performed since that was not the subject under investigation at the time. The bithermal testing technique has been applied to several wrought and cast alloys. Wrought alloys included 304 (ref. 149) and 316 (refs. 10 and 130) austenitic stainless steels, A-286 (ref. 149), 2-1/4 Cr-1Mo steel (ref. 130), and the tantalum alloys ASTAR 811C (ref. 146) and T-111 (ref. 146). Cast superalloys examined were the aluminide coated cobalt-base alloy MAR-M-302 (ref. 144) and the nickel-base alloy B-1900 + Hf (ref. 150).

B. BITHERMAL FATIGUE RESULTS

As early as 1971, the bithermal fatigue cycling technique was used by Manson, Halford and Hirschberg (ref. 10) to characterize the isothermal Strain-range Partitioning (SRP) behavior of 316 austenitic stainless steel and 2-1/4Cr-1Mo steel. The peak temperature in the cycle was considered to be the important temperature, and results were compared with isothermal results for approximately the same temperature. The concept behind the technique was to ensure that only time-independent plastic deformation was encountered in the half cycle of interest by reducing the temperature below the creep range. No attempt was made at the time to consider the bithermal cycle as an approximation to a thermomechanical fatigue cycle. However, since these bithermal results agreed well with isothermal results (ref. 131 for the two alloys studied, it is anticipated that isothermal behavior could be used to predict thermomechanical fatigue lives. This assumption was reinforced in 1976 for the 316 austenitic stainless steel (ref. 131).

The agreement of bithermal and thermomechanical results for 316 stainless steel is illustrated in figure 22. Results for both in-phase (CP) and out-of-phase (PC) cycles are shown. For the in-phase cycles, it appears that bithermal cycling produces slightly lower lives than TMF cycling. This is rationalized by noting that the bithermal cycles contain a greater proportion of the highly damaging CP strainrange component than to the TMF cycles. For example, in the case of inelastic strainranges below 0.01, the fraction of the inelastic strainrange that is of the CP type is approximately 0.225 (ref. 131), whereas for the two bithermal tests, this fraction is 0.365 and 0.475 (ref. 10). By applying the interaction damage rule of the SRP method, these two sets of results can be brought into even closer agreement. In reference 10, photomicrographs were presented showing the extensive intergranular cracking present in the in-phase bithermal experiments. Similar intergranular cracking was also documented for the in-phase TMF tests reported in reference 131. Since the basic failure mechanism was the same for the two types of testing, it is not surprising that the cyclic lives are comparable. Differences in lives between the in-phase and the out-of-phase cycles are explained by the more benign transgranular cracking mechanisms in the bithermal and TMF out-of-phase experiments.

In 1972, Sheffler and Doble (ref. 146) of TRW, under contract to NASA, also performed bithermal fatigue tests on the tantalum alloys T-111 and ASTAR 811C in ultrahigh vacuum. Comparisons of bithermal and thermomechanical fatigue tests can be made only for the ASTAR 811; results are shown in figure 23(a) and (b) for in-phase (CP) and out-of-phase (PC) cycles, respectively. The bithermal cycles are more severe than the TMF cycles. Again, this would be expected based upon the greater degree of damaging creep strains present in the bithermal cycles compared to the TMF cycles. Greater creep strains occur in the bithermal tests since all of the inelastic deformation is

imposed at the peak temperature, whereas in the case of linear thermal ramping for TMF cycling, the inelastic deformation within a half cycle is imposed at a considerably lower average temperature.

The results discussed above are the only known examples for which both bithermal and TMF tests have been conducted for the same alloy during the same investigation.

Bithermal data in ultra high vacuum have been reported for 304 austenitic stainless steel (ref. 149) and A-286 (ref. 140) as well as for aluminide coated MAR-M-302, a cast cobalt-base superalloy (ref. 144). For these three alloys, there is no valid basis for judging whether the bithermal cycling results are compatible with TMF or isothermal creep-fatigue behavior, since the latter type tests were not performed.

Preliminary bithermal fatigue results have been generated by Halford, McGaw, Bill and Fantl (ref. 150) for B-1900 + Hf. Only PP and PC bithermal results have been reported, and no TMF results had been conducted as yet. The PP and PC bithermal data were essentially coincident on a plot of total inelastic strainrange versus cycles to complete failure. Test temperatures were 483 °C in tension and 871 °C in compression. Their results are shown in figure 24, and are compared to isothermal PP results for the two temperatures. Surprisingly, the bithermal results agree very closely with the higher temperature, higher life, isothermal PP data.

While bithermal cycling offers several advantages over conventional thermomechanical cycling, other forms of strain-temperature cycles have also been used to advantage by researchers in the field. For example, Lindholm and Davidson (ref. 141) have employed phased strain-temperature cycles that are similar to the bithermal cycle-the chief exception being that both tensile and compressive deformation is imposed at both the maximum and minimum temperatures in their work. This aspect can introduce features not found in thermally driven service cycles. Another form of cycling, referred to as a dog-leg cycle, is one in which the tensile and compressive straining is imposed at a single temperature (either maximum or minimum), and at some point in each cycle, the specimen is subjected to a thermal excursion during which no mechanical strain is allowed to be experienced by the specimen. This form of cycling does introduce some aspects of a service cycle, but not to the same extent as does the bithermal cycle. Cycles have also been conducted in which the strain and temperature are phased by 90° in an attempt to simulate special thermal fatigue cycles. These TMF cycles are referred to as "baseball" cycles (ref. 81) because of the diamond shape of the strain-temperature path.

In this section the philosophy has been adopted that complex thermomechanical fatigue behavior can be approximated by simpler bithermal fatigue experiments. For the approximation to be acceptable, the same basic deformation, crack initiation, and crack propagation mechanisms must be present in both types of cycles. And, in order to directly compare the results of one type of test to the other, a damage accumulation, i.e., life prediction, theory must be invoked. The SRP framework has been utilized herein.

The principal reason for promoting bithermal fatigue testing as a viable technique is to provide a simple test procedure that captures the first order aspects of more complex TMF cycling, and does so by taking advantage of isothermal testing philosophy.

From the limited experience to-date, it is apparent that bithermal fatigue testing can be used to impose more creep damage per cycle than a comparable TMF cycle. Consequently, bithermal cycling could be used to determine lower bounds on TMF life, or at least to determine a conservative life. For alloys whose TMF behavior and bithermal behavior can be predicted directly from isothermal behavior, there is less of a need for the bithermal approach. However, for other alloys in which TMF is not directly predictable from isothermal behavior because of new mechanisms of deformation and cracking, the bithermal cycling procedure offers a useful means for ascertaining TMF resistance. The bithermal technique is also advantageous from the standpoint of interpreting the mechanisms of cyclic deformation and cracking since only two distinct temperatures are involved. TMF cycling includes the complete spectrum of temperature from minimum to maximum, and mechanistic interpretation could be hampered by the integrated effects of a spectrum of damage mechanisms.

The principal features of the bithermal fatigue philosophy can be summarized as follows:

1. Bithermal fatigue testing is a simple alternative to thermomechanical fatigue testing, and can provide a conservative determination of TMF life.
2. Bithermal fatigue results can be directly related to TMF fatigue results through the use of an appropriate damage rule.
3. Bithermal fatigue may be related to isothermal fatigue provided that no new mechanisms of deformation and cracking are introduced by the change in temperature required by the bithermal experiments.
4. The micromechanisms of cyclic deformation and cracking should be easier to interpret for bithermal cycles than for thermomechanical cycles because of the discrete nature of bithermal cycling compared to the continuous spectrum of TMF cycling.
5. Bithermal fatigue testing could be accomplished in any high-temperature fatigue laboratory with a minimum of alterations to the instrumentation. Current testing procedures utilizing computer control and data acquisition and handling are ideally suited for bithermal fatigue experimentalization.

ISOTHERMAL LIFE PREDICTION MODELS

High temperature fatigue life prediction models have been developed almost exclusively under isothermal conditions. The mere fact that a model was developed with isothermal conditions in mind does not, in itself, exclude the model from applicability to TMF or thermal fatigue life prediction. However, if the constants in the model are evaluated only under isothermal test conditions with no regard to prior thermal history, the model should be used with caution before applying to a thermal cycling fatigue problem. Some of the proposed models can be applied readily to thermal cycling conditions provided the constants are known as a function of temperature, and an analysis has been made of the cyclic stress-strain-temperature-time history at the critical crack initiation location. The classic time- and cycle-life fraction approach (ref. 152) and the Continuum Damage method of LeMaitre and Chaboche (ref. 153) fall into this category. However, the predicted lives are excessively dependent upon the

accuracy of the stress-temperature-time history. For thermal fatigue life prediction, strain based approaches, especially those based on total strainrange, are much less sensitive to the accuracy of the input analyses.

The life prediction models would be relatively simple were it not for the time-dependent damaging mechanisms that are introduced by high temperature exposure. In fact, many of the methods are simply extension of low temperature methods. The principal damaging mechanisms are creep (particularly grain boundary related creep phenomena), oxidation (particularly at surface connected grain boundaries), and metallurgical instabilities promoted by the combination of crystallographic slip and thermal exposure. Consequently, every high-temperature life prediction model features some aspect of time-dependency. However, few methods can truly distinguish which time dependency is being accounted for when the constants are being evaluated from test results.

The primary variables of concern are the strainranges (both inelastic and total), stresses (range, peak tensile, mean stress, and the stress-temperature-time history), time (strain rate, frequency, hold time, total elapsed time), temperature, stress or strain intensity, crack size, and rates of oxidation.

Exactly how these variables enter into the various life prediction methods is what distinguishes one from the other. All rely upon stress or strain related parameters as the prime variable, but they differ on how time enters. Some, such as Coffin's Frequency Modified Life or Frequency Separation methods and Ostergren's Approach treat time (frequency) directly in their formulations. On the other hand, the Strainrange Partitioning method incorporates time indirectly through a knowledge of the percentage of creep strain present in a cycle. Obviously, the greater the elapsed time/cycle, the greater the amount of creep strain. In either case, all time-dependent effects (creep, oxidation, metallurgical changes) are accounted for when constants in the models are evaluated from tests that cover a limited time span. Extrapolating life predictions to significantly longer times will be acceptable provided only the same mechanisms continue to operate, and operate at the same rates as in the evaluation tests.

A summary of the 30 isothermal high-temperature life prediction models proposed over the past three decades is contained in table II. The table also lists the 13 different reviews of these methods. Because of the large number of models, it is not possible to review and do proper justice for each and every model; such an undertaking shall be reserved for a future review chapter. In the meantime, the reader is referred to some of the more extensive reviews, in particular, Manson (refs. 154 and 155), Coffin (refs. 156 and 157), Lundberg and Sandstrom (ref. 158), and Miller, Priest, and Ellison (ref. 159). The reader is encouraged to examine the well-thought out criteria for judging methods that was used by Manson (ref. 154) in his 1976 review. The very same criteria should be applied to the numerous life prediction models that have been proposed since that time. Manson's criteria are:

1. Accountability for Data Trends
2. Viability of Basic Mechanism
3. Applicability to Realistic Design
4. Required Input Data
5. Special Range of Utility

For every isothermal life prediction method proposed to-date, accountability for data trends is the first and foremost criterion that has been

applied and found to be acceptable, at least for the range of variables considered by the method developer. A shortcoming of most of the high-temperature methods has been the limitation placed on the range of applicability. This is particularly true when it comes to the prediction of TMF and thermal fatigue lives. While successful thermal cycling fatigue life predictions have been demonstrated for the time- and cycle-fraction approach as utilized by Spera (ref. 188), Strainrange Partitioning (ref. 131), Exhaustion of Ductility (ref. 189), Continuum Damage (ref. 190), and Pawa SRP Combustor Model (ref. 191), such successes can hardly be expected on a more routine basis. Examination of the TMF crack initiation data trends in table 1 clearly shows the diversity of behavior that has been observed, and hence the improbability of an existing isothermal model being able to deal accurately with all conditions and all materials.

The following section takes an in-depth look at the prediction of TMF lives using three selected isothermal life models with idealized characteristics. Even under the highly simplified conditions, it will be seen that isothermal life models can give erroneous TMF life predictions.

PREDICTION OF TMF LIVES USING IDEALIZED ISOTHERMAL CHARACTERISTICS

Thermomechanical fatigue (TMF) life predictions in design are often made on the basis of established isothermal fatigue behavior (ref. 19). Strong economic and engineering reasons exist for continuing to rely upon the vast quantity of existing isothermal material characterizations for life prediction data bases. However, recognition of the inadequacies in the use of isothermal behavior to predict TMF life of certain classes of materials has been increasing.

Accuracy of TMF life predictions is generally recognized to be considerably poorer than corresponding isothermal life predictions. The primary deficiency lies in the simple fact that isothermal testing and characterization can never capture those micromechanisms which become manifest under thermal cycling conditions. For example, alloys with strengthening precipitates can experience an additional localized component of cyclic strain during thermal cycling because of the differential thermal expansion between the precipitate and the matrix metal; such an additional cyclic strain would not be present during isothermal cycling. Imposing identical global mechanical strains during both types of cycling would not produce the same local strains, and hence the test with the highest local strain would likely have the shortest life. Numerous other micromechanisms of cyclic deformation also may be present depending upon the material involved and the circumstances in a thermal cycling test.

The purpose of this section is to examine a few of the simpler isothermal life prediction models, and to explore the logical implications of these methods when applied to TMF problems. The study is analytic and avoids the uncertainties that tend to confuse pure experimental comparisons of isothermal and TMF behavior. To keep the analysis as basic as possible, only the simplest of possible assumptions are made. It is assumed, for example, that the alloy and its environment are such that no additional thermal cycling mechanisms, above and beyond that encountered in isothermal cycling, are present. Only one dominant isothermal inelastic deformation mechanism (for example, to and fro crystallographic slip) is assumed to be present. This is obviously the simplest

of all conditions to consider, and consequently serves as an excellent base from which to formulate future studies. Under these conditions, it is reasonable to expect that an isothermal fatigue model based upon the single mechanism would be able to predict thermal cycling fatigue lives. Hence, it is possible to establish a required condition for a valid isothermal fatigue life prediction method. If an isothermal method doesn't accurately predict a thermal cycling fatigue life under these idealized conditions, then the method is considered to be technically deficient.

Historically, investigators have sought an equivalence between TMF and isothermal fatigue by postulating the existence of a single isothermal temperature level for which the low-cycle fatigue resistance is the same as the TMF resistance. Suggested temperature levels have been: maximum thermal cycling temperature (ref. 19), minimum temperature, average temperature, or more complex choices such as an equivalent temperature (ref. 187) or the temperature within the thermal cycling range for which the isothermal fatigue resistance is minimum (ref. 188). A uniquely defined single temperature level has not been found thus far that can represent all thermal cycling conditions for all materials.

The proper basis for comparison of isothermal and TMF resistance has also been open to debate. Quoted isothermal and TMF results may differ considerably, depending upon the choice of parameter used for comparison. In fact, the relative fatigue resistances can reverse depending upon the parameters used. Comparisons have been made on the basis of inelastic strainrange, total strainrange, stress range, peak tensile stress, and a variety of other failure criteria or damage factors. This issue, of course may never be experimentally resolved because of the host of differing damage accumulation mechanisms from one material to the next, and because of the potential for differing damage accumulation mechanisms between isothermal fatigue and TMF. Numerous examples from the literature were surveyed in a previous section, and a wide range of behaviors between isothermal and TMF have been noted. Thermal fatigue lives are almost invariably less than or equal to isothermal fatigue lives when the basis for comparison is constant inelastic strainrange. However, if the total strainrange is used as the basis of comparison, the order may be reversed, particularly if the inelastic strainrange is small compared to the total strainrange.

Another complication arises when dealing with TMF because of the potentially pronounced effect of temperature and strain phasing. In-phase thermal cycling (high temperature at maximum strain) produces lives that can be either greater than, nearly equal to, or less than, out-of-phase cycling (low temperature at maximum strain) depending upon the material and environment involved. Hence, if isothermal fatigue life prediction methods are to be able to predict phase effects, they would have to recognize the different mechanistic aspects of the two different phases. In this section, the idealized behavior is limited to a single operative crack initiation mechanisms, and consequently, no temperature/strain phase effect is introduced. Some isothermal life prediction methods attempt to distinguish the effects of phasing, others do not. The approach of Ostergren (ref. 71) predicts an effect of phasing, and will be examined later in this section.

The approach is to assume an idealized isothermal behavior for a material, then infer what the likely thermomechanical response would be. History independence of flow behavior is assumed, and no additional flow or damage mechanisms are permitted during the thermal excursions. Such idealizations are seldom, if ever, achieved in real materials. However, they do serve a useful purpose in providing a simple, common basis, for directly comparing various life prediction approaches. If an isothermal life prediction method properly predicts the idealized TMF behavior, a required condition has been achieved for assessing the validity of the method. On the other hand, if incorrect TMF behavior is predicted, the prediction method is faulty.

A. CONSTANT MANSON-COFFIN FAILURE CRITERION

Two distinct material behaviors are examined; time-independent cyclic stress strain behavior over the entire temperature range of interest, and time-dependent behavior within the higher temperature region. In all cases considered in this subsection (A), it is assumed the inelastic strainrange versus cyclic life relation, i.e., the Manson-Coffin (refs. 167 and 5) relation, is independent of both temperature and time. Hence, the inelastic strainrange uniquely defines the cyclic lifetime.

1. TMF Life Prediction for Time-Independent Constitutive Behavior

Although the cyclic stress-strain properties are assumed to be independent of time, they are recognized to be temperature-dependent. Figure 25 schematically illustrates the form of the cyclic stress-strain relation used; linear elastic strain plus power-law plastic strain-stress response,

$$\Delta\epsilon = \Delta\epsilon_e] + \Delta\epsilon_i]n = \Delta\sigma/E + (\Delta\sigma/K)^{1/n} \quad (1)$$

The three material constants, E, K, and n, are taken to vary with temperature according to the straight line relations shown in figure 26. A temperature range from 0 to 1000 °C has been considered for sake of numerical example. While the numerical values are arbitrary, the trends reflect realistic engineering material behavior.

The temperature-independent inelastic strainrange versus life relationship shown in figure 27 is of the Manson-Coffin form,

$$\Delta\epsilon_i]n = B(N_f)^\beta \quad (2)$$

By fixing the constants in the cyclic stress-strain relation and in the inelastic strainrange versus life relation, the elastic strainrange versus life relation (fig. 28) becomes fixed at each temperature.

$$\Delta\epsilon_e] = A(N_f)^\alpha \quad (3)$$

Since β and n are constant at all temperatures, α is also temperature independent ($\alpha = \beta n$). The constant A varies with temperature because of the corresponding temperature dependence of K and E (i.e., $A = KB^n/E$). The constants for the inelastic and elastic strainrange versus life relations are presented in figure 29 for the temperature range considered.

Since the inelastic strainrange versus life relation is not a function of temperature, and since no new deformation or crack initiation micromechanism is permitted due to thermal cycling, it can be deduced that a TMF cycle will have exactly the same life as any isothermal cycle with the same inelastic strainrange.

Consequently, the life of any TMF cycle can be determined simply by knowing its inelastic strainrange. Now, we are in a position to ask what other life prediction methods (which utilize other criteria for failure) would predict under these circumstances.

Two failure criteria are examined; (a) total strainrange of the cycle at some prescribed temperature and (b) the approach of Ostergren (ref. 71) (with no time dependencies) that postulates that the product of the inelastic strainrange and the peak tensile stress is a power function of the cyclic life. Alternatively, the product can be interpreted as representative of the tensile hysteresis energy of the cycle. This alternative is also examined by considering the integrated hysteresis energy of the tensile half of the loops.

a. Total Strain Range Criterion

The isothermal total strainrange versus life relations for any temperature can readily be computed from the originally adopted constitutive and failure behavior. Calculated curves for the maximum, average, and minimum temperatures are presented in figure 30. We are now in a position to examine a TMF cycle and predict its life based upon the total strainrange versus life relations of figure 30.

For the sake of an example, an inelastic strainrange of 0.005 is assumed, and the TMF hysteresis loop of figure 31 is calculated from the assumed constitutive behavior for a temperature range of 0 to 1000 °C. The cyclic life for this loop is determined using equation (2) and is 400 cycles. The loop shown in the figure does not include the elastic strain. However, the only important elastic strains are those at the extreme temperatures and strains of the TMF cycle. In this case, the elastic strainrange of 0.00300 is composed of the 0 °C amplitude of 0.00233 and the 1000 °C amplitude of 0.00067. The total strainrange is thus 0.00800.

If we enter the isothermal total strainrange versus life curve for the maximum temperature of the TMF cycle we would predict a life of 233 cycles to failure. This number, however, is in disagreement with what we know to be the correct life of 400 cycles to failure based upon an inelastic strainrange of 0.005. Similar calculations for other isotherms reveal the predictions shown in table III.

None of the three predictions agree with the known life. Since the known life is between the extreme predictions, it is obvious that a temperature level (equal-life temperature) exists for which the prediction would be equal to the known life. However, that temperature can be shown to be a function of the values of the constants in the cyclic stress-strain curve, and the constants in the failure curves themselves. Calculations show that the equal-life temperature is also a function of the temperature range and peak temperature. Since the equal-life temperature is dependent upon all of the variables involved, it

has no special significance. Blind use of a total strainrange failure criterion for a preselected isothermal temperature fails to produce correct life predictions.

b. Ostergren Approach

The Ostergren failure criterion for time-independent behavior is the product of the inelastic strainrange and the peak tensile stress of the cycle. This quantity is directly related to the tensile hysteresis energy for isothermal fatigue cycles. For the presently assumed cyclic stress-strain behavior and a constant value of $n = 0.2$, the product and the energy term are linearly related by a factor of 2/3. For isothermal life prediction, there is little need to distinguish between the two. However, the criteria begin to deviate when TMF cycles are involved. The reasons for the divergent behavior will become apparent later. We will examine the product form first, i.e.:

$$(\Delta\epsilon_{in}) (\sigma_T) = F (N_f)^\gamma \quad (4)$$

Equation (4) is shown in figure 32 for several temperature levels. The constants F and γ are derivable from the previously assumed constants, i.e., $F = (K/2)(B)^{1+n}$ and $\gamma = \alpha + \beta$.

The isothermal curves for the tensile hysteresis energy criterion of failure would lie a factor of 2/3 below the curves of figure 32.

Reexamining the in-phase TMF hysteresis loop of figure 31, we can determine the product, $(\Delta\epsilon_{in}) (\sigma_T)$. In this case $\sigma_T = 210$ MPa (30.8 ksi) at point B, $\Delta\epsilon_{in} = 0.005$, and the product is 1.05 MPa (0.154 ksi). Following the same procedure as used in examining the total strainrange failure criterion, we can examine the maximum, average, and minimum temperature. For an in-phase cycle, a fourth temperature might also be selected, i.e., the temperature of which the peak tensile stress is encountered (point B, figure 31). For an out-of-phase TMF cycle, the peak tensile stress of 477 MPa (69.87 ksi) occurs at the maximum strain and minimum temperature. Table IV compares the TMF life predictions at the four isotherms with the previously determined life known to exist for the inelastic strainrange of 0.005. Both in-phase and out-of-phase TMF cycles are examined.

Again, it is readily apparent that none of the in-phase predictions are in agreement with the known life of 400 cycles. An equal-life temperature in this case as well, is so highly dependent upon all of the input variables, the idea of treating the parameter $(\Delta\epsilon_{in}) (\sigma_T)$ and an equal-life temperature as a failure criterion, is not appealing.

For the out-of-phase cycle, agreement is achieved by using the minimum temperature of the cycle. This agreement, however, is circumstantial and is far from being a general conclusion. For example, if the point of view is taken that the tensile hysteresis energy is a more appropriate term, then the above noted successful prediction is no longer correct. By integrating the tensile hysteresis energy for the loop of figure 31 (or the other half of the loop in the case of an out-of-phase TMF cycle) and entering isothermal failure curves based on tensile hysteresis energy, the predictions of table V are obtained.

For this case, there is no agreement between predictions and known life of 400 cycles.

2. TMF Life Prediction for Time-Dependent Constitutive Behavior

In addition to the previously adopted temperature dependence of the cyclic stress-strain behavior, let us now examine the consequences of assuming a time-dependency. The assumed time-dependency begins below an arbitrarily set inelastic strain rate (1.0 sec^{-1} in the present case). The degree of time-dependency increases as the temperature increases. As stated earlier, the failure behavior, which is taken to be inelastic strainrange versus life, is not assumed to be time-dependent, nor is it temperature dependent.

Figure 33 illustrates the time-dependency employed for the cyclic stress-strain curve. The constants K and n are previously designated and retain their originally assigned values. The inelastic strain rate hardening exponent, m , has been assumed to vary with temperature in an exponential manner as shown in figure 34. Based upon these assumptions, it follows that the elastic strainrange versus life relationships are both time- and temperature-dependent. This behavior is shown in figure 35. The total strainrange versus life relationships are also time- and temperature-dependent, as indicated in figure 36.

Since the inelastic strainrange versus life relation is not a function of temperature or time, and since no new deformation or crack initiation micro-mechanism is permitted, it is logical to deduce that a TMF cycle will again have exactly the same life as any isothermal cycle with the same inelastic strainrange. Thus, we can deduce the life of any TMF cycle simply by knowing its inelastic strainrange. The fact that the stress response is time-dependent dictates that the total strainrange and the Ostergren models exhibit time-dependent failure curves. For the sake of an example, we select a single, slow inelastic strain rate of 0.0001 sec^{-1} for evaluation of the TMF and isothermal fatigue lives. An inelastic strainrange of 0.005 is again assumed. The TMF hysteresis loop for an in-phase cycle of an inelastic strain rate of 0.0001 sec^{-1} and temperature extremes of 0 to $1000 \text{ }^\circ\text{C}$ is shown in figure 37.

a. Total Strain Range Criterion

The isothermal total strainrange versus life relations for the slow strain rate of 0.0001 sec^{-1} are shown in figure 38 for the minimum, average, and maximum temperatures. The effect of the low strain rate on the $1000 \text{ }^\circ\text{C}$ curve is quite apparent when compared with figure 30.

The total strainrange is now only 0.00756 (the $1000 \text{ }^\circ\text{C}$ tensile elastic strain amplitude is only 0.00025), and the TMF life is 400 cycles to failure as determined earlier. Life predictions based on the three isothermal total strainrange fatigue curves of figure 38 are listed in table VI. Life predictions at a given temperature are the same for in-phase and out-of-phase TMF cycles.

b. Ostergren Approach

With the introduction of time dependency of the stress response, the Ostergren Approach (ref. 71) can no longer be taken in its time-independent form. Instead, the equation can be written as:

$$(\Delta \epsilon_{in}) (\sigma_T) = F (\dot{\epsilon}_{in})^m (N_f)^{\alpha+\beta} \quad (5)$$

where $F = (K/2) (B)^{1+n}$.

Since the isothermal and TMF inelastic strain rates are identical, no interpolation or extrapolation is required with respect to time-dependent effects. Furthermore, the tensile and compressive inelastic strain rates are also identical, thus eliminating the need to consider the time-dependent wave-form effects that are handled in the Ostergren approach by special interpretation of tensile and compressive going frequencies.

For an inelastic strain rate of 0.0001 sec^{-1} and an inelastic strain-range of 0.005, a life can be calculated from each of the three isothermal temperatures of interest from figure 39. These represent isothermal life predictions of the TMF cycle. For an in-phase TMF cycle, a fourth isothermal temperature may have significance, i.e., the temperature at which the maximum tensile stress occurs (pt. B in fig. 37).

Table VII summarizes the life calculations.

Again, it is obvious that there is general disagreement between the established life and the isothermally predicted lives. The only point of agreement is for the out-of-phase cycle for which the minimum isothermal temperature conditions exist. Again, this is somewhat circumstantial, and it would be dangerous to generalize the agreement for other conditions. To illustrate the point, one need only look at the tensile hysteresis energy representation of the time-dependent Ostergren approach. Predictions for the same TMF cycle are shown in table VIII.

Here it is seen that the previously obtained agreement (using time-independent properties) for the min temp prediction of the out-of-phase cycle is no longer upheld.

Life prediction calculations have also been made for a broader range of the variables of interest. Such calculations are readily obtainable from the computer program prepared for this purpose, and several such calculations have been made. These results are contained in the next several figures for the range of temperatures considered and for an additional inelastic strainrange of only 0.0002. Figure 40 displays the TMF fatigue life predictions based upon the isothermal total strainrange criterion for the two strainranges and for both time-dependent and time-independent behavior. Predictions are identical for in-phase and out-of-phase TMF cycles. The known TMF lives are also independent of phasing for the present case. Note that there are two total strainrange values for each inelastic strainrange. This is because of the different elastic strainrange contributions to the total strainrange resulting from the time-independent and time-dependent TMF loops.

Similar results are displayed in figures 41(a) and (b) and 42(a) and (b) for the two formulations of the Ostergren Approach. The same general trends as found for the 0.005 inelastic strainrange calculations apply for the smaller strainrange.

The above subsections dealt with a temperature-independent inelastic strainrange versus cyclic life criterion of failure. Other temperature-independent criteria will now be examined. Namely, total strainrange and the Ostergren parameter.

B. CONSTANT TOTAL STRAIN RANGE FAILURE CRITERION

When considering the total strainrange criterion it quickly becomes apparent that the only way to make this criteria independent of temperature is to have two conditions fulfilled. The first condition is to have the cyclic strength decrease with increasing temperature at exactly the same rate as the decrease of the modulus of elasticity with temperature, i.e., the elastic strainrange versus life relations must be independent of temperature (and also must be independent of time or strain rate effects). The second condition is that the inelastic strainrange versus cyclic life relation must be temperature independent. However, this is exactly the failure criterion just examined. Hence, there is no merit in further pursuit of the total strainrange criterion.

C. CONSTANT OSTERGREN FAILURE CRITERION

1. Time-Independent Constitutive Behavior

We will now examine the Ostergren Approach [71]. Selecting the time-independent, product-form, (eq. (4)), we see that the constants F and Y must be independent of temperature in order that the failure criterion be temperature independent. Hence, $F = (K/2)(B)^{1+n} = \text{const}$ and $Y = \alpha + \beta = \text{const}$.

In all previous analyses in this study, it was assumed that $n (= 0.2)$, $\alpha (= -0.1)$, and $\beta (= -0.5)$ were constant with respect to temperature. Then, $Y = (-0.1) + (-0.5) = -0.6$, and $(K/2)B^{1.2} = \text{const}$. It is thus necessary for K and B to vary with temperature according to this constraint. Previously, B was considered to be temperature independent. To do so now would also require that the strength coefficient in the cyclic stress-strain curve, K , be a constant. Such a condition is unrealistic since strength decreases as temperature increases. Hence, K is selected to vary with temperature as assumed earlier, $K = 2733 - 2.187T$ (fig. 2). Thus, B must vary with temperature according to:

$$B = \frac{\text{const.}}{(1367 - 1.094T)^{\frac{1}{1+n}}} \quad (6)$$

The constant in the above expression will be taken arbitrarily at a value of 51.74 (previous value at 500 °C with $B = 0.1$) for the sake of example. Thus,

$$B = (26.42 - 0.02113T)^{-0.833} \quad (7)$$

B varies from 0.065 at 0 °C to 0.245 at 1000 °C. Note that it is necessary for B to increase as temperature is increased. While this is not normal engineering material behavior, it is physically viable. Such a trend has been observed by Annis, et al. (ref. 192) for some nickel-base superalloys at high homologous temperatures (>0.7).

Before pursuing the implications to TMF life predictions, time-dependent constitutive response and its affect on the Ostergren approach will be examined.

2. Time-Dependent Constitutive Behavior

From equation (5), we find that $(\alpha + \beta)$ must be temperature independent, and that $K(B)^{1+n}(\dot{\epsilon}_{1n})^m = \text{const.}$, where $K = (2733 - 2.187T)$ and $m = 0.001 \exp(0.004605T)$. Hence, B must vary with both temperature and inelastic strain rate in a highly constrained, physically improbable manner. For example, as the strain rate decreases, the value of B (an indicator of "ductility") must increase. Such response is extremely uncommon except within the realm of superplastic behavior at extremely high homologous temperatures (>0.9).

For an inelastic strain rate of unity or greater, the time-dependent constitutive response degenerates to the time-independent case.

3. TMF Life Prediction for Time-Independent and Time-Dependent Cases

Obviously, if the Ostergren failure criterion is independent of temperature, then the prediction of TMF life using the Ostergren approach is trivial, i.e., the TMF life is identical to the isothermal life. The TMF cycles of interest have already been discussed. The TMF cycle parameters are as listed in table IX. Time-independent values ($\dot{\epsilon}_{1n} \geq 1.0 \text{ sec.}^{-1}$) are shown first, followed by time-dependent ($\dot{\epsilon}_{1n} = 0.0001 \text{ sec.}^{-1}$) values.

a. Ostergren Approach

For time-independent conditions, an in-phase value of 1.05 for the Ostergren product results in an isothermal life of 660 cycles to failure, and thus a TMF life also of 660 cycles to failure. For the time-dependent case, the life is 625 cycles. Similarly the out-of-phase, time-independent and time-dependent lives are 169 and 147 cycles to failure. TMF lives calculated using the Ostergren tensile hysteresis energy parameter were numerically different, but exhibited identical trends.

b. Manson-Coffin Failure Criterion

Evaluation of the Manson-Coffin equation for $B = (26.42 - 0.021131)T^{-0.833}$, i.e. for time-independent constitutive behavior, results in lives for an inelastic strainrange of 0.005 of 169, 400, and 2500 respectively for 0, 500, and 1000 °C. Examining a low inelastic strain rate of 0.0001 sec.^{-1} at an inelastic strainrange of 0.005 results in calculated TMF lives of 149, 400, and 9920 respectively for 0, 500, and 1000 °C. None of these lives are in agreement with what is being forced to be the correct life, i.e., 660 cycles. There is no influence of temperature-strain phasing for this failure criterion. Note again, that by assuming a constant Ostergren failure criterion, independent of temperature, that the predicted TMF lives increase as the isothermal temperature used in the prediction is increased. Also, the lives are greater for the lower strain rate at the highest temperature. These are uncommon trends.

c. Total Strain Range Criterion

For a constant Ostergren failure criterion, the isothermal total strainrange versus life curves must differ from one another at different temperatures. In the present case, both the inelastic and the elastic life line must vary considerably. This is particularly true for time-dependent cases.

For the total strainrange values listed in table IX, the corresponding isothermally predicted TMF lives are as shown in table X below:

Calculated lives are independent of the temperature-strain phasing of the TMF cycle. Again, the lives listed in table 10 increase as temperature increases and as strain rate decreases. Both trends are uncommon.

The above results are displayed in figures 43(a) and (b) for time-independent and time-dependent material behavior respectively. In addition, a much smaller strainrange condition is examined, i.e., $\Delta\epsilon_{1n} = 0.0002$. These figures display the diversity in predicted lives that result from the various failure criteria.

D. INTERPRETATION OF ANALYSES

The objectives have been achieved by examining simple isothermal fatigue life prediction models, and exploring the logical implication of applying these to thermal cycling conditions. Simple sets of assumptions were made regarding isothermal cyclic flow and failure behavior. These were made to permit easier interpretation of the thermomechanical cycling behavior. Cyclic life predictions of selected TMF cycles were based upon the various assumed isothermal fatigue resistances. Of the three basic failure criteria examined, inelastic strainrange, total strainrange, and two versions of the Ostergren Approach, it is concluded that use of an inelastic strainrange criterion gave the most reasonable interpretation of TMF behavior. The other criteria were shown to require improbable material flow and or failure behavior in order to produce numerically correct TMF life predictions. The reason for their poor performance lies in the fact that the failure criteria for each is composed of two contributions, one related to failure (inelastic strain), and the other related to the nonlinear cyclic flow behavior (stress or elastic strain). A similar set of conclusions are projected for the future when other phenomenological life prediction methods are analyzed that incorporate both flow and failure characteristics into their damage parameter.

For a paper study, it is by far the simplest to assume that the failure criterion of interest was independent of temperature and time. Procedures for handling a nonconstant failure criteria have as yet to be established. However, assumptions would have to be made as to how to incrementally add damage in going through each TMF cycle. For example, the cycle could be broken up into equal increments of inelastic strain. Each increment would have its damage tied to the rate of doing damage at the temperature of that increment. The linear summation of the increments of damage over a cycle could be straightforward. While this type of procedure could be applied to the inelastic strain criterion, it is not at all clear as to how to incrementally sum damage due to a total strain criterion, or due to a product of the peak tensile stress and plastic strain.

A key feature of the present analytic study is the assumption that no new deformation or failure mechanisms were introduced by the thermal cycling. While this is not particularly realistic for many materials, it is not an unreasonable one for others. For example, a relatively pure single phase material subjected to fatigue in an inert atmosphere over a relatively narrow, lower-temperature regime could readily fall into this category.

By ruling out additional mechanisms due to TMF, one can potentially achieve a TMF life prediction based solely upon isothermal material behavior. Consequently one can determine which isothermal life prediction methods can meet this necessary (although not-sufficient) condition of validity. Further study will be required to examine more complex cycles, more realistic failure behavior as a function of temperature and time, and to examine additional phenomenological life prediction methods. In particular, it will be necessary to incorporate the numerous imbalances of mechanisms of deformation and cracking that were discussed in detail in a previous section.

THERMAL FATIGUE LIFE PREDICTIONS OF ENGINEERING STRUCTURAL COMPONENTS

The principal reason for pursuing thermal fatigue life prediction is to solve or lessen the problems of thermal fatigue failures in engineering structural components. Such failures are quite expensive, costing the economy many millions of dollars/yr. Most thermal fatigue cracking problems are not of a life-threatening nature involving safety considerations. Rather, they are of a nuisance nature that requires expensive replacement of parts that can no longer properly perform their intended design function. If the thermal fatigue sensitive components can be visually inspected on a regular basis, the thermal fatigue cracks can be detected prior to the onset of catastrophic fracturing into two or more pieces. For example, thermal fatigue cracking frequently encountered in aeronautical gas turbine engine inlet guide vanes can be detected during routine inspection. If the cracks are only in the coating, the coating is stripped and the vanes are recoated and reinstalled in the engine. If cracks are deep enough and penetrate into the metal airfoil, they may be welded shut, or if quite small, may be ground and polished out. On the other hand, in certain equipment, such as a nuclear reactor in a commercial power plant, it is not always possible to inspect for thermal fatigue cracks because of radioactive contamination. Even if inspection were possible, part replacement would be prohibitive from the standpoint of the replacement part costs, and because of loss of revenue during down times. In the case of dies for high temperature die casting, thermal fatigue cracks interfere with a smooth surface on the die faces and thus produce an inferior surface finish on the cast parts. Again, replacement is expensive and the down time of the equipment is expensive in terms of lost revenue. From these examples it is seen that thermal fatigue cracking is an important engineering problem. For relatively inexpensive components that are easy to inspect and replace, the problem is simply a mild nuisance with moderate associated costs. For the large irreplaceable components, adequate thermal fatigue resistance must be designed in at the beginning. If not, the economic consequences are too great, and financial disaster would ensue.

A problem has existed over the years in documenting thermal fatigue failures of inservice components, their analyses, and their solutions. This is because few manufacturers are willing to publicly acknowledge and provide details of problems associated with their products. Nor are they interested

in giving their competition insights into their design schemes. Nevertheless, some important case histories have been published in the open literature. In this section, a representative sampling of these publications will be discussed. The principal concerns herein are for the techniques employed in predicting the thermal fatigue lives, as opposed to the techniques used for thermal and structural analyses. However, it must be emphasized that all contributing subanalyses are of extreme importance to the proper solution of the problem, and that any errors introduced by a subanalysis directly impacts the errors observed in subsequent analyses.

A block flow diagram is shown in figure 44 for an overall analysis of structural loading, thermal and structural response, material stress-strain-temperature-time response (constitutive behavior), cyclic life calculation, and comparison with service or simulated service experience. Although the diagram was created to be used in conjunction with the Strainrange Partitioning method, it is of general applicability and is valuable in pointing out the numerous aspects of a thorough thermal fatigue analysis.

By the early 1970s, high-temperature structural analyses involving creep and plasticity calculations were just beginning to become a workable tool for failure and design analyses. Similarly, high-temperature material constitutive behavior models were refined enough to permit reasonable estimates of the local cyclic stress strain response in complex shaped structural components. Consequently, the technical literature on the subject began to grow, and papers dealing with sophisticated thermal fatigue life predictions of structural components appeared. The International Conference on Creep and Fatigue in Elevated Temperature Applications (ref. 41) contained several such papers (refs. 193 and 195) of direct interest.

Before discussing four specific examples of thermal fatigue life prediction of engineering structural components, reference should be made to the 150 page manual prepared by Saugerud [196] of the Marine Technology Center of the University of Trondheim, Trondheim, Norway. Entitled, "Fatigue Life Prediction of Thermally Loaded Engine Components," it is directed specifically at internal combustion engine thermal fatigue problems. The manual is presented in an easy to follow textbook fashion and is exceptionally informative to a designer facing thermal fatigue problems in heat engines of all sorts.

A. HEAT EXCHANGER INLET NOZZLE

Gangadharan et al. (ref. 193) examined the expected thermal fatigue resistance of a primary inlet nozzle of a sodium intermediate heat exchanger. The heat exchanger was destined for the fast flux test facility which was to have been built as a part of a United States program to develop Liquid Metal Fast Breeder Reactors for electric power. The cyclic thermal history for the nozzle involved an excursion in temperature from 149 to 566 °C with a duration of approximately one week at the peak temperature. The pressure loading was constant at approximately 13 atmospheres. Results of the decoupled creep and plasticity structural analysis revealed a hysteresis loop as shown in figure 45. The inelastic strainrange was determined to be 0.29 percent. Damage during the thermal fatigue cycle was assessed using a version of the time-and cycle-fraction method that was similar to the method that had been adopted by the ASME Boiler and Pressure Vessel Code Committee at the time (Code Case 1331-4 and -5, Currently Code Case N-47-22(19)). Creep damage was found to be negligible while the fatigue damage was determined from a design

curve based upon isothermal strain cycling fatigue data generated at 538 °C for austenitic stainless steels. A life estimate of 3800 cycles to cracking was enough in excess of the desired 800 cycles of operation that the design was judged adequate to resist thermal fatigue. Both the creep-rupture curves and the fatigue curves used in the design calculations have large factors of safety built into them, so the judgement of design adequacy was likely accurate. It is in this manner that the ASME Code Case works best. The life prediction method utilizes large factors of safety to guard against the many unknowns in the problem, and as such should not be considered an accurate tool for life prediction. Instead, it permits components to be designed to have a high probability of not failing.

B. TURBINE ROTOR

Briner and Beglinger [195] presented the results of an analysis of thermal fatigue cracks that had been observed in the root attachment grooves of a large industrial gas turbine rotor. A thorough thermal analysis was made of the rotor, including the transients during heat up and cool down. Finite element techniques were used to perform an elastic structural analysis. Since a multi-axial strain state existed at the base of the groove where cracks had initiated, an equivalent total strainrange was calculated and compared to isothermal fatigue curves (with no creep) of the rotor alloy (12 percent Cr steel) at the maximum cycle temperature. The authors rationalized that this provided an upper bound on expected life of 1100 cycles. The method of Strainrange Partitioning (ref. 10) was used to estimate a lower bound life of 450 cycles. Experience had indicated cracking of the rotor after about 700 start-stop cycles. The agreement between operation and prediction was reasonable considering the numerous assumptions that were required.

C. HIGH PRESSURE TURBINE BLADE

One of the most sophisticated thermal-structural-life analyses performed up to 1983 was reported by McKnight, et al. (ref. 136) for a first-stage, high-pressure turbine blade used in the General Electric CF6 high-by-pass-ratio gas turbine engine. These analyses have been summarized by Kaufman and Halford (ref. 197). The blades are cast of the nickel-base superalloy, Rene 80, and have an aluminide coating. Versions of this engine power McDonnell-Douglas DC10 and Boeing 747 aircraft. The tips of these blades had experienced unwanted thermal fatigue cracking that was causing excessive hot gas leakage past the tip seals. This state of affairs reduced fuel efficiency at a time when fuel costs were soaring. The problem was thus an economic nuisance. Extensive thermal analyses, two- and three-dimensional structural analyses, and state-of-the-art life prediction analyses were performed. Figure 46 shows a thermal fatigue hysteresis loop for the critical location of the blade tip. It was clearly demonstrated that the problem was almost exclusively a thermal problem. The constitutive stress-strain model was the classical creep and plasticity approach in which no interaction between time-dependent and time-independent components was recognized. Two life prediction models, Frequency Modified Life (ref. 70) and Strainrange Partitioning (ref. 10), were applied. Both were evaluated using isothermal creep-fatigue properties. Despite the many necessary assumptions, the observed 3000 cycle crack initiation life was reasonably bound by calculated lives ranging between 1200 and 4420 cycles.

As a direct result of having performed this program under contract to the NASA Lewis, the General Electric Company gained enough confidence to apply similarly sophisticated analyses to numerous other turbine engine components within the hot section. Only 3 yr later, significant advances have been made in the performance of thermal analyses, transferring the thermal analyses to the structural analyses, structural analysis techniques, unified constitutive theories and life prediction. The hot section technology (HOST) program (ref. 198) of NASA-Lewis is largely responsible for instigating these advances in technology.

D. COMBUSTOR LINER

Extensive thermal/structural/life analyses have also been performed on an annular combustor liner by Moreno, Meyer, Kaufman and Halford (ref. 199). This was a parallel program to the turbine blade tip durability analysis discuss in the previous section. The hardware studied was a half-size simulated combustor liner that was otherwise identical to the liners used in Pratt and Whitney, JT9D, high-by-pass-ratio gas turbine engines.

Using induction heating and forced air cooling, temperature extremes at the edge of the Hastelloy X louver lip (where thermal fatigue cracks invariably formed) ranged between 504 and 954 °C. Cycle timing was such that 20 sec was required during heat up, 40 sec for steady state, and 30 sec for cool down. Cracking was observed after 1000 cycles of testing. Three-dimensional heat transfer analyses were matched with thermocouple outputs at known locations on the louver lip and in the colder "knuckle" region. Transient and steady state analyses were performed. The MARC general purpose finite element computer program was used to calculate structural response, and hence the cyclic stress-strain history at the critical cracking location. At the time, the best available and numerically evaluated constitutive models were based upon distinct, noninteractive, creep-plasticity equations. In fact, when used in the MARC program, it was necessary to alternatively turn on and off first the plasticity, and then the creep; the two modes of deformation could not be handled simultaneously. Now, unified constitutive models [63] are available and offer a more accurate representation of concurrent creep and plastic deformations. Stress-strain hysteresis loops for the first two thermal fatigue cycles at the edge of the louver lip are shown in figure 47. Considerable inelastic deformation was present in each cycle, giving rise to the low cycle fatigue life of 1000 cycles to crack initiation. To confirm the predicted hysteresis loop, an axial-loaded TMF specimen was programmed to follow the calculated strain-time and temperature-time history of the crack prone area. Excellent agreement was observed between the experimental TMF hysteresis loop and the analytically predicted loop. Life predictions were made by relying upon two strain based methods: Strainrange Partitioning (SRP) and the method used by Pratt and Whitney (based upon SRP concepts) in the design of commercial combustor liners. Both have their bases in isothermal methodology, and model constants were evaluated from laboratory data at the maximum temperature of the thermal fatigue cycle. Both life models over predicted the half-scale liner life by factors of between 1.7 (Pratt and Whitney Method) and 8.5 (SRP), thus suggesting that thermal strain cycling causes fatigue damage to accumulate at a higher rate than isothermal strain cycling. The Pratt and Whitney combustor design approach relies heavily upon being able to calibrate the life prediction models against actual engine durability results, thus overcoming the life prediction versus observation discrepancies of the SRP method noted above.

DOs AND DON'Ts IN DESIGN AGAINST THERMAL FATIGUE

Our state of understanding of the processes of low-cycle thermal fatigue is primarily qualitative. Quantitative understanding, while improving at a rapid rate, still does not permit us to predict thermal fatigue lives with a very high degree of accuracy. For new or different material systems, for which we have little experimental data, we cannot expect better than order-of-magnitude life estimates. For data rich alloys, it is possible to achieve better than factor-of-two life estimates under well-controlled laboratory conditions, but because of uncertainties in operating conditions, thermal and structural analyses, cyclic constitutive behavior, and life prediction models, factors of three to four are more likely for newly designed components put into service for the first time. As experience is gained and in-service thermal fatigue failures are documented and correlations established with the thermal fatigue theories and data bases, more accurate life predictions become possible. However, factors of near two or slightly better are about as accurate as can be expected, since statistical scatter in even the best of thermal fatigue results is approximately a factor of two in crack initiation life.

The bottom line analysis is that thermal fatigue life prediction for service remains, to this date, heavily tied to background service experience despite intense research activities to provide better understanding and analyses. Because of this reliance upon experience, it is appropriate to compile as many generalities as possible concerning thermal fatigue and how to ameliorate thermal fatigue problems. An important observation drawn from the summary of existing TMF and isothermal results is that isothermal low-cycle fatigue resistance measured at the maximum temperature of the TMF cycle does not provide a conservative estimate of TMF life. This is in contradiction to the major high temperature design codes such as the ASME Code Case N-47 (ref. 19). The conclusion drawn herein is certainly not new, since nearly every research paper on TMF since the very beginning [5] has drawn the same conclusions.

There are three distinct aspects to thermal fatigue problems, (1) the thermal forcing function, i.e., the thermal environmental history, (2) the geometry of the structural component with its thermal and physical properties, and finally (3) the material mechanical response to the thermal stresses and strains, i.e., the cyclic stress-strain and cracking responses.

A. THE THERMAL FORCING FUNCTION

The range of temperature, ΔT , of the environment is the most obvious variable that should be minimized to reduce thermal stress and strains, and hence improve cyclic life. While it may not be possible to alter ΔT of the thermal environment, it may be possible, for example, to preheat a component in order to cut down on the effective ΔT that the surface will experience. In this regard, it should be pointed out that the widespread practice of internal turbine airfoil cooling that has become necessary in current gas turbine engines to permit higher temperatures and more efficient combustion is intensifying the thermal fatigue environment. The increased thermal efficiencies and improvements in materials, however, have outweighed the thermal fatigue debit.

The value of the maximum temperature can also be detrimental. The higher the temperature, the poorer is the mechanical strength and fatigue resistance of most alloys (with the obvious exception of ceramic coatings and other materials that may become more ductile and hence strain resistant at the higher temperatures). Time at high temperature is also important, because it usually results in further deterioration of exposed materials. At the other temperature extreme, it is possible to encounter embrittling mechanisms in certain classes of materials and for certain environments. Embrittling regions should obviously be avoided, too, particularly if tensile stresses would be present during the time when such temperatures are encountered. The time rate of change of the environmental temperature should also be kept to a minimum to help lower the transient thermal stresses and strains. In hardware such as the Space Shuttle Main Engine (SSME), for example, the liquid oxygen/hydrogen fuel system requires start-up and shut-down sequences to occur within a matter of a second or two. Thermal gas transients on the order of 10 000 °C/sec have been inferred from limited measurements during engine firings. Once at steady state operating temperatures, the thermal gradients in SSME components such as turbine airfoils are small and resultant thermal stresses and strains are of no consequence to durability of the blades (ref. 200 and 201). If the sharp thermal transients could be avoided, thermal fatigue cracking of the airfoil sections would not be a problem.

The heat capacity (and potential for heat transfer to a solid because of density and pressure) of the thermal environment is also quite important to the problem. Reducing the rate of heat transfer across the gas/solid interface will aid in the relief of thermal fatigue problems.

The chemical reactivity of the thermal environment is also of considerable concern, since thermal fatigue is highly sensitive to the conditions at free surfaces. Oxygen in air, sulphur in the petroleum by-products of combustion, ion transport in liquid cooled systems, very high pressure hydrogen gas in oxygen/hydrogen fueled systems, etc. can severely reduce a material's thermal fatigue resistance by embrittling or otherwise disturbing the near surface layer. Surface protective coatings have been developed to help guard against such attack. However, while solving one aspect of the overall problem, they frequently introduce additional but lower priority problems, such as bonding compatibility with substrate.

B. GEOMETRY OF STRUCTURAL COMPONENTS AND THERMAL/PHYSICAL PROPERTIES

Since thermal fatigue results from the self-constraint imposed by a component subjected to alternating temperatures, those features should be avoided that promote deformation constraint at the surface location of concern. That is, a compliant structural configuration is desirable. The most obvious detrimental geometric feature is a sharp thin edge on an otherwise massive component. The edge is severely constrained due to equilibrium and compatibility requirements by the massive bulk material. In addition, such an edge has a high surface to volume ratio which means that it can absorb heat from the environment quite rapidly. It also has a reduced path through which to conduct heat to the bulk of the component. The local material therefore sees very high temperatures and very high thermal strains, thus compromising its thermal fatigue durability.

Surface finish is still another consideration, since it can dictate the nature of high velocity gas flow at the boundary layer, which in turn impacts the rate of heat transfer to and from the component. Low heat transfer coefficients are desirable in relieving the thermal fatigue problem.

A high thermal conductivity within the structural component is desirable in permitting heat to flow more rapidly, thus lowering temperature gradients and hence thermal constraint. High thermal conductivity also helps to keep the peak surface temperatures down when some form of cooling is provided to draw the heat away. While thermal conductivity is seldom considered in selecting alloys to resist thermal fatigue (because other characteristics are usually more important), there are some extreme examples whereby it is of paramount importance. The metallic liner in the main combustion chamber of the SSME, for instance, is made of a copper alloy, NARloy Z. A copper alloy was chosen because it was the only alloy known to man with a high enough melting temperature that also could conduct heat fast enough to prevent itself from melting in this particular application. This liner is highly cooled by the passage of massive amounts of cryogenic hydrogen fuel through channels imbedded within the liner wall.

Another interesting consideration involving thermal conductivity involves the design of thickwall, high-velocity (hypersonic), high-temperature nozzles, subjected to intermittent high temperature operation. A viable approach is to select an alloy with poor thermal conductivity, thus producing a steep thermal gradient at the inside hot gas wall, but a very low gradient throughout the balance of the thickness. Thermal fatigue cracks would be encouraged to form at the hot surface. Because of the rapidly decaying temperature gradient, however, the stress-strain field ahead of the crack would be so benign that the surface cracks would lack the potential driving energy to propagate into the bulk of the thickness, hence they would rather quickly arrest. The end result would be a nozzle with a highly compliant bore (due to extensive thermal fatigue cracking) and a stiff and strong outer shell. A similar condition could be designed in by intentionally slotting the bore material to a depth below the steep portion of the temperature gradient. The only potential hazard would be if cracks were to change direction and link up, causing segments of the bore material to separate and enter the high velocity gas stream. Such segments could cause damage to any models or instrumentation downstream.

Probably the most crucial material property is the coefficient of thermal expansion, α , since it influences in direct proportionality the thermal strains that are induced. Low thermal expansion coefficients are desirable. The ceramic cookware pioneered by Corning which can be thermally shocked without fear of fracture is an excellent example of designing a material with a very low coefficient of thermal expansion. Not only is α important, it can create additional problems when solids with different values of α are bonded together into a composite material. Any differential between the two coefficients of expansion will give rise to added thermal strains. A composite solid with no thermal gradients can experience large internal thermal strains due to this affect alone. The cases discussed earlier regarding thermal fatigue of coated superalloys point up the importance of designing composite systems with a minimum differential of coefficients of thermal expansion.

C. MATERIAL MECHANICAL RESPONSE CHARACTERISTICS

The principal mechanical properties of importance are the elastic constants (modulus of elasticity and Poisson's ratio), the temperature- and time-dependent flow strength in the cyclic state, ductility, fracture toughness, and the resistance to repeated stress and inelastic deformation. For elastic thermal strain response, the modulus of elasticity directly dictates the thermal stresses that develop. Thus, if it is desirable to keep the thermal stresses low, then a low modulus of elasticity is beneficial. If yielding occurs during thermal cycling, then it is desirable to have as high a yield strength as possible to minimize this inelastic component of strain. For a given amount of inelastic strain/cycle, materials with high ductility and resistance to environmental embrittlement tend to fare the best in resisting thermal fatigue failure.

When single crystal and directionally solidified alloys were being developed about two decades ago, the chief feature being claimed was that transverse grain boundaries had been eliminated. Grain boundaries had been the source of creep deformation and premature high temperature intergranular cracking. These new materials while having greater creep resistance, have nearly the same yield strengths as their polycrystalline counterparts. As it has turned out, however, they are much better in thermal fatigue resistance than polycrystalline alloys of the same basic composition. The real reason for improved thermal fatigue resistance was due to the significantly lower modulus of elasticity of the directional structure of these alloys. The low modulus cube axis of the face-centered-cubic nickel alloy is aligned with the growth direction, which is taken as the longitudinal direction of the airfoil portion of turbine blades. Because of the low modulus, almost all of the thermal strains are absorbed elastically, thus greatly reducing the amounts of inelastic strains that would have been induced in a polycrystalline alloy. Examination of figure 15 clearly shows that the directionally solidified alloys are superior in their thermal fatigue resistance to polycrystalline alloys of the same nominal composition. This conclusion applies to either coated or bare alloys.

REFERENCES

1. Duga, J.J., et al.: Fracture Costs US \$119 Billion A Year, Says Study by Battelle/NBS. *Int. J. Fract.*, vol. 23, 1983, pp. R81-R83.
2. Dennis, A.J., and Cruse, T.A.: Cost Benefits from Improved Hot Section Life Prediction Technology. AIAA Paper 79-1154, June 1979.
3. Wetenkamp, H.R.; Sidebottom, O.M.; and Schrader, H.J.: The Effect of Brake Shoe Action on Thermal Cracking and on Failure of Wrought Steel Railway Car Wheels. *Engineering Experiment Station Bulletin Series No. 387, University of Illinois Bulletin*, vol. 47, no. 77, June 1950.
4. Coffin, L.F., Jr.; and Wesley, R.P.: Apparatus for Study of Effects of Cyclic Thermal Stresses on Ductile Metals. *Trans. ASME*, vol. 76, no. 6, Aug. 1954, pp. 923-930.
5. Coffin, L.F., Jr.: A Study of the Effects of Cyclic Thermal Stresses on a Ductile Metal. *Trans., ASME*, vol. 76, no. 6, Aug. 1954, pp. 931-950.
6. Manson, S.S.: *Thermal Stress and Low-Cycle Fatigue*, McGraw-Hill, New York, 1966, p. 194.
7. Manson, S.S.: Fatigue: A Complex Subject-Some Simple Approximations. *Exp. Mech.*, vol. 5, no. 7, July, 1965, pp. 193-226.
8. Manson, S.S.; and Halford, G.R.: A Method of Estimating High-Temperature Low-Cycle Fatigue Behavior of Materials. *Thermal and High-Strain Fatigue, Metals and Metallurgy Trust*, London, 1967, pp. 154-170.
9. Manson, S.S.; Halford, G.R.; and Spera, D.A.: The Role of Creep in High Temperature Low-Cycle Fatigue. *Advances in Creep Design*, A. I. Smith and A. M. Nicolson, eds., Halsted Press, 1971, pp. 229-249.
10. Manson, S.S.; Halford, G.R.; and Hirschberg, M.H.: Creep-Fatigue Analysis by Strain-Range Partitioning. *Design for Elevated Temperature Environment*, S.Y. Zamrik, ed., ASME, 1971, pp. 12-28.
11. Manson, S.S.: *Thermal Stress and Low-Cycle Fatigue*, McGraw-Hill, 1966.
12. Glenny, R.J.E.: Thermal Fatigue. *High-Temperature Materials in Gas Turbines*, P.R. Sahm and M.O. Speidel, eds. Elsevier, Amsterdam, 1974, pp. 257-281.
13. Spera, D.A.: What is Thermal Fatigue? *Thermal Fatigue of Materials and Components*, D.A. Spera and D.F. Mowbray, eds., ASTM STP-612, ASTM, 1976, pp. 3-9.
14. Majors, H., Jr.: Thermal Shock and Fatigue--A Literature Survey. Technical Report No. 1, Bureau of Engineering Research, University of Alabama, Sept. 1956.

15. Swindeman, R.W.; and Douglas, D.A.: The Failure of Structural Metals Subjected to Strain-Cycling Condition. *J. Basic Eng.*, vol. 81, no. 2, June 1959, pp. 203-212.
16. Taira, S.: Lifetime of Structures Subjected to Varying Load and Temperature. *Creep in Structures*, N. J. Hoff, ed., Academic Press, 1962, pp. 96-124.
17. Robinson, E.L.: Effect of Temperature Variation on the Long-Time Strength of Steels. *Trans. ASME*, vol. 74, no. 5, July 1952, pp. 777-781.
18. Spera, D.A.: A Linear Creep Damage Theory for Thermal Fatigue of Materials. Doctoral Thesis, University of Wisconsin, 1968.
19. Boiler and Pressure Vessel Piping Code Case N-47-22, Section III, Nuclear Components, ASME, New York City, NY, 1983.
20. Benham, P.P.: Fatigue of Metals Caused by Relatively Few Cycles of High Load or Strain Amplitude. *Metall. Rev.*, vol. 3, no. 11, 1958, pp. 203-234.
21. Benham, P.P.: Axial-Load and Strain-Cycling Fatigue of Copper at Low Endurance. *J. Inst. Met.*, vol. 89, 1961, pp. 328-338.
22. Benham, P.P.: Low Endurance Fatigue. *Thermal Stress*, P.P. Benham and R. Hoyle, eds., Sir Isaac, Pitman & Sons, 1964, pp. 163-181.
23. Glenny, E., et al.: A Technique for Thermal-Shock and Thermal-Fatigue Testing, Based on the Use of Fluidized Solids. *J. Inst. Met.*, vol. 87, 1958-59, pp. 294-302.
24. Glenny, E.; and Taylor, T.A.: A Study of the Thermal-Fatigue Behaviour of Metals: The Effect of Test Conditions on Nickel-Base High-Temperature Alloys. *J. Inst. Met.*, vol. 88, 1959-60, pp. 449-461.
25. Howes, M.A.H.: Evaluation of Thermal Fatigue Resistance of Metals Using the Fluidized Bed Technique. *Fatigue at Elevated Temperatures*, A.E. Carden, A.J. McEvily and C.H. Wells, eds., ASTM STP-520, ASIM, 1973, pp. 242-254.
26. Forrest, P.G.; and Penfold, A.B.: New Approach to Thermal Fatigue Testing. *Engineering (London)*, vol. 192, no. 4983, Oct. 20, 1961, pp. 522-523.
27. Thielsch, H.: Thermal Fatigue and Thermal Shock. *Weld. Res. Council Bull.*, no. 10, Apr. 1952.
28. Miller, D.R.: Bibliography on Thermal Stresses and Low-Cycle Fatigue. KAPL-2048, Knolls Atomic Power Laboratory, Aug. 1959.
29. Glenny, E.: Thermal Fatigue. *Metall. Rev.*, vol. 6, no. 24, 1961, pp. 387-465.
30. Yen, T.C.: Thermal Fatigue--A Critical Review. *Weld. Res. Council Bull.*, No. 72, October 1961.

31. Akimov, L.M.; and Sklyarov, N.M.: Investigation Methods for Thermal Stability of Heat-Resistant Alloys. *Termostoikost Zharoprochynykh Splavov*, Sbornik State1, Moscow, 1962, pp. 5-52. (in Russian)
32. Gusenkov, A.P.; and Kotov, P.I.: Low-Cycle Fatigue Under Nonisothermal Loading. *Izdatel'stvo Mashinostroenie*, Moscow, 1983. (in Russian).
33. Carden, A.E.: An Abstracted Bibliography of the Thermal Fatigue Literature for the Years 1954-1963. Memorandum Report No. 26, Bureau of Engineering Research, University of Alabama, Apr. 1964.
34. Baron, H.G.: Thermal Shock and Thermal Fatigue. *Thermal Stress*, P.P. Benham and R.D. Hoyle, eds., Pitman, London, 1964, pp. 182-206.
35. Freudenthal, A.M.; Boley, B.A.; and Liebowitz, H.; eds.: *High Temperature Structures and Materials*, Pergamon Press, 1964.
36. Joint International Conference on Creep, Proc. I. Mech. Eng., vol. 178, part 3A, Institution of Mechanical Engineers, London, 1965.
37. *Thermal and High-Strain Fatigue*, Monograph and Report Series No. 32, The Institute of Metals, London, 1967.
38. Littler, D.J., ed.: *Thermal Stresses and Thermal Fatigue*, Butterworths, London, 1969.
39. Zamrik, S.Y., ed.: *Symposium on Design for Elevated Temperature Environment*, American Society of Mechanical Engineers, New York, 1971.
40. Carden, A.E.; McEvily, A.J.; and Wells, C.H.; eds.: *Fatigue at Elevated Temperatures*, ASTM STP-520, ASTM, 1973.
41. *Creep and Fatigue in Elevated Temperature Applications*, Institution of Mechanical Engineers, London, 1974.
42. Sahm, P.R.; and Speidel, M.O.; eds.: *High-Temperature Materials in Gas Turbines*, Elsevier, 1974.
43. Coffin, L.F., Jr., et al.: *Time-Dependent Fatigue of Structural Alloys - A General Assessment (1975)*, ORNL-5073, Oak Ridge National Laboratories, 1977.
44. Spera, D.A.; and Mowbray, D.F.: *Thermal Fatigue of Materials and Components*, ASTM STP-612, American Society for Testing and Materials, 1976.
45. Curren, R.M., ed.: *1976 ASME-MPC Symposium on Creep-Fatigue Interaction*, American Society of Mechanical Engineers, 1976.
46. Bathgate, R.G., ed.: *Fatigue Testing and Design*, Society of Environmental Engineers, Havant, England 1976.
47. Cruse, T.A.; and Gallagher, J.P., eds.: *Fatigue Life Technology*, American Society of Mechanical Engineers, 1977.

48. Louthan, M.R.; and McNitt, R.P.; eds.: Environmental Degradation of Engineering Materials, Blacksburg, VA, 1977, Virginia Tech Printing Department, Blacksburg, VA, 1977.
49. Coutsouradis, D.; et al.: High Temperature Alloys for Gas Turbines, Applied Science Publishers, London, 1978.
50. Characterization of Low Cycle High Temperature Fatigue by the Strain-range Partitioning Method, AGARD CP-243, Advisory Group for Aerospace Research and Development, France, 1978.
51. Ostergren, W.J.; and Whitehead, J.R., eds.: Methods for Predicting Material Life in Fatigue, American Society of Mechanical Engineers, 1979.
52. Burke, J.J.; and Weiss, V., eds.: Fatigue, Environment and Temperature Plenum Press, 1983.
53. Wells, C.H., ed.: Analysis of Life Prediction Methods for Time-Dependent Fatigue Crack Initiation in Nickel-Base Superalloys, NMAB-347, National Materials Advisory Board, Washington, D.C., 1980.
54. Wilshire, B.; and Owen, D.R.J., eds.: Creep and Fracture of Engineering Materials and Structures, Pineridge Press, Swansea, U.K., 1981.
55. Zamrik, S.Y.; and Dietrich, D., eds.: Pressure Vessels and Piping: Design Technology - 1982 - A Decade of Progress, American Society of Mechanical Engineers, 1982.
56. Baylac, G., ed.: Inelastic Analysis and Life Prediction in Elevated Temperature Design, Orlando, American Society of Mechanical Engineers, 1982.
57. Brunetaud, R., et al., eds.: High Temperature Alloys for Gas Turbines, D. Reidel Publishing Co., 1982.
58. Woodford, D.A.; and Whitehead, J.R., eds.: ASME International Conference on Advances in Life Prediction Methods, American Society of Mechanical Engineers, 1983.
59. Jaske, C.E.; Hudak, S.J.; Jr.; and Mayfield, M.E.; eds.: Thermal and Environmental Effects in Fatigue: Research - Design Interface, American Society of Mechanical Engineers, 1983.
60. Wilshire, B.; and Owen, D.R.J., eds.: Proceedings of the Second International Conference on Creep and Fracture of Engineering Materials and Structures, Pineridge Press, Swansea, U.K., 1984.
61. Beevers, C.J., ed.: Fatigue 84, Engineering Materials Advisory Services Ltd., West Midlands, U.K., 1984.
62. Laflen, J.H.; and Cook, T.S.: Equivalent Damage: A Critical Assessment. (R82-AEG533, General Electric Co.; NASA Contract NAS3-22534) NASA CR-167874, 1982.

63. Kaufman, A.; Laflen, J.H.; and Lindholm, U.S.: Unified Constitutive Material Models for Nonlinear Finite-Element Structural Analysis. AIAA Paper 85-1418, July, 1985.
64. McDowell, D.L.: Transient Nonproportional Cyclic Plasticity. Design and Materials Division Report No. 107, UILU-ENG 83-4003, Dept. of Mech. and Ind. Engineering, University of Illinois, Urbana, June 1983.
65. Robinson, D.N.; and Bartolatta, P.A.: Viscoplastic Constitutive Relationships with Dependence on Thermomechanical History. NASA CR-174836, 1985.
66. Taira, S.; and Inoue, T.: Thermal Fatigue Under Multiaxial Thermal Stresses. Thermal Stresses and Thermal Fatigue, D.J. Littler, ed., Butterworths, London, 1969, Paper No. 3.
67. Moreno, V.; Nissley, D.; and Liu, L.S.: Creep Fatigue Life Prediction for Engine Hot Section Materials (Isotropic). (PWA-5894-34, Pratt and Whitney Aircraft; NASA Contract NAS3-23288) NASA CR-174844, 1985.
68. Tavernelli, J.F.; and Coffin, L.F., Jr.: A Compilation and Interpretation of Cyclic Strain Fatigue Tests on Metals. Trans. ASM, vol. 51, 1959, pp. 438-453.
69. Halford, G.R.; Saltsman, J.F.; and Hirschberg, M.H.: Ductility Normalized-Strainrange Partitioning Life Relations for Creep-Fatigue Life Prediction. Environmental Degradation of Engineering Materials, M.R., Louthan Jr. and R.P. McNitt, eds., Virginia Tech. Printing Dept., Blacksburg, VA, 1977, pp. 599-612.
70. Coffin, L.F., Jr.: The Effect of Frequency on High-Temperature, Low-Cycle Fatigue. Proceedings of the Air Force Conference on Fracture and Fatigue of Aircraft Structures, AFFDL-TR-70-144, 1970, pp. 301-312.
71. Ostergren, W.J.: Damage Function and Associated Failure Equations for Predicting Hold Time and Frequency Effects in Elevated Temperature, Low Cycle Fatigue. J. Test. Eval., vol. 4, no. 5, Sept. 1976, pp. 327-339.
72. Coffin, L.F.: The Concept of Frequency Separation in Life Prediction for Time-Dependent Fatigue. 1976, ASME-MPC Symposium on Creep-Fatigue Interaction, R.M. Curran, ed., 1976, pp. 349-363.
73. Halford, G.R.; Hirschberg, M.H.; and Manson, S.S.: Temperature Effects on the Strainrange Partitioning Approach for Creep-Fatigue Analysis. Fatigue at Elevated Temperatures, A.E. Carden, A.J. McEvily and C.H. Wells, eds., ASTM STP-520, ASTM, 1973, pp. 658-669.
74. Morrow, J.: Fatigue Properties in Metals. Section 3.2, Fatigue Design Handbook, J.A. Graham, ed., SAE, 1968, pp. 21-29.
75. Halford, G.R.; and Nachtigall, A.J.: Strainrange Partitioning Behavior of an Advanced Gas Turbine Disk Alloy AF2-10A. J. Aircr., vol. 17, no. 8, Aug. 1980, pp. 598-604.

76. Manson, S.S.: Thermal Stresses in Design, Part 20 - Thermal Cycling with Steady Stress. Mach. Des., vol. 32, July 21, 1960, pp. 161-167.
77. Zamrik, S.Y.; and Billir, O.G.: Analysis of Biaxial-Fatigue Damage at Elevated Temperatures. Exp. Mech., vol. 16, no. 10, Oct. 1976, pp. 373-379.
78. Socie, D.F., et al.: Observations of Small Cracks in Biaxial Fatigue. Fatigue 84, vol. 2, C.J. Beevers, ed., Engineering Materials Advisory Services Ltd., West Midlands, U.K., 1984.
79. Jordan, E.H.: Elevated Temperature Biaxial Fatigue. NASA CR-175795, 1984.
80. Bannantine, J.; and Socie, D.F.: Observations of Cracking Behavior in Tension and Torsion Low Cycle Fatigue. Presented at the Symposium on Low Cycle Fatigue - Directions for the Future, ASTM, Bolton Landing, New York, Sept. 30-Oct. 4, 1985.
81. Leverant, G.R.; Strangman, T.E.; and Langer, B.S.: Parameters Controlling the Thermal Fatigue Properties of Conventionally-Cast and Directionally-Solidified Turbine Alloys. Superalloys: Metallurgy and Manufacture, B.H. Kear, et al. eds., Claitor's Publishing Division, Baton Rouge, 1976, pp. 285-295.
82. Bill, R.C., et al.: Preliminary Study of Thermomechanical Fatigue of Polycrystalline MAR-M 200. NASA TP-2280, 1984.
83. Rau, C.A., Jr.; Gemma, A.E.; and Leverant, G.R.: Thermal-Mechanical Fatigue Crack Propagation in Nickel- and Cobalt-Base Superalloys Under Various Strain-Temperature Cycles. Fatigue at Elevated Temperatures, ASTM STP-520, A.E. Carden, A.J. McEvily and C.H. Wells, eds., ASTM, 1973, pp. 166-178.
84. Gemma, A.E.; Langer, B.S.; and Leverant, G.R.: Thermomechanical Fatigue Crack Propagation in an Anisotropic (Directionally Solidified) Nickel-Base Superalloy. Thermal Fatigue of Materials and Components, ASTM STP-612, D. A. Spera and D. F. Mowbray, eds., ASTM, 1976, pp. 199-213.
85. Meyers, G.J.: Fracture Mechanics Criteria for Turbine Engine Hot Section Components, (PWA-5772-23, United Technologies Corp.; NASA Contract NAS3-22550) NASA CR-167896, 1982.
86. Marchand, N.; and Pelloux, R.M.: Thermal-Mechanical Fatigue Crack Growth in Inconel X-750. NASA CR-174740, 1984.
87. Blackburn, W.S.: Path Independent Integrals to Predict Onset of Crack Instability In An Elastic Plastic Material. Int. J. Fract. Mech., vol. 8, 1972, pp. 343-346.
88. Ainsworth, R.A.; Neale, B.K.; and Price, R.H.: Fracture Behavior in the Presence of Thermal Strains. Tolerance of Flaws in Pressurized Components, Mechanical Engineering Publications, London, 1978, pp. 171-178.

89. Kishimoto, K.; Aoki, S.; and Sakata, M.: On the Path-Independent Integral-J. Eng. Fract. Mech., vol. 13, no. 4, 1980, pp. 841-850.
90. Atluri, S.N.; Nishioka, T.; and Nakagaki, M.: Incremental Path-Independent Integrals in Inelastic and Dynamic Fracture Mechanics. Eng. Fract. Mech., vol. 20, no. 2, 1984, pp. 209-244.
91. Gemma, A.E.; Ashland, F.X.; and Masci, R.M.: The Effects of Stress Dwells and Varying Mean Strain on Crack Growth During Thermal Mechanical Fatigue, J. Test. Eval., vol. 9, no. 4, July 1981, pp. 209-215.
92. Okazaki, M.; and Koizumi, T.: Crack Propagation During Low Cycle Thermal-Mechanical and Isothermal Fatigue at Elevated Temperatures. Metall. Trans. A., vol. 14A, no. 8, Aug. 1983, pp. 1641-1648.
93. Liu, H.W.; and Oshida, Y.: Literature Survey on Oxidations and Fatigue Lives at Elevated Temperatures. NASA CR-174639, 1984.
94. Miller, R.A.; and Lowell, C.E.: Failure Mechanisms of Thermal Barrier Coatings Exposed to Elevated Temperatures. Thin Solid Films, vol. 95, 1982, pp. 265-273.
95. Liebert, C.H.; and Miller, R.A.: Ceramic Thermal Barrier Coatings. Ind. Eng. Chem. Prod. Res. Dev., vol. 23, no. 3, Sept. 1984, pp. 344-349.
96. Strangman, T.E.: Thermal Fatigue of Oxidation Resistant Overlay Coatings for Superalloys. PhD Thesis, University of Connecticut, 1978.
97. Strangman, T.E.; and Hopkins, S.W.: Thermal Fatigue of Coated Superalloys. Am. Ceram. Soc. Bull., vol. 55, no. 3, Mar. 1976, pp. 304-307.
98. Warren, R., et al.: Thermal Cycling of W-Wire Reinforced Metal Matrix Composites, Progress in Science and Engineering of Composites, T. Hayashi, K. Kawata and S. Umekawa, eds., Japan Society for Composite Materials, Tokyo, 1982, pp. 1419-1426.
99. Hirschberg, M.H.: Elevated Temperature Fatigue Testing of Metals. Fatigue Test Methodology, AGARD LS-118, Advisory Group For Aerospace Research and Development, France, 1981, pp. 7-1 to 7-18.
100. Lampson, F.K.; Tsareff, T.C., Jr.; and Green, A.W.F.: Thermal Shock Testing Under Stress of Certain High Temperature Alloys. Proc. Am. Soc. Test. Mater., vol. 57, 1957, pp. 965-976.
101. Mowbray, D.F.; and Woodford, D.A.: Observations and Interpretations of Crack Propagation Under Conditions of Transient Thermal Strain. Creep and Fatigue in Elevated Temperature Applications, Institution of Mechanical Engineers, London, 1974, pp. 179-1 to 179-11.
102. Bizon, P.T.; and Spera, D.A.: Thermal-Stress Fatigue Behavior of Twenty-Six Superalloys. Thermal Fatigue of Materials and Components, ASTM STP-612, D.A. Spera and D.F. Mowbray, eds., ASTM, 1976, pp. 106-122.

103. Bizon, P.T., et al.: Three-Dimensional Finite-Element Elastic Analysis of a Thermally Cycled Single-Edge Wedge Geometry Specimen. NASA TM-79026, 1979.
104. Kamachi, K., et al.: Thermal Fatigue Test by Direct Passage Method of Large Electric Current on Stainless Steels. Mechanical Behavior of Materials -- IV, vol. 1, J. Carlsson and N.G. Ohlson, eds., Pergamon Press, Oxford, 1984, pp. 175-182.
105. Radeker, W.: Stahl u. Eisen, vol. 75, 1955, p. 1252.
106. Spera, D.A.; Calfo, F.D.; and Bizon, P.T.: Thermal Fatigue Testing of Simulated Turbine Blades. SAE Paper 710459, May 1971.
107. Humphreys, V.E.: Thermal Fatigue and Oxidation Data for Coating Variations of Army Helicopter Engine Materials. NASA CR-(in-press), IITRI-M6001-107, 1985.
108. Hofer, K.E.; and Humphreys, V.E.: Thermal Fatigue and Oxidation Data of TAZ-8A and M22 Alloys and Variations. (IITRI-M6001-89, IIT Research Institute; NASA Contract NAS3-17787) NASA CR-165407, 1981.
109. Hofer, K.E.; Hill, V.L.; and Humphreys, V.E.: Thermal Fatigue and Oxidation Data of Oxide Dispersion-Strengthened Alloys. (IITRI-M6001-82, IIT Research Institute; NASA Contract NAS3-17787) NASA CR-159842, 1980.
110. Hill, V.L.; and Humphreys, V.E.: Thermal Fatigue and Oxidation Data of Superalloys Including Directionally Solidified Eutectics. (IITRI-B6124-48, IIT Research Institute; NASA Contract NAS3-17787) NASA CR-135272, 1977.
111. Hill, V.L.; and Humphreys, V.E.: Thermal Fatigue and Oxidation Data for Alloy/Braze Combinations. (IITRI-B6134-25, IIT Research Institute; NASA Contract NAS3-18942) NASA CR-135299, 1977.
112. Hill, V.L.; and Humphreys, V.E.: Thermal Fatigue and Oxidation Data for Directionally Solidified MAR-M 246 Turbine Blades. (IITRI-M6003-53, IIT Research Institute; NASA Contract NAS3-19696) NASA CR-159798, 1980.
113. Humphreys, V.E.; and Hofer, K.E.: Thermal Fatigue Performance of Integrally Cast Automotive Turbine Wheels. (IITRI-M06003-54, IIT Research Institute; NASA Contract NAS3-19696) NASA CR-165227, 1980.
114. Solomon, H.D.: Low Frequency, High Temperature Low Cycle Fatigue of Solders. Presented at the ASTM Symposium on Low Cycle Fatigue --- Directions for the Future, Bolton Landing, New York, Sept. 30-Oct. 4, 1985.
115. Shine, M.C.; Fox, L.R.; and Sofia, J.W.: Fatigue of Solder Joints in Surface Mounted Devices. Presented at the ASTM Symposium on Low Cycle Fatigue --- Directions for the Future, Bolton Landing, New York, Sept. 30-Oct. 4, 1985.

116. Lake, J.K.; and Wild, R.N.: Some Factors Affecting Leadless Chip Carrier Solder Joint Fatigue Life. *Materials and Processes-Continuing Innovations*, SAMPE, 1983, pp. 1406-1424.
117. Rauschenbach, H.S.: *Electrical Elements, Solar Cell Array Design Handbook*, Rauschenbach Van Norstrand Reinhold Co., New York, 1980, p. 270.
118. Hopkins, S.W.: *Low-Cycle Thermal Mechanical Fatigue Testing. Thermal Fatigue of Materials and Components*, ASTM STP-612, D.A. Spera and D.F. Mowbray, eds., ASTM, 1976, pp. 157-169.
119. Kuwabara, K.; Nitta, A.; and Kitamura, T.: *Thermal-Mechanical Fatigue Life Prediction in High-Temperature Component Materials for Power-Plant. Advances in Life Prediction Methods*, D.A. Woodford and J.R. Whitehead, eds., ASME, 1983, pp. 131-141.
120. Jaske, C.E.: *Thermal-Mechanical, Low-Cycle Fatigue of AISI 1010 Steel. Thermal Fatigue of Materials and Components*, ASTM STP-612, D.A. Spera and D.F. Mowbray, eds., ASTM, 1976, pp. 170-198.
121. Westwood, H.J.; and Lee, W.K.: *Creep-Fatigue Crack Initiation in 1/2 Cr-Mo-V Steel. Creep and Fracture of Engineering Materials and Components*, B. Wilshire and D.R.J. Owen, eds., Pineridge Press, Swansea, U.K., 1981, pp. 517-530.
122. Taira, S.; Fujino, M.; and Ohtani, R.: *Collaborative Study on Thermal Fatigue Properties of High Temperature Alloys in Japan, Fatigue of Engineering Materials and Structures*, vol. 1, no. 4, 1979, pp. 495-508.
123. Fujino, M.: *The Role of Cyclic Temperature on Failure Mechanisms of Low Cycle Fatigue of Steels. PhD Thesis, Department of Mechanical Engineering, Kyoto University, Kyoto, Japan, 1975.*
124. Udoguchi, T.; and Wada, T.: *Thermal Effect on Low-Cycle Fatigue Strength of Steels, Thermal Stresses and Thermal Fatigue*, D.J. Littler, ed., Butterworths, London, 1969, pp. 109-123.
125. Sandstrom, R., et al.: *Crack Initiation and Growth during Thermal Fatigue of Aluminum Caster Shells, Scand. J. Metall.*, vol. 12, no. 3, 1983, pp. 99-106.
126. Taira, S.; Fujino, M.; and Haji, T.: *A Method for Life Prediction of Thermal Fatigue by Isothermal Fatigue Testing. Mechanical Behavior of Materials*, The Society of Materials Science, Kyoto, Japan, 1974, pp. 257-264.
127. Carden, A.E.; and Sodergren, J.H.: *The Failure of 304 Stainless Steel by Thermal Strain Cycling at Elevated Temperature. ASME Paper 61-WA-200, Dec. 1961.*
128. Stentz, R.H.; Berling, J.T.; and Conway, J.B.: *A Comparison of Combined Temperature and Mechanical Strain Cycling Data with Isothermal Fatigue Results, 1st International Conference on Structural Mechanics in Reactor Technology, Berlin, 1971.*

129. Westwood, H.J.: High Temperature Fatigue of 304 Stainless Steel under Isothermal and Thermal Cycling Conditions. *Fracture 77-Advances in Research on the Strength and Fracture of Materials*, D.M.R. Taplin, ed., Pergamon, 1978, pp. 755-765.
130. Saltsman, J.F.; and Halford, G.R.: Application of Strainrange Partitioning to the Prediction of Creep-Fatigue Lives of AISI Types 304 and 316 Stainless Steel. *J. Pressure Vessel Technol.*, vol. 99, no. 2, May, 1977, pp. 264-271.
131. Halford, G.R.; and Manson, S.S.: Life Prediction of Thermal-Mechanical Fatigue Using Strainrange Partitioning. *Thermal Fatigue of Materials and Components*, ASTM STP-612, D.A. Spera and D.F. Mowbray, eds., ASTM, 1976, pp. 239-254.
132. Carden, A.E.: Thermal Fatigue of a Nickel-Base Alloy. *J. Basic Eng.* vol. 87, no. 1, Mar. 1965, pp. 237-244.
133. Kaufman, A.; and Halford, G.R.: Engine Cyclic Durability by Analysis and Material Testing. *Engine Cyclic Durability by Analysis and Testing*, AGARD CP-368, AGARD France, 1984, pp. 12-1 to 12-12.
134. Vogel, W.H.; and Carden, A.E.: Thermal Mechanical Fatigue of Some Superalloys, ASM Paper C7-21.3, Presented at ASM National Metal Congress, Cleveland, OH, Oct. 16-19, 1967.
135. Ostergren, W.J.; and Embley, G.T.: Mechanical Property Requirements for Hot Section Components of Gas Turbines. Presented at 2nd Conference on Advanced Materials for Alternate Fuel Capable Heat Engines, Monterey, CA, 1981.
136. McKnight, R.L., et al.: Turbine Blade Nonlinear Structural and Life Analysis, *J. Aircr.*, vol. 20, no. 5, May, 1983, pp. 475-480.
137. Sheinker, A.A.: Exploratory Thermal-Mechanical Fatigue Results for Rene' 80 in Ultrahigh Vacuum. (TRW ER-8028, TRW Inc.; NASA Contract NAS3-21019) NASA CR-159444, 1978.
138. Cook, T.S.; and Laflen, J.H.: Considerations for Damage Analysis of Gas Turbine Hot Section Components. ASME Paper 84-PVP-77, June 1984.
139. Tilly, G.P.: Laboratory Simulation of Thermal Fatigue Experienced by Gas Turbine Blading. *Thermal Stresses and Thermal Fatigue*, D.J. Littler, ed., Butterworths, London, 1969, Paper No. 11.
140. Bill, R.C., et al.: Preliminary Study of Thermomechanical Fatigue of Polycrystalline MAR-M 200. NASA TP 2280, 1984.
141. Lindholm, U.S.; and Davidson, D.L.: Low-Cycle Fatigue with Combined Thermal and Strain Cycling. *Fatigue at Elevated Temperatures*, ASTM STP-520, A.E. Carden, A.J. McEvily and C.H. Wells, eds., ASTM, 1973., pp. 473-481.

142. Bashunin, A.I.; and Kotov, P.I.: Method of Investigating the Rules of Deformation and Failure under Conditions of Low-Cycle Nonisothermal Loading. Ind. Lab. (Engl. Transl.), vol. 48, no. 12, June, 1983, pp. 1216-1219.
143. Rezaei-Aria, F., et al.: Thermal Fatigue Behavior of MAR M509 Superalloy. Mechanical Behavior of Materials --- IV, vol. 1, J. Carlsson and N.G. Ohlson, eds., Pergamon Press, Oxford, 1983, pp. 247-253.
144. Sheffler, K.D.: The Partitioned Strainrange Fatigue Behavior of Coated and Uncoated MAR-M 302 at 1000°C (1832°F) in Ultrahigh Vacuum. (TRW ER-7723, TRW Inc.; NASA Contract NAS3-17786) NASA CR-134626, 1974.
145. Conway, J.B.; Stentz, R.H.; and Berling, J.T.: High Temperature, Low-Cycle Fatigue of Copper-Base Alloys in Argon; Part III - Zirconium Copper; Thermal-Mechanical Strain Cycling, Hold-Time and Notch Fatigue Results. (MTI-R003-2-3, Mar-Test Inc.; NASA Contract NAS3-16753) NASA CR-121261, 1973.
146. Sheffler, K.D.; and Doble, G.S.: Influence of Creep Damage on the Low Cycle Thermal-Mechanical Fatigue Behavior of Two Tantalum Base Alloys. (TRW ER-7592, TRW Inc.; NASA Contract NAS3-13228) NASA CR-121001, 1972.
147. Koizumi, T.; and Okazaki, M.: Crack Growth and Prediction of Endurance in Thermal-Mechanical Fatigue of 12 Cr-Mo-V-W Steel. Fatigue Eng. Mater. Struct., vol. 1, no. 4, 1979, pp. 509-520.
148. Taira, S.; Fujino, M.; and Maruyama, S.: Effects of Temperature and the Phase Between Temperature and Strain on Crack Propagation in a Low Carbon Steel During Thermal Fatigue. Mechanical Behavior of Materials, Society of Materials Science, Kyoto, Japan, 1974, pp. 515-524.
149. Sheffler, K.D.: Vacuum Thermal-Mechanical Fatigue Testing of Two Iron Base High Temperature Alloys. (TRW ER-7697, TRW Inc.; NASA Contract NAS3-6010) NASA CR-134524, 1974.
150. Halford, G.R., et al.: Bi-Thermal Fatigue - A Link Between Isothermal and Thermomechanical Fatigue, Presented at the ASTM Symposium on Low Cycle Fatigue - Directions for the Future. Bolton Landing, NY, Sept. 30 - Oct. 4, 1985.
151. Halford, G.R.; Manson, S.S.; and Hirschberg, M.H.: Temperature Effects on the Strainrange Partitioning Approach for Creep Fatigue Analysis. Fatigue at Elevated Temperatures, ASTM STP-520, A.E. Carden, A.J. McEvily, and C.H. Wells, eds., ASTM, 1972, pp. 658-667.
152. Taira, S.: Lifetime of Structures Subjected to Varying Load and Temperature. Creep in Structures, N.J. Hoff, ed., Academic Press, 1962, pp. 96-124.
153. LeMaitre, J.; Chaboche, J-L.; and Munakata, Y.: Method of Metal Characterization for Creep and Low Cycle Fatigue Prediction in Structures - Example of Udimet 700. Mechanical Behavior of Materials, Kyoto, Society of Materials Science, Kyoto, Japan, 1973, pp. 239-249.

154. Manson, S.S.: Observations and Correlations Emphasizing Wave Shape and Other Salient Features, Time-Dependent Fatigue of Structural Alloys, A General Assessment (1975), ORNL-5073, L.F. Coffin Jr., et al., eds, Oak Ridge National Laboratories, 1977, pp. 155-332.
155. Manson, S.S.: A Critical Review of Predictive Methods for Treatment of Time-Dependent Metal Fatigue at High Temperatures. Pressure Vessels and Piping: Design Technology - 1982 - A Decade of Progress, S.Y. Zamrik and D. Dietrich, eds., ASME, New York, 1982, pp. 203-225.
156. Coffin, L.F., Jr.: Observations and Correlations Emphasizing Frequency and Environmental Effects. Time-Dependent Fatigue of Structural Alloys, A General Assessment (1975), ORNL-5073, L.F. Coffin Jr., et al., eds., Oak Ridge National Laboratories, 1977, pp. 37-153.
157. Coffin, L.F.: A Review of Fatigue Predictive Methods in the Regime Where Inelastic Strains Dominate. Methods for Predicting Material Life in Fatigue, W.J. Ostergren and J.R. Whitehead, eds., ASME, 1979, pp. 1-24.
158. Lundberg, L.; and Sanderstrom, R.: Application of Low Cycle Fatigue Data to Thermal Fatigue Cracking, Scand. J. Metall., vol. 11, no. 2, 1982, pp. 85-104.
159. Miller, D.A.; Priest, R.H.; and Ellison, E.G.: A Review of Material Response and Life Prediction Techniques under Fatigue-Creep Loading Conditions. High Temp. Mater. Processes, vol. 6, no. 3-4, 1984, pp. 155-194.
160. Chen, W.C.: A Literature Review on Fatigue and Creep Interaction. (MTS-HWL-4116-776, Syracuse Univ.; NASA Grant NGR-33-022-157), NASA CR-135305, 1977.
161. Low Cycle Fatigue. Metals Handbook, Ninth Edition, vol. 3, ASM, 1980, pp. 235-237.
162. Nazmy, M.Y.; and Wuthrich, C.: The Predictive Capability of Three High Temperature Low Cycle Fatigue Models in the Alloy IN-738. Mechanical Behavior of Materials --- IV, vol. 1, J. Carlsson and N.G. Ohlson, eds., Pergamon Press, Oxford, 1984, pp. 183-189.
163. Cailletaud, C., et al.: A Review of Creep-Fatigue Life Prediction Methods. Proceedings of the 7th International Seminar on Computational Aspects of the Finite Element Method (CAFEM-7), J.F. Gloudeman, et al., eds., ONERA TP 1983-122, 1983.
164. Radhakrishnan, V.M.: An Assessment of Time Dependent Fatigue Life. SAMPE Q., vol. 15, no. 1, Oct. 1983, pp. 45-50.
165. Bernstein, H.L.: An Evaluation of Four Current Models to Predict the Creep-Fatigue Interaction in Rene' 95. AFML-TR-79-4075, Wright-Patterson Airforce Base, 1979 (AD-A077168).

166. Batte, A.D.: Creep-Fatigue Life Predictions. Fatigue at High Temperature, R.P. Skelton, ed., Applied Science Publishers, London, 1983, pp. 365-401.
167. Manson, S.S.: Behavior of Materials Under Conditions of Thermal Stress. NACA TN-2933, 1953.
168. Morrow, J.: An Investigation of Plastic Strain Energy as a Criterion for Finite Fatigue Life. Garrett Corp., Phoenix, AZ., Aug. 1960.
169. Manson, S.S.: Thermal Stress in Design, Part 19, Cyclic Life of Ductile Materials. Mach. Des., vol. 32, pp. 139-144, July 7, 1960.
170. Tomkins, B.: Fatigue Crack Propagation--An Analysis. Philos. Mag., vol. 18, no. 155, Nov. 1968, pp. 1041-1066.
171. Berling, J.T.; and Conway, J.B.: A New Approach to the Prediction of Low-Cycle Fatigue Data. Metall. Trans., vol. 1, no. 4, Apr. 1970, pp. 805-809.
172. Ellis, J.R.; and Esztergar, E.P.: Considerations of Creep-Fatigue Interaction in Design Analysis. Design for Elevated Temperature Environment, S.Y. Zamrik, ed., ASME, 1971, pp. 29-43.
173. Lagneborg, R.; and Attermo, R.: The Effect of Combined Low-Cycle Fatigue and Creep on the Life of Austenitic Stainless Steel. Metall. Trans., vol. 2, no. 7, July 1971, pp. 1821-1827.
174. Saheb, R.E.; and Bui-Quoc, T.: Role of the Strain-Hardening Exponent in Life-Prediction in High Temperature Low Cycle Fatigue. Creep and Fatigue in Elevated Temperature Applications, Institute of Mechanical Engineers, London, 1974.
175. Solomon, H.D.; and Coffin, L.F., Jr.: The Effects of Frequency and Environment on Fatigue Crack Growth in A286 at 1100°F. Fatigue at Elevated Temperatures, ASIM STP-520, A.E. Carden, A.J. McEvily and C.H. Wells, eds., ASIM, 1973, pp. 112-22.
176. Carden, A.E.: Parametric Analysis of Fatigue Crack Growth, Proc., Conference on Creep and Fatigue, Philadelphia, PA, 1973.
177. Majumdar, S.; and Maiya, P.S.: A Damage Equation for Creep-Fatigue Interaction, 1976 ASME-MPC Symposium on Creep-Fatigue Interaction, R.M. Curran, ed., ASIM, 1976, pp. 323-336, 1976.
178. Vogel, W.H.; Soderquist, R.W.; and Schlein, B.C.: Application of Creep-LCF Cracking Model to Combustor Durability Prediction. Fatigue Life Technology, T.A. Cruse and J.P. Gallagher, eds., ASME, 1977, pp. 22-31.
179. Leis, B.N.: An Energy-Based Fatigue and Creep-Fatigue Damage Parameter, J. Pressure Vessel Technol., vol. 99, no. 4, Nov. 1977, pp. 524-533.

180. McLean, D.; and Pineau, A.: Grain-Boundary Sliding as a Correlating Concept for Fatigue Hold-Times, *Met. Sci.*, vol. 12, no. 7, July 1978, pp. 313-316.
181. Antolovich, S.D.; Domas, P.; and Strudel, J.L.: Low Cycle Fatigue of Rene 80 as Affected by Prior Exposure. *Metall. Trans. A*, vol. 10A, no. 12, Dec. 1979, pp. 1859-68.
182. Bernstein, H.: A Stress-Strain-Time Model (SST) for High Temperature Low Cycle Fatigue. *Methods for Predicting Material Life in Fatigue*, W.J. Ostergren and J.R. Whitehead, eds., ASME, 1979, pp. 89-100.
183. Majumdar, S.; and Maiya, P.S.: A Mechanistic Model for Time-Dependent Fatigue. *J. Eng. Mater. Tech.*, vol. 102, no. 1, Jan. 1980, pp. 159-167.
184. Lavaillant, C.; and Pineau, A.: Assessment of High-Temperature LCF Life of Austenitic Stainless Steels by Using Intergranular Damage as a Correlating Parameter. *LCF and Life Prediction*, ASTM STP-770, C. Amzallag, B.N. Leis, and P. Rabbe, eds., ASTM, 1982, pp. 169-193.
185. Halford, G.R.; and Saltsman, J.F.: Strainrange Partitioning - A Total Strainrange Version. *ASME, International Conference on Advances in Life Prediction Methods*, D.A. Woodford and J.R. Whitehead, eds., ASME, 1983, pp. 17-26.
186. Moreno, V., et al.: Application of Two Creep-Fatigue Life Models for the Prediction of Elevated Temperature Crack Initiation of a Nickel-Base Alloy. *AIAA Paper 85-1420*, July 1985.
187. Taira, S.: Relationship Between Thermal Fatigue and Low-Cycle Fatigue at Elevated Temperature. *Fatigue at Elevated Temperatures*, ASTM STP-520, A.E. Carden, A.J. McEvily and C.H. Wells, eds., ASTM, 1973, pp. 80-101.
188. Spera, D.A.: Comparison of Experimental and Theoretical Thermal Fatigue Lives for Five Nickel-Base Alloys. *Fatigue at Elevated Temperatures*, ASTM STP-520, A.E. Carden, A.J. McEvily and C.H. Wells, eds., ASIM, 1973, pp. 648-657.
189. Polhemus, J.F.; Spaeth, C.E.; and Vogel, W.H.: Ductility Exhaustion for Prediction of Thermal Fatigue and Creep Interaction. *Fatigue at Elevated Temperatures*, ASIM STP-520, A.E. Carden, A.J. McEvily and C.H. Wells, eds., ASIM, 1973, pp. 625-635.
190. Lesne, P.M.; and Chaboche, J.L.: Prediction of Crack Initiation Under Thermal Fatigue and Creep, *Fatigue 84*, vol. 3, C.J. Beevers, ed., Engineering Materials Advisory Services Ltd., West Midlands, U.K., 1984, pp. 1903-1912.
191. Vogel, W.H.; Soderquist, R.W.; and Schlein, B.C.: Application of Creep-LCF Cracking Model to Combustor Durability Prediction. *Fatigue Life Technology*, T.A. Cruse and J.P. Gallagher, eds., ASME, 1977, pp. 23-31.

192. Annis, C.G.; VanWanderham, M.C.; and Wallace, R.M.: Strainrange Partitioning Behavior of an Automotive Turbine Alloy. (PWA FR-7424, Pratt and Whitney Aircraft, NASA Contract NAS3-18930) NASA CR-134974, 1976.
193. Gangadharan, A.C.; Pai, D.H.; and Berman, I.: Non-Linear Creep Fatigue Analysis of a Sodium Heat Exchanger Component for the Fast Flux Test Facility. Creep and Fatigue in Elevated Temperature Applications, Institution of Mechanical Engineers, London, 1974, pp. 215.1-215.8.
194. Featherstone, P.F.; Hother-Lushington, S.; and Proctor, E.: Thermal Behavior of Turbine Casings in High Output Generating Plant. Creep and Fatigue in Elevated Temperature Applications, Institution of Mechanical Engineers, London, 1974, pp. 189.1-189.7.
195. Briner, M.; and Beglinger, V.: Thermal Fatigue Analysis of a Large Gas Turbine Rotor. Creep and Fatigue in Elevated Temperature Applications, Institution of Mechanical Engineers, London, 1974, pp. 220.1-220.8.
196. Sangerud, O.T.: Fatigue Life Prediction of Thermally Loaded Engine Components. Report No. UR-81-11, Marine Technology Center, Trondheim, Norway, 1981.
197. Kaufman, A.; and Halford, G.R.: Engine Cyclic Durability by Analysis and Material Testing. Engine Cyclic Durability by Analysis and Testing, AGARD-CP-368, AGARD, France, 1984, pp. 12-1 to 12-12.
198. Sokolowski, D.E.; and Ensign, C.R.: Improved Durability in Advanced Combustors and Turbines through Enhanced Analytical Design Capability. AIAA Paper 85-1417, July 1985.
199. Moreno, V.; et al.: Nonlinear Structural and Life Analyses of a Combustor Liner. Comput. Struct., vol. 16, no. 1-4, 1983, pp. 509-515.
200. Manderscheid, J.M.; and Kaufman, A.: Cyclic Structural Analyses of Anisotropic Turbine Blades for Reusable Space Propulsion Systems. NASA TM-86990, 1985.
201. Kaufman, A.; and Manderscheid, J.M.: Cyclic Structural Analysis of SSME Turbine Blades. Structural Integrity and Durability of Reusable Space Propulsion Systems, NASA CP-2381, 1985, pp. 147-154.

TABLE 1. - SUMMARY OF TMF BEHAVIOR

Alloy	Tmax °C	Tmin °C	Freq., Hz. TMF	Freq., Hz. ISO	Response type		Iso./TMF $\Delta\epsilon_T$		Iso./TMF $\Delta\epsilon_{in}$		Ref.
					$\Delta\epsilon_T$	$\Delta\epsilon_{in}$	Out	In	Out	In	
Steels											
AISI 1010 (H.R.)	316	93	0.0067	?	?	?	A	?	A	?	Jaske [120]
	427	93	.0067	?	?	?	A	?	A	?	
	538	93	.0067	0.1-1.3	?	?	A	A	A	A	
1/2 Cr-Mo-V (N&T)	667	300	.00058- .00074	.00058- .00074	?	?	?	A	?	A	Westwood [121]
Cr-Mo-V (forging)	550	300	.0083	.0083	0	0	N	N	N	N	Kuwabara [119]
Cr-Mo-V (forging)	550	300	.0083	.0083	E	E	B	N	N	N	Taira [122]
Cr-Mo-V (forging)	600	300	.0083	.0083	I	I	N	A	N	A	Taira [122]
Cr-Mo-V (cast)	538	300	.0083	.0083	I	I	N	A	N	A	Kuwabara [119]
Ni-Mo-V (forging)	538	300	.0083	.0083	0	0	N	B	N	N	Kuwabara [119]
1.25Cr- 0.5 Mo.	538	300	.0083	.0083	0	0	N	N	N	N	Kuwabara [119]
2.25Cr - 1 Mo	538	300	.0083	.0083	0	0	N	N	N	N	Kuwabara [119]
0.15%C Steel	400	100	.0167	.0167	0	0	N	N	A	A	Fujino [123]
0.15%C Steel	500	200	.0167	.0167	I	I	A	A	A	A	Fujino [123]
12 Cr-Mo-W-V	550	300	.0083	.0083	0	0	N	N	N	N	Taira [122]
12 Cr-Mo-W-V	600	300	.0083	.0083	0	0	N	N	N	N	Taira [122]
A 286 (forging)	650	300	.0056	.0056	E	E	B	B	N	N	Kuwabara [119]
S40C (Carbon Steel)	300	100	.0167	.0500	?	?	?	?	A	?	Udoguchi [124]
S40C	400	100	.0167	.0500	?	?	?	?	A	?	Udoguchi [124]
Cr - Mo-V	620	80	?	.0002- .0008 sec. ⁻¹	?	?	?	?	N	?	Sandstrom [125]
2.25 Cr-1Mo.	594	316	var.	var.	?	?	?	?	N	?	Manson [10]
2.25 Cr-1Mo.	510	316	var.	var.	?	?	?	?	N	?	Manson [10]
0.16%C steel (S15C)	400	100	.011- .016	.011- .016	?	?	?	?	N	?	Taira [126]
0.16%C steel (S15C)	500	200	.011- .016	.011- .016	?	?	?	?	A	?	Taira [126]
0.16%C steel (S15C)	550	150	.011- .016	.011- .016	?	?	?	?	A	?	Taira [126]
0.16%C steel (S15C)	600	100	.011- .016	.011- .016	?	?	?	?	A	?	Taira [126]
0.16%C steel (S15C)	600	300	.011- .016	.011- .016	?	?	?	?	N	?	Taira [126]

TABLE 1. - Continued.

Alloy	Tmax °C	Tmin °C	Freq., Hz. TMF	Freq., HZ. ISO	Response Type		Iso./TMF $\Delta\epsilon_T$		Iso./TMF $\Delta\epsilon_{in}$		Ref.
					$\Delta\epsilon_T$	$\Delta\epsilon_{in}$	Out	In	Out	In	
Stainless Steels											
304 (Mat. A)	550	200	0.0083	0.0083	E	E	N	N	N	N	Kuwabara [119]
304	550	200	.0083	.0083	E	I'	N	N	N	N	Fujino [123]
304 (Mat. B)	600	300	.0083	.0083	E	E	N	N	N	N	Kuwabara [119]
304	600	300	.0083	.0083	E	E	N	N	N	N	Taira [122]
304	700	300	.0056	.0056	I'	I'	N	A	N	A	Taira [122]
304	750	200	.0083	.0083	I	I	N	A	A	A	Fujino [123]
304 Annealed	var.	var.	.0094- .037	?	?	?	A	-	A	-	Carden [127]
304 Annealed	650	427	.00115- .0024	.0001- .0100	?	?	N	A	N	A	Stentz [128]
304	700	350	.0012- .0015	?	?	I	N	N	N	N	Westwood [129]
316 (Annealed)	647	316	var.	var.	?	?	N	N	N	N	Saltsman [130]
316	705	316	var.	var.	?	?	N	N	N	N	Saltsman [130]
316	815	316	var.	var.	?	?	N	N	N	N	Saltsman [130]
316 (Annealed)	760	230	.00056	var.	?	?	N	N	N	N	Halford [131]
321	650	450	.0033	.0033	E	I	N	N	A	A	Kuwabara [119]
347	600	100	var.	-	-	-	?	-	?	-	Coffin [5]
347	500	200	.0167	.050	?	?	?	?	A	?	Udoguchi [124]
347	600	100	.0167	.050	?	?	?	?	A	?	Udoguchi [124]
347	600	300	.0167	.050	?	?	?	?	A	?	Udoguchi [124]
347	700	400	.0167	.050	?	?	?	?	?	?	Udoguchi [124]
347	700	200	.0167	.050	?	?	?	?	?	?	Udoguchi [124]
347	600	200	.011- .016	.011- .016	?	?	N	?	?	?	Taira [126]
347	650	300	.011- .016	.011- .016	?	?	N	?	?	?	Taira [126]
347	700	300	.011- .016	.011- .016	?	?	N	?	?	?	Taira [126]
347	750	250	.011- .016	.011- .016	?	?	N	?	?	?	Taira [126]
347	800	400	.011- .016	.011- .016	?	?	N	?	?	?	Taira [126]
H46 Martensitic S.S.	700	400	.0167	.050	?	?	?	?	A	?	Udoguchi [124]
H46 Martensitic S.S.	700	200	.0167	.050	?	?	?	?	A	?	Udoguchi [124]
H46 Martensitic S.S.	600	300	.0167	.050	?	?	?	?	A	?	Udoguchi [124]
H46 Martensitic S.S.	600	100	.0167	.050	?	?	?	?	A	?	Udoguchi [124]
H46 Martensitic S.S.	500	200	.0167	.050	?	?	?	?	A	?	Udoguchi [124]

TABLE 1. - Continued.

Alloy	Tmax °C	Tmin °C	Freq., Hz. TMF	Freq., Hz. ISO	Response type		Iso./TMF $\Delta\epsilon_T$		Iso./TMF $\Delta\epsilon_{in}$		Ref.
					$\Delta\epsilon_T$	$\Delta\epsilon_{in}$	Out	In	Out	In	
Nickel-Base Alloys											
HASTELLOY N wrought	871	205	0.00118	?	?	?	N	-	N	-	Carden [132]
	871	var.	var.	?	?	?	N	-	N	-	
	871	var.	var.	?	?	?	N	-	N	-	
	871	var.	var.	?	?	?	N	-	N	-	
	871	650	.0239	?	?	?	N	-	N	-	
	705	50	.0010	?	?	?	N	-	N	-	
	705	var.	var.	?	?	?	N	-	N	-	
	705	var.	var.	?	?	?	N	-	N	-	
	705	260	.0200	?	?	?	N	-	N	-	
HASTELLOY X	705	300	.0083	0.0083	I	I	?	?	N	A	Taira [122]
	900	300	.0083	.0083	I	I	?	?	N	A	
HASTELLOY X wrought	927	427	.0167	.0167	?	?	N	-	N	-	Kaufman [133]
INCONEl 600 wrought	871	538	?	.00833	?	?	N	-	N	-	Swindeman [15]
INCONEl 718 forged	650	300	.0056	.0056	I'	I'	B	N	B	N	Kuwabara [119]
UDIMET 700	983	205	.0067	.133	?	?	-	A	-	A	Vogel [134]

TABLE 1. - Continued.

Alloy	Tmax °C	Tmin °C	Freq., Hz. TMF	Freq., Hz. ISO	Response type		Iso./TMF $\Delta\epsilon_T$		Iso./TMF $\Delta\epsilon_{in}$		Ref.
					$\Delta\epsilon_T$	$\Delta\epsilon_{in}$	Out	In	Out	In	
Nickel-Base Alloys											
INCONEL 738LC cast	900	300	0.0056	0.0056	0	I	N	B	A	A	Kuwabara [119]
IN-738 cast	?	?	?	?	?	?	?	?	?	?	Ostergren [135]
INCONEL 939 cast	900	300	.0056	.0056	I'	I	B	N	A	A	Ostergren [135]
MAR M247 cast	900	300	.0056	.0056	I'	I'	N	N	A	A	Ostergren [135]
René 80 cast	900	300	.0056	.0056	0	I	N	N	A	A	Ostergren [135]
René 80 cast	1000	344	.0049	.0049	?	?	A	-	A	-	Mcknight [136]
René 80 (vac) cast	1000	400	.0014	.007- .050	I	I	-	A	-	A	Sheinker [137]
René 80 cast	1093	649	?	?	?	?	?	-	?	-	Cook [138]
B1900 cast	983	205	.0067	.133	?	?	A	-	A	-	Vogel [134]
Nimonic 90	1000	350	?	?	?	?	-	A	?	?	Tilly [139]
MAR-M200 cast	1000	500	.0037	.200- .00006	?	I	A	A	A	A	Bill [140]
8Cr-10Co-6Al-6Mo-1Ti	927	594	.013	.013	?	?	N	A	?	?	Lindholm [141]
ÉP 693VD Alloy	800	200	.009	?	?	I	?	?	?	?	Bashunin [142]
	700	200	.009	?	?	I	?	?	?	?	Bashunin [142]
	860	700	.009	?	?	I	?	?	?	?	Bashunin [142]
	860	200	.009	?	?	I	?	?	?	A	Bashunin [142]
	700	200	.009	?	?	I	?	?	?	A	Bashunin [142]
	860	700	.009	?	?	I	?	?	?	A	Bashunin [142]

TABLE 1. - Concluded.

Alloy	Tmax °C	Tmin °C	Freq., Hz. TMF	Freq., Hz. ISO	Response Type		Iso./TMF $\Delta\epsilon_T$		Iso./TMF $\Delta\epsilon_{in}$		Ref.
					$\Delta\epsilon_T$	$\Delta\epsilon_{in}$	Out	In	Out	In	
Cobalt-Base Alloys											
MAR-M509 cast	1100	200	0.0125	0.025- .100	?	?	A	?	?	?	Rezai-Aria [143]
WI-52 cast	983	205	.0067	?	?	?	A	?	?	Vogel [134]	
MAR-M302 cast	1000	500	.0065	.0065	?	0	A	N	A	N	Sheffler [144]
Copper-Base Alloys											
AMZIRC-1/2 Hard	538	260	.00125	.00333	I	I	A	A	A	A	Conway [145]
Tantalum-Base Alloys											
T-111	1150	205	.0065	.0065	I	I	N	A	N	A	Sheffler [146]
ASTAR 811C	1150	205	.0065	.0065	I	I	A	A	A	A	Sheffler [146]

ORIGINAL PAGE IS
OF POOR QUALITY

TABLE 2. - SUMMARY OF REVIEWS OF ISOTHERMAL LIFE PREDICTION METHODS

Year intro- duced	Reviewers*	1	2	3	4	5	6	7	8	9	10	11	12	13
	Engineering life prediction models for high temperatures													
1953	Manson-Coffin Law [167] [5]	X	X	-	X	-	X	X	-	-	-	-	-	-
1960	Hysteresis Energy [168]	-	-	-	-	-	X	-	-	-	-	-	-	-
1960	Exhaustion of Ductility [169]	X	-	-	-	-	-	-	-	-	-	-	-	X
1962	Time & Cycle Fraction [152]	X	-	X	X	-	X	X	X	X	-	-	-	X
1965	Universal Slopes [7]	X	X	X	X	-	X	X	-	-	-	-	-	-
1967	10% Rule [8]	X	-	X	X	-	X	X	-	-	-	-	-	-
1968	Crack Growth Model (Tomkins) [170]	-	X	-	X	-	-	-	-	-	-	-	-	X
1969	Frequency Modified Life [70]	X	X	X	X	-	X	X	X	X	-	-	-	-
1970	Characteristic Slopes [171]	X	-	-	-	-	-	-	-	-	-	-	-	-
1971	Modified Time & Cycle Fraction [9]	X	-	-	X	-	-	X	-	-	-	-	-	-
1971	Strainrange Partitioning [10]	X	X	X	X	X	X	X	X	X	X	X	X	X
1971	Time-Cycle Failure Diagram [172]	-	-	-	X	-	X	X	-	-	-	-	-	-
1971	Interactive Time & Cycle Fraction [173]	-	X	X	-	-	-	-	-	-	-	-	-	-
1973	Saheb and Bui-Quoc [174]	X	-	-	X	-	-	X	-	-	-	-	-	-
1973	Crack Growth Model (Solomon) [175]	X	X	-	X	-	-	-	-	-	-	-	-	-
1973	Crack Growth Model (Carden) [176]	X	-	X	-	-	-	-	-	X	-	-	-	-
1975	Continuum Damage [153]	-	-	-	-	-	-	-	-	-	-	-	-	-
1976	Damage Rate [177]	-	-	-	X	X	X	X	-	-	-	X	-	X
1976	Frequency Separation [72]	-	X	-	X	X	-	X	X	X	X	X	X	X
1976	Ostergren Approach [71]	-	X	-	X	X	-	X	X	-	X	X	-	-
1976	P&WA SRP Combustor Model [178]	-	-	-	-	-	-	-	-	-	-	-	-	-
1977	Leis Energy Model [179]	-	-	-	-	-	-	-	-	-	-	-	-	-
1978	Grain Boundary Sliding [180]	-	-	-	-	-	-	-	X	-	-	-	-	-
1978	Ductility Normalized SRP [69]	-	-	-	-	-	-	X	-	-	-	-	-	X
1979	Stress-Crack Tip Oxidation [181]	-	-	-	-	-	-	-	-	-	-	-	-	-
1979	SST Model [182]	-	-	-	-	-	-	-	-	-	-	-	-	-
1980	Modified Damage Rate [183]	-	-	-	-	-	-	X	-	-	-	-	-	X
1982	Ecole de Mines de Paris SRP Model [184]	-	-	-	-	-	-	-	-	-	-	X	-	-
1982	Radhakrishnam Crack Tip Energy Model [164]	-	-	-	-	-	-	-	-	-	-	-	X	-
1983	Total Strainrange - SRP [185]	-	-	-	-	-	-	-	-	-	-	-	-	X
1985	Cyclic Damage Accumulation [186]	-	-	-	-	-	-	-	-	-	-	-	-	-

- *1 - Manson, 1976 [154]
- 2 - Coffin, 1976 [156]
- 3 - Wen-Ching Chen, 1977 [160]
- 4 - Coffin, 1979 [157]
- 5 - Bernstein, 1979 [165]
- 6 - Halford, 1980 [161]
- 7 - Manson, 1982 [155]
- 8 - Lundberg and Sandstrom, 1982 [158]
- 9 - Batte, 1983 [166]
- 10 - Nazmy and Wuthrich, 1983 [162]
- 11 - Cailletaud and Nouailhas, 1983 [163]
- 12 - Radhakrishnam, 1984 [164]
- 13 - Miller, Priest, and Ellison, 1984 [159]

TABLE 3. - TOTAL
STRAINRANGE
CRITERION
PREDICTIONS,
TIME-INDEPENDENT

Isothermal temperature, °C	Predicted life, cycles
Min. 0	740
Avg. 500	560
Max. 1000	233

TABLE 4. - OSTERGREN APPROACH
($\Delta\epsilon_{in}$)(σ_T), TIME-DEPENDENT

Isothermal temperature, °C	Predicted life, cycles	
	In-phase	Out-of-phase
Min. 0	1547	400
Pt. B. 410	797	---
Avg. 500	660	169
Max. 1000	106	27

TABLE 5. - OSTERGREN APPROACH
(TENSILE HYSTERESIS ENERGY),
TIME-INDEPENDENT

Isothermal temperature, °C	Predicted life, cycles	
	In-phase	Out-of-phase
Min. 0	1249	717
Pt. B. 410	644	---
Avg. 500	533	306
Max. 1000	85	49

TABLE 6. - TOTAL
 STRAINRANGE
 CRITERION
 PREDICTIONS,
 TIME-DEPENDENT

Isothermal temperature, °C	Predicted life, cycles
Min. 0	910
Avg. 500	474
Max. 1000	205

TABLE 7. - OSTERGREN APPROACH
 $(\Delta \epsilon_{iN})(\sigma_T)$, TIME-DEPENDENT

Isothermal temperature, °C	Predicted life, cycles	
	In-phase	Out-of-phase
Min. 0	1681	400
Pt. B. 370	874	---
Avg. 500	625	147
Max. 1000	25	6

TABLE 8. - OSTERGREN APPROACH
 (TENSILE HYSTERESIS ENERGY),
 TIME-DEPENDENT

Isothermal temperature, °C	Predicted life, cycles	
	In-phase	Out-of-phase
Min. 0	1621	794
Pt. B. 370	842	---
Avg. 500	602	295
Max. 1000	24	12

TABLE 9. - TMF PARAMETERS (0 TO 1000 °C)

Parameter	In-phase	Out-of-phase
$\Delta\epsilon_{in}$	0.005/0.00500	0.005/0.00500
$\Delta\epsilon$	0.008/0.00756	0.008/0.00756
$\Delta\epsilon_{in\sigma_T, MPa}$	1.05/0.991	2.38/2.36
$\Delta W_T, MPa$	0.800/0.667	1.11/1.04

TABLE 10. - TOTAL STRAINRANGE APPROACH

Isothermal temperatures, °C	Predicted life, cycles	
	Time-independent	Time-dependent
0	320	330
500	450	484
1000	1450	5110

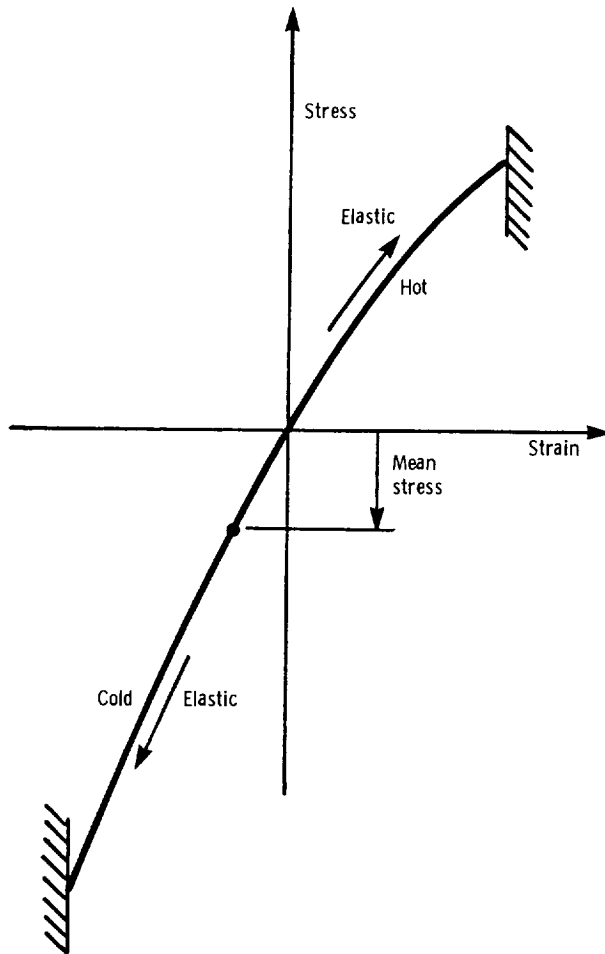


Figure 1. - In-phase thermomechanical hysteresis loop for elastic conditions.

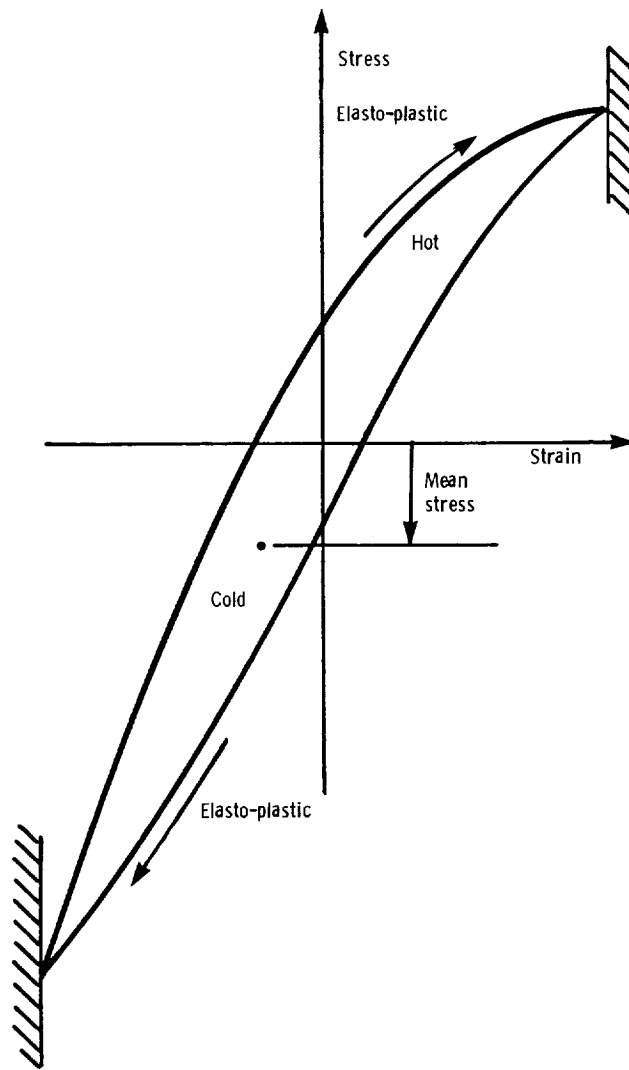


Figure 2 - In-phase thermomechanical hysteresis loop for elasto-plastic conditions.

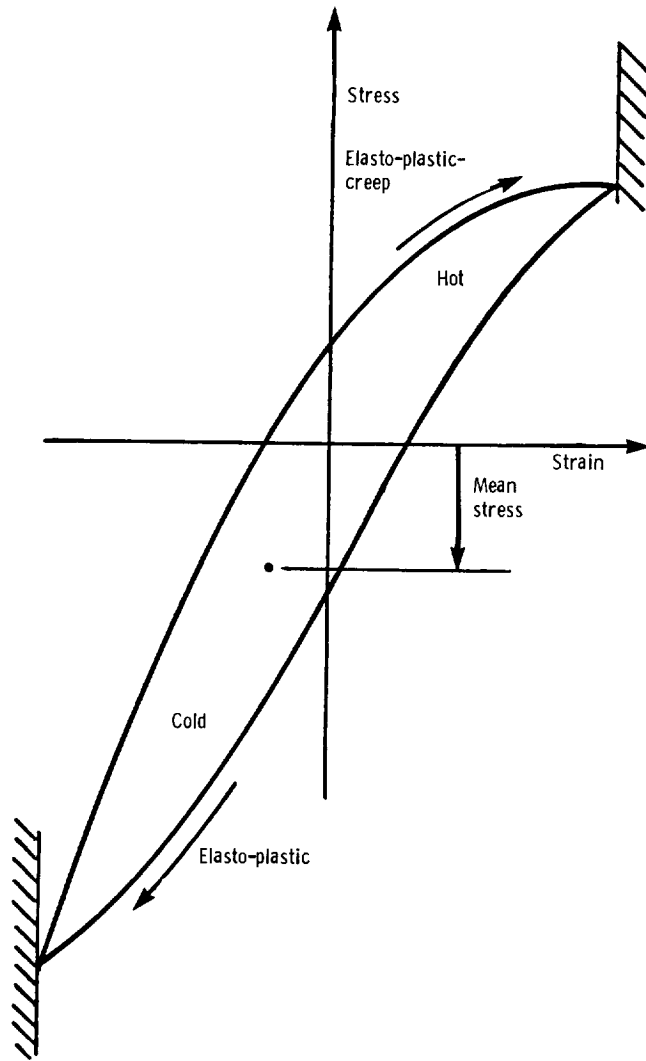


Figure 3. - In-phase thermomechanical hysteresis loop for elasto-plastic-creep conditions.

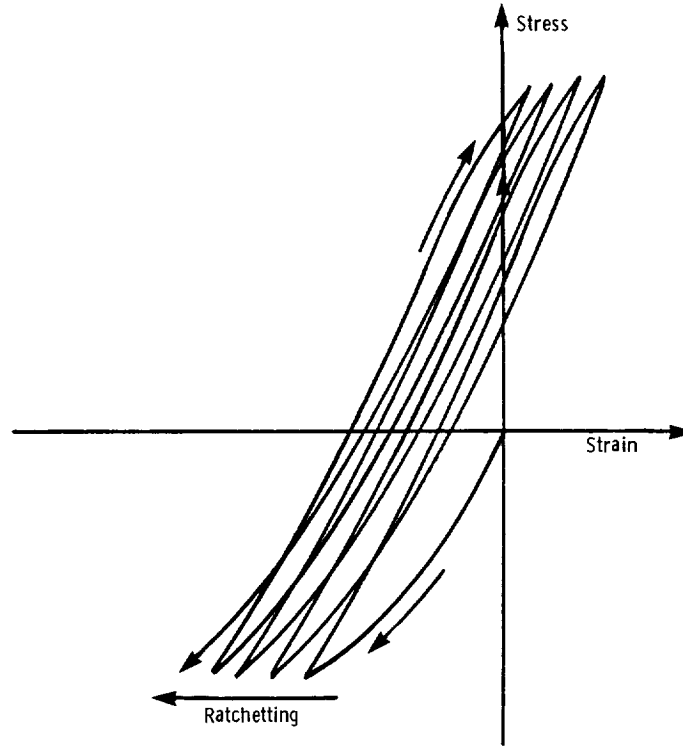
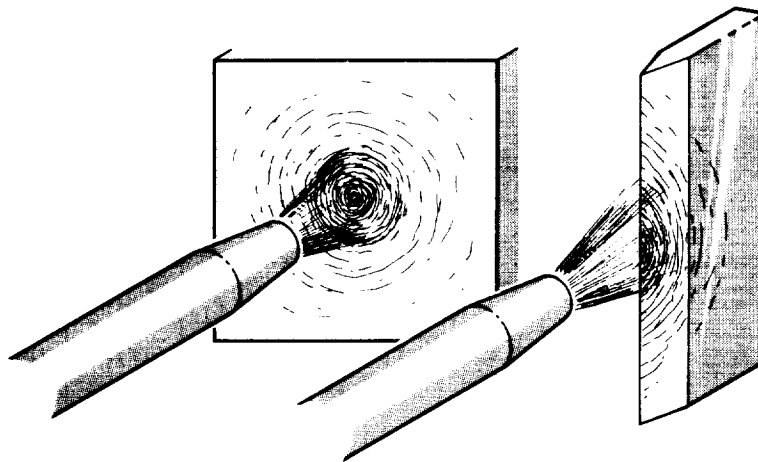


Figure 4. - Compressive creep ratchetting in thermal fatigue.



(a) Flat plate-equibiaxial.

(b) Thin edge-uniaxial.

Figure 5. - Extremes of biaxial thermal stress fields.

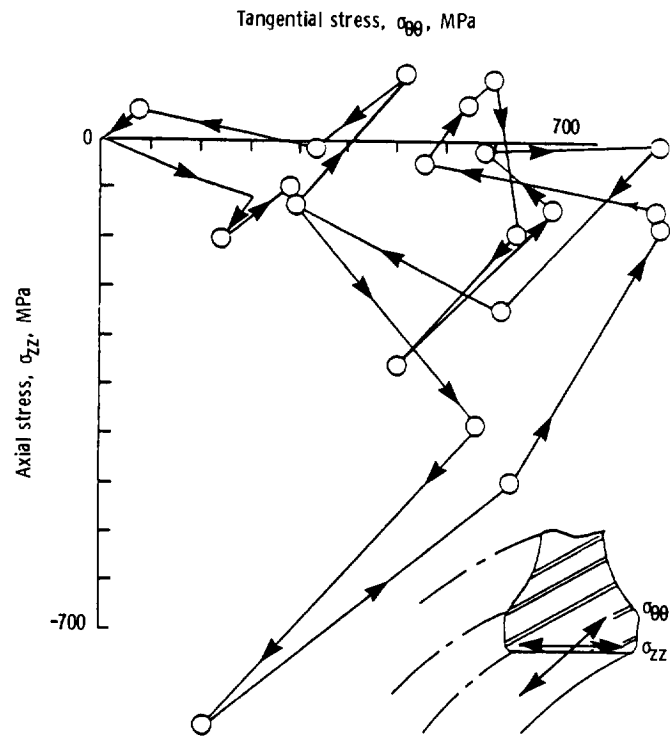


Figure 6. - Example of complex states of stress that can evolve during a simulated mission in a disk bore. After Laffen and Cook (62).

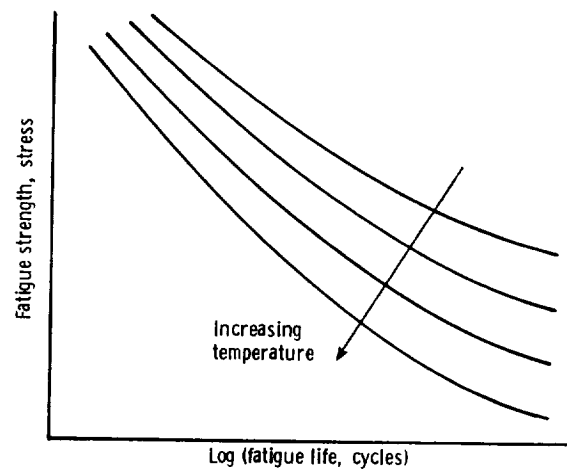


Figure 7. - Stress-fatigue resistance decreases with increasing temperature.

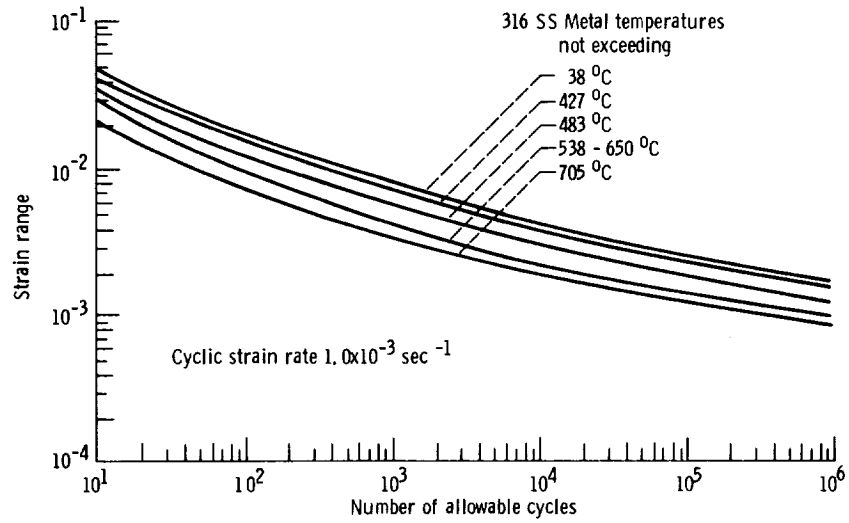


Figure 8. - Fatigue design curves for austenitic stainless steel 316, ASME Code Case N-47-22 (19). Reprint with permission of the American Society of Mechanical Engineers.

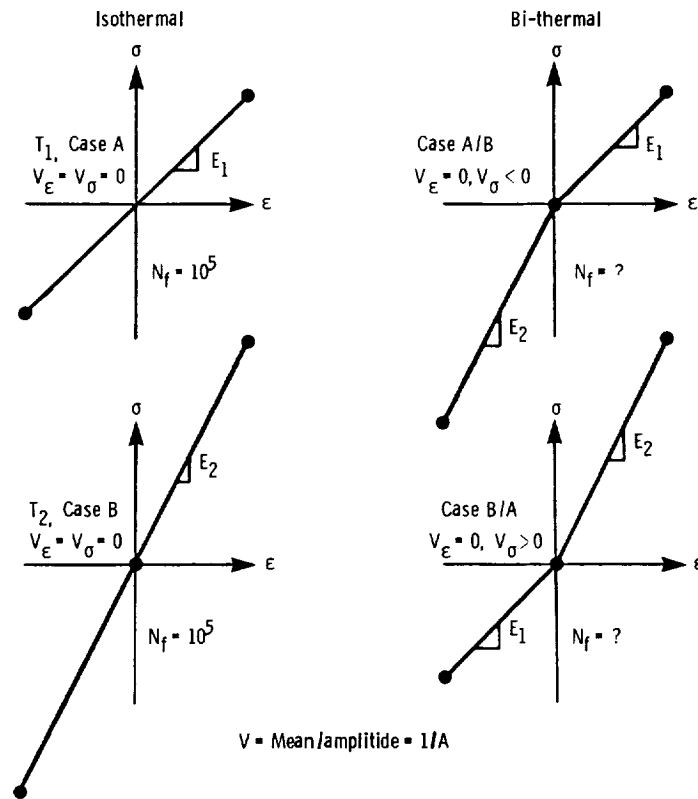


Figure 9. - The case for mean elastic strain in thermal fatigue.

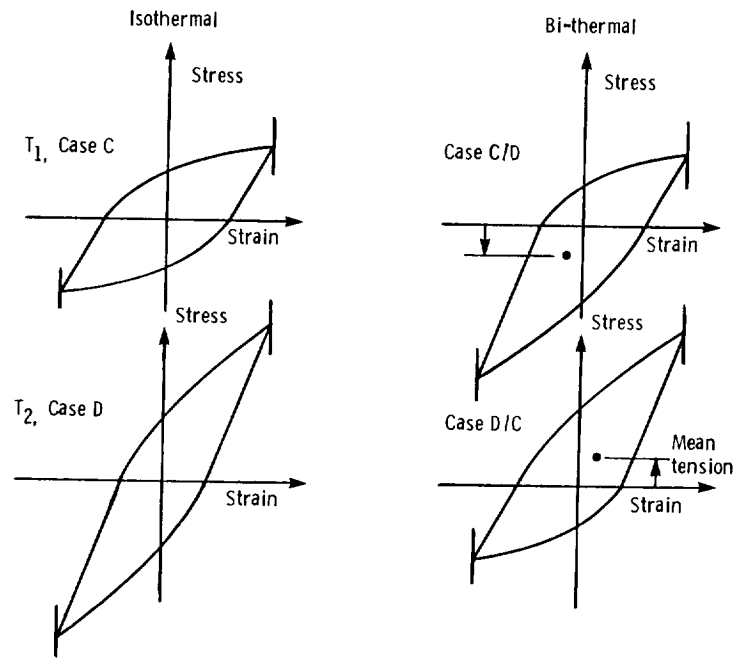


Figure 10. - Mean stresses in Bi-thermal cycles.

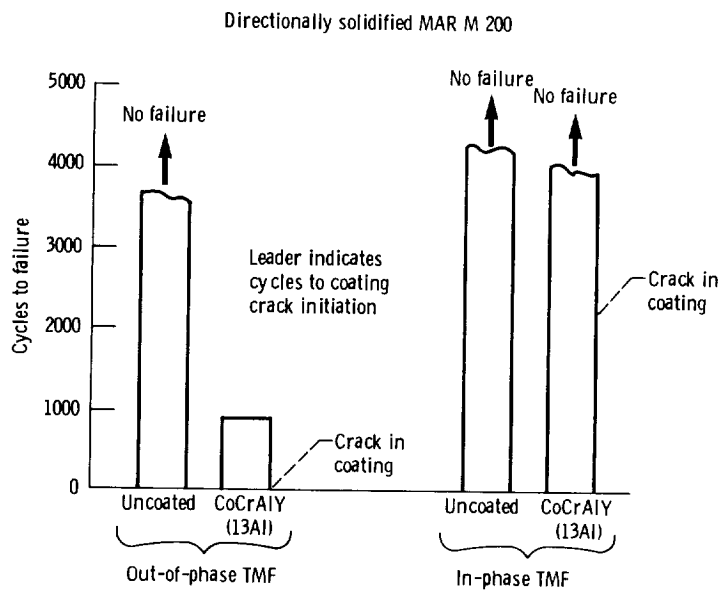


Figure 11. - Early TMF crack initiation in low ductility coating during out-of-phase cycling TMF cycling between 427 and 1038 C at 0.0074 Hz. After Leverant, et al (81). Reprinted by permission of Claitor's Law Books and Publishing Division, P.O. Box 333, Baton Rouge, LA 70821.



Single edge



Double edge

Figure 14. - Single edge and double edge wedge thermal fatigue specimens for use in fluidized bed facility at IITRI.

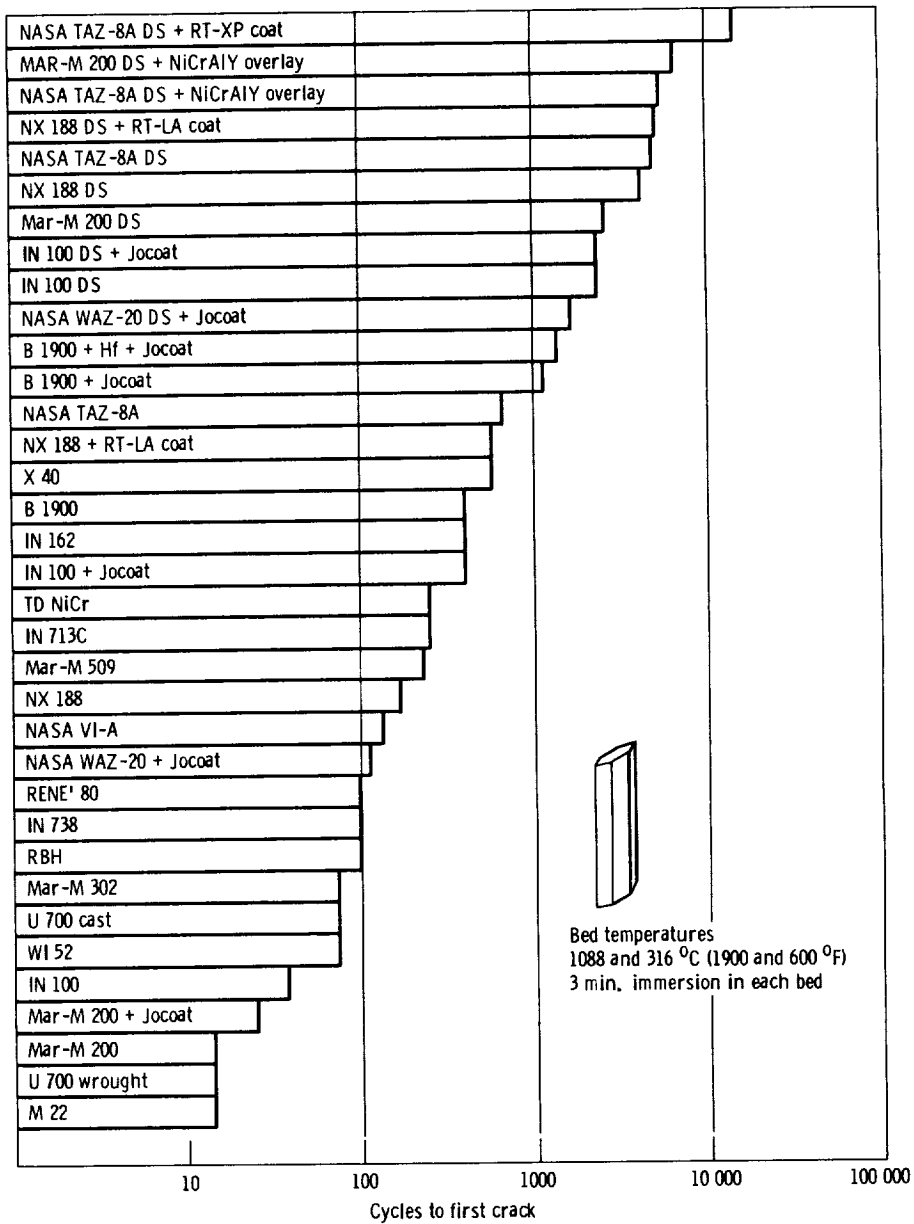


Figure 15. - Comparative thermal fatigue resistances of Nickel- and Cobalt-base alloys. After Bizon and Spera (102).

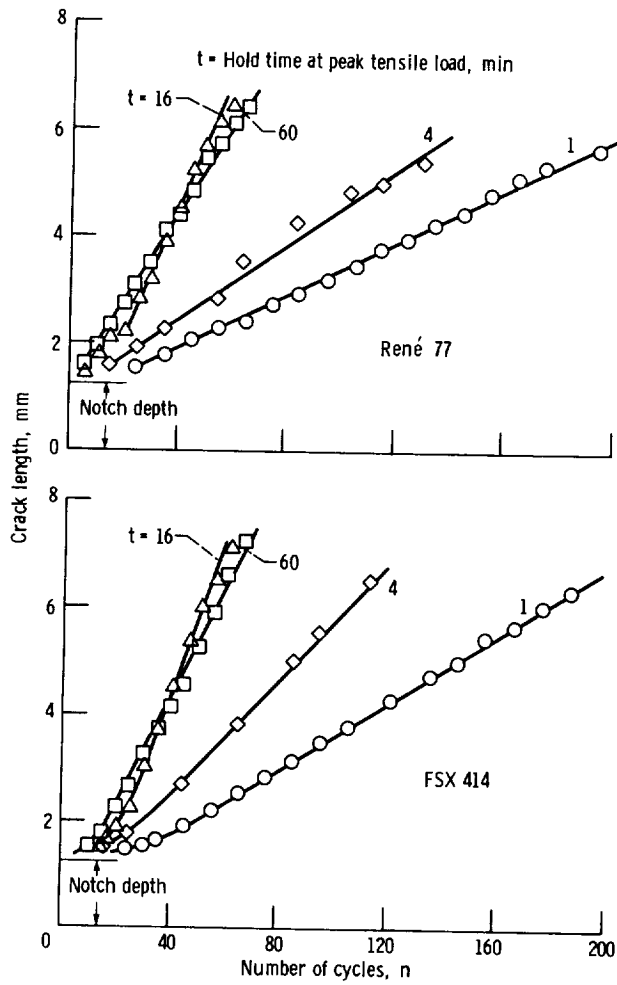


Figure 16. - TMF Crack growth curves showing effect of hold time at 970 °C maximum temperature (range of temperature = 946 °C). After Mowbray and Woodford (101). Reprinted by permission of the Council of the Institution of Mechanical Engineers.

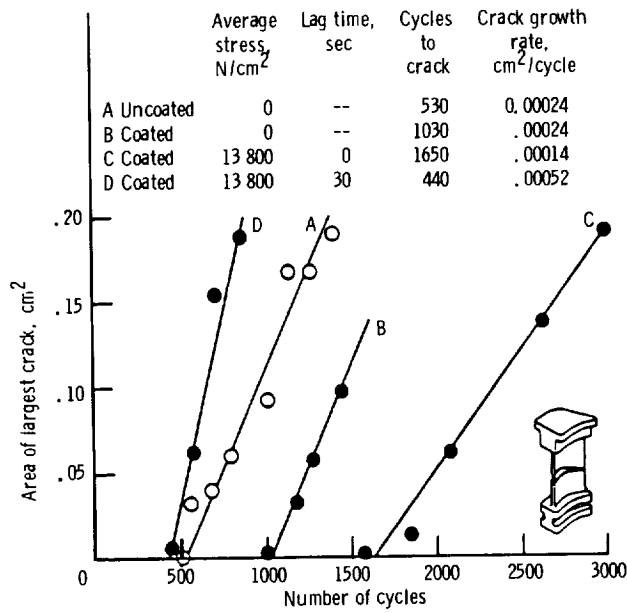


Figure 17. - Thermal fatigue crack propagation in IN 100 simulated turbine blades (87 to 952 °C). After Spera, Calfo and Bizon (106).

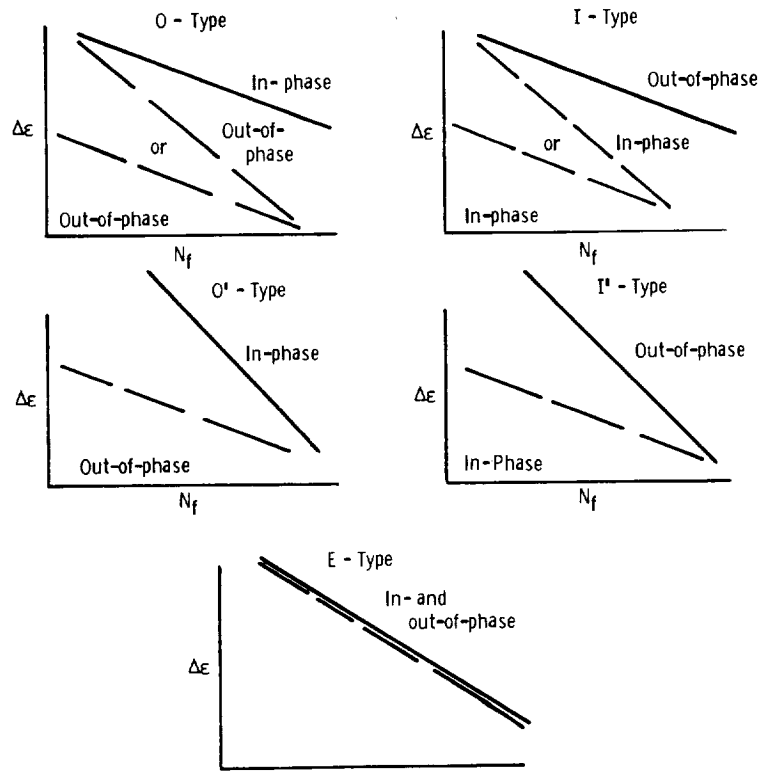


Figure 18. - Coding systems used to describe TMF behavior for in-phase and out-of-phase cycles.

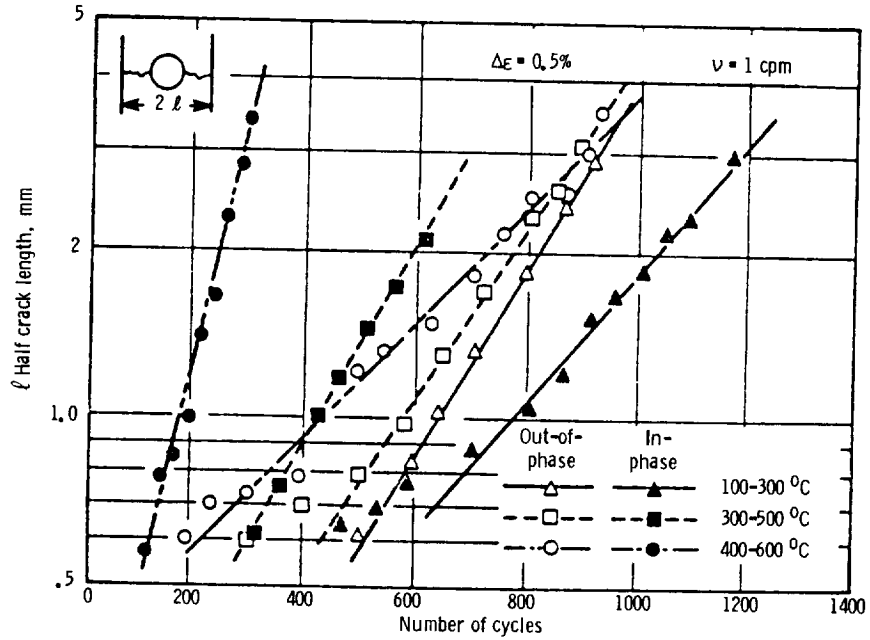


Figure 19. - Thermal fatigue crack length versus number of cycles under 0.5% strain range (0.16% carbon steel). After Taira, Fujino and Maruyama (148).

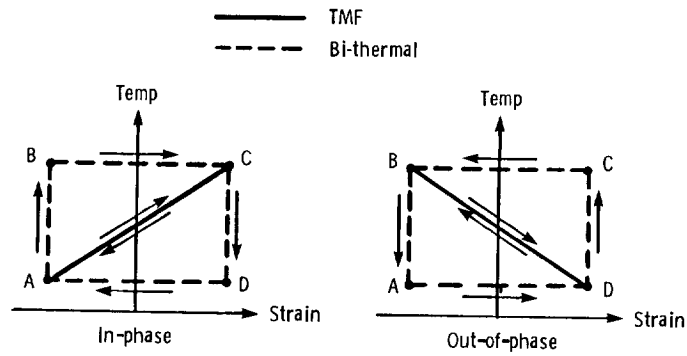


Figure 20. - Temperature/strain patterns for TMF and bi-thermal strain cycles.

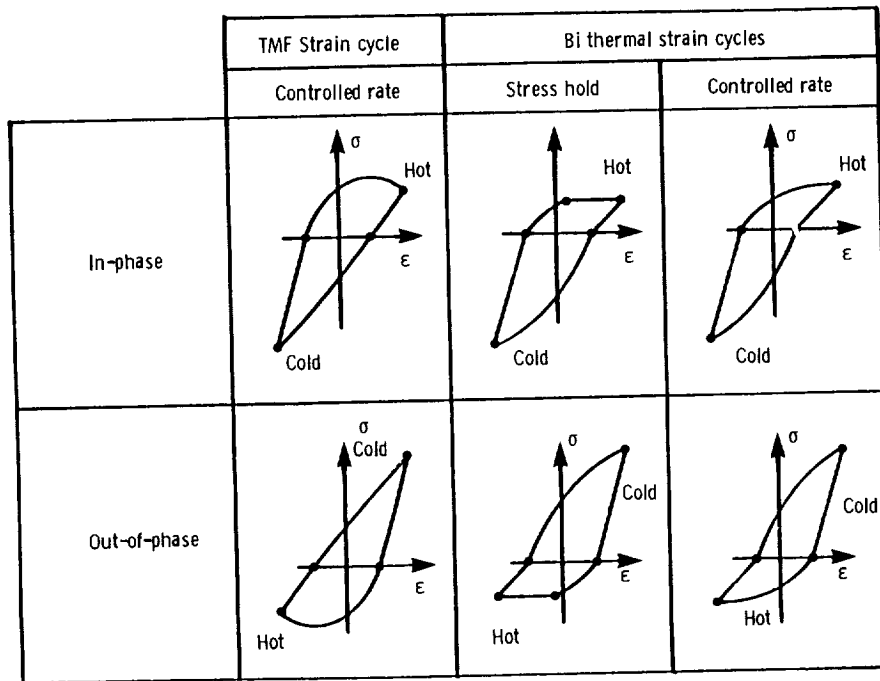


Figure 21. - Schematic hysteresis loops for TMF and bi-thermal cycles.

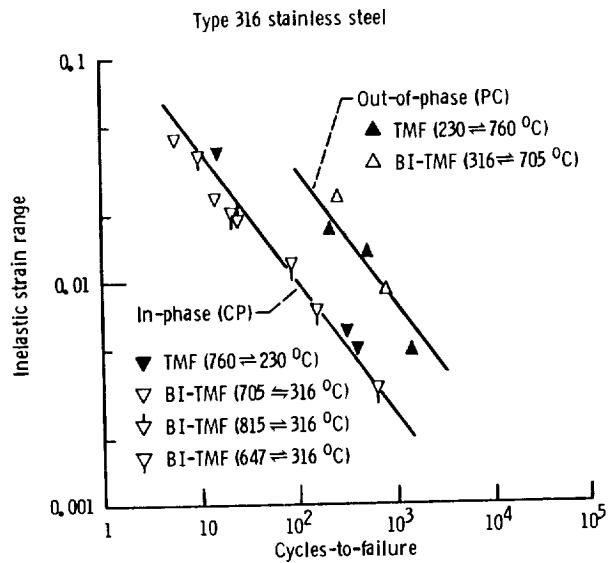


Figure 22. - Comparison of bi-thermal and TMF LCF behavior of AISI type 316 stainless steel. Bi-thermal results re-reported by Saltsman and Halford (130); TMF results are NASA data generated by Halford and Manson, and partially reported in ref. (131).

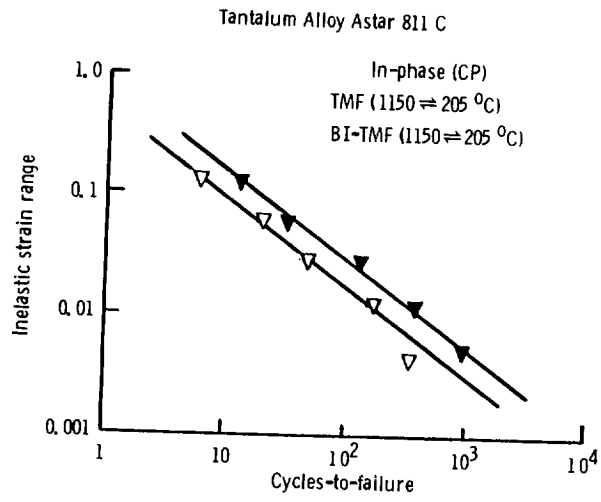


Figure 23, - Comparison of bi-thermal and TMF LCF behavior of a ductile refractory alloy in ultra-high vacuum, after Sheffler and Doble (146).

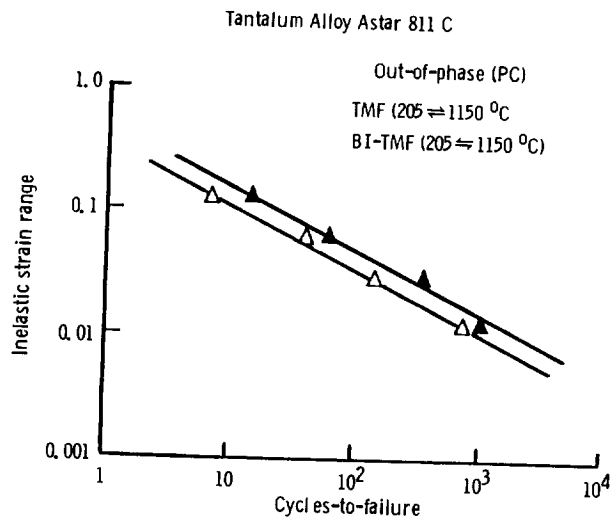


Figure 23, - Concluded.

C-2

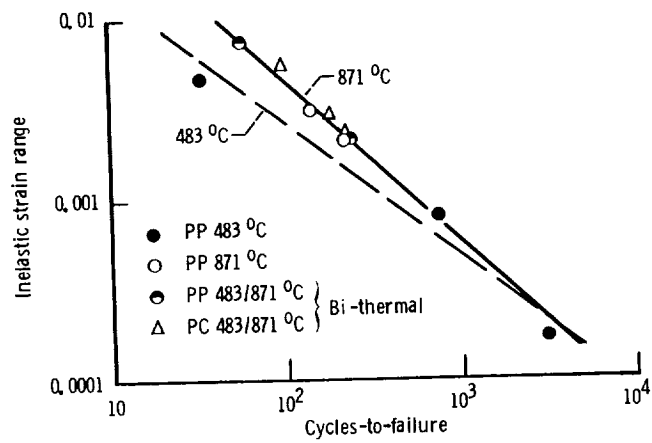


Figure 24. - Isothermal and bi-thermal creep-fatigue results for B-1900 + Hf. After Halford, et al (150).

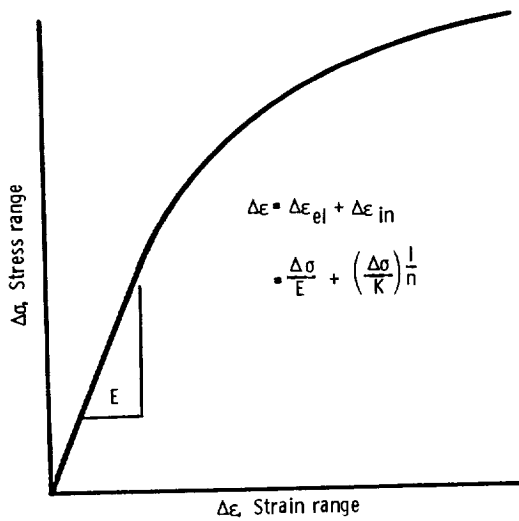


Figure 25. - Cyclic stress-strain relation for hypothetical material with time-independent behavior.

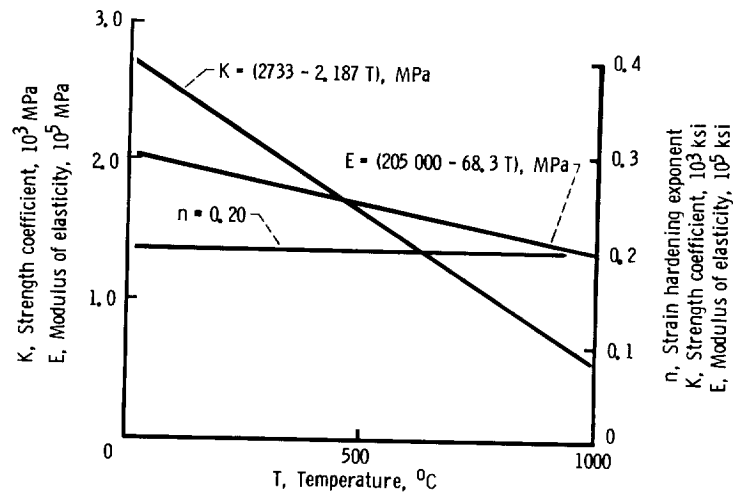


Figure 26. - Temperature dependence of cyclic stress-strain constants, E, K, and n.

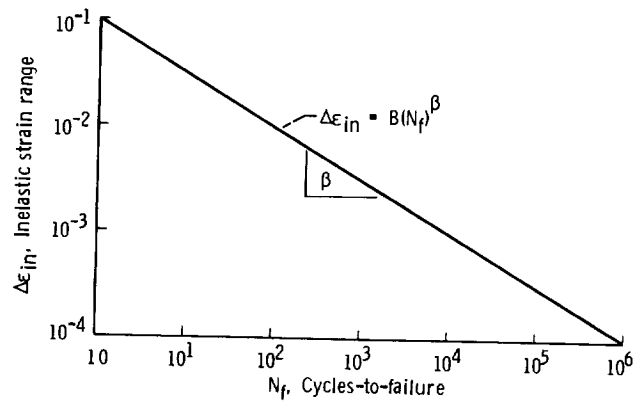


Figure 27. - Inelastic strain range versus cyclic life relation for hypothetical material with time- and temperature-independent behavior.

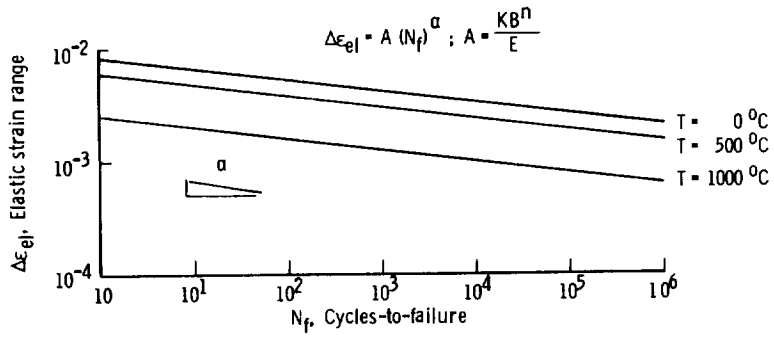


Figure 28. - Elastic strain range versus cyclic life relation for hypothetical material with time-independent behavior.

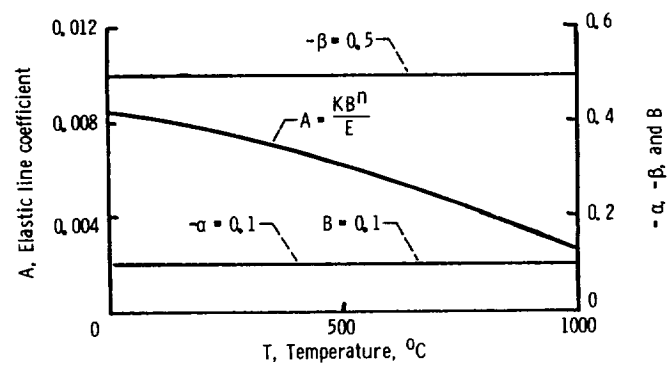


Figure 29. - Temperature dependence of time-independent fatigue constants.

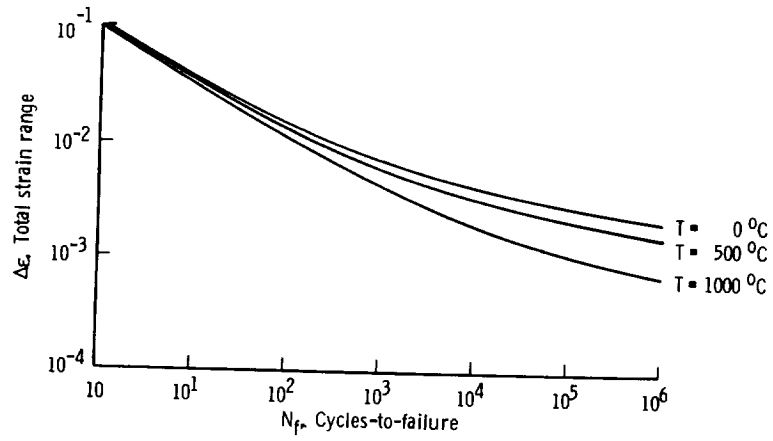


Figure 30. - Total strain range versus cyclic life relation for hypothetical material with time-independent behavior. Curves for minimum, average, and maximum temperatures of TMF cycle.

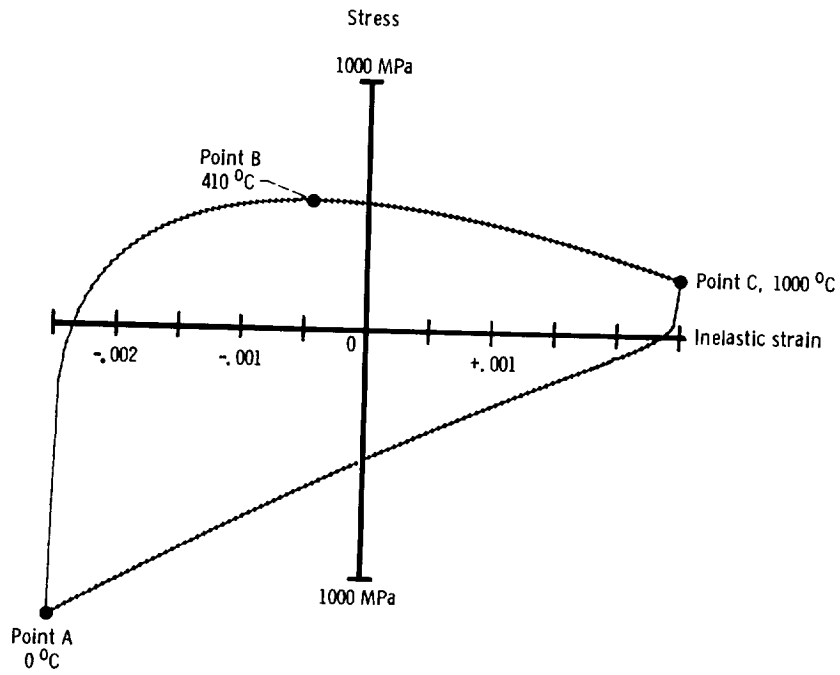


Figure 31. - TMF Hysteresis loop, in-phase, inelastic strain range = 0.005, max. temperature of 1000 °C, min temperature of 0 °C, $\epsilon_{in} \geq 1.0 \text{ sec}^{-1}$.

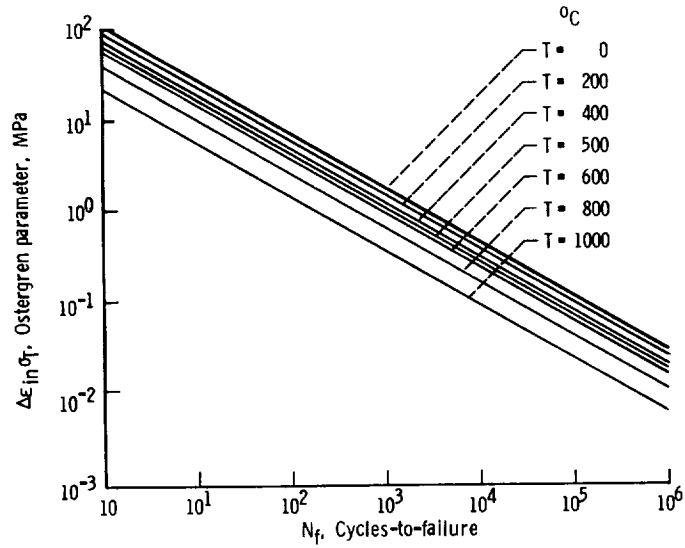


Figure 32, - Isothermal failure criterion using Ostergren's time-independent stress-inelastic strain range product form.

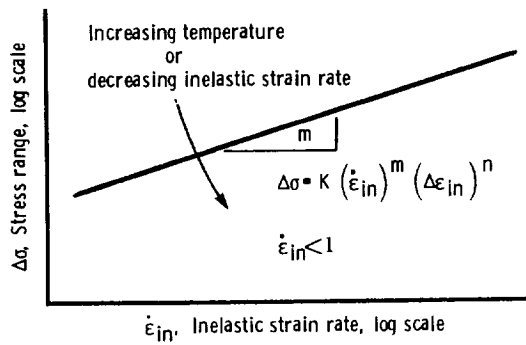


Figure 33, - Inelastic strain rate dependency of cyclic-stress-strain curve. Strain range and temperature constant.

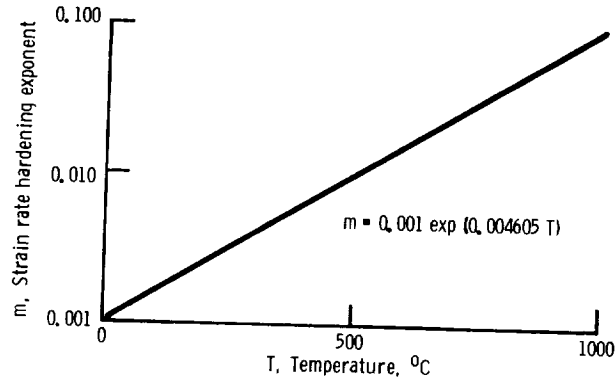


Figure 34. - Temperature dependence of strain rate hardening exponent, m .

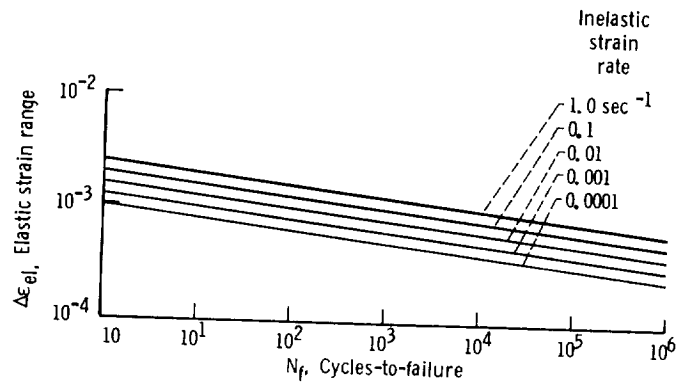


Figure 35. - Time-dependent elastic strain range versus cyclic life as function of inelastic strain rate. Curves shown for 1000 °C.

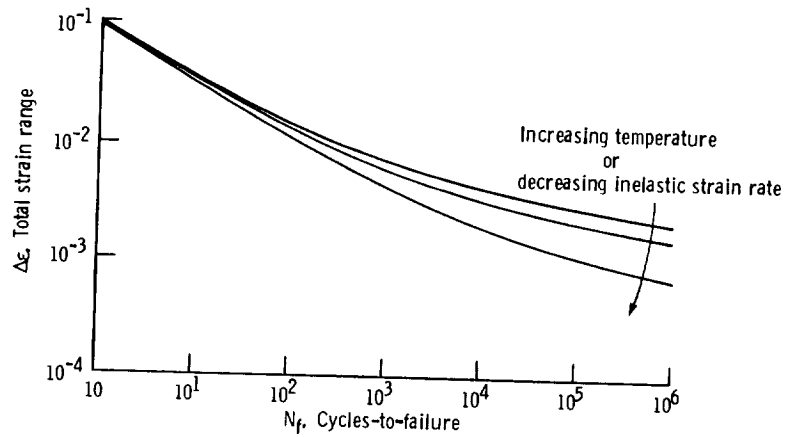


Figure 36. - Total strain range versus cyclic life relations for hypothetical material. Curves shown for constant inelastic strain rate and constant temperature. Elastic contribution is time- and temperature-dependent.

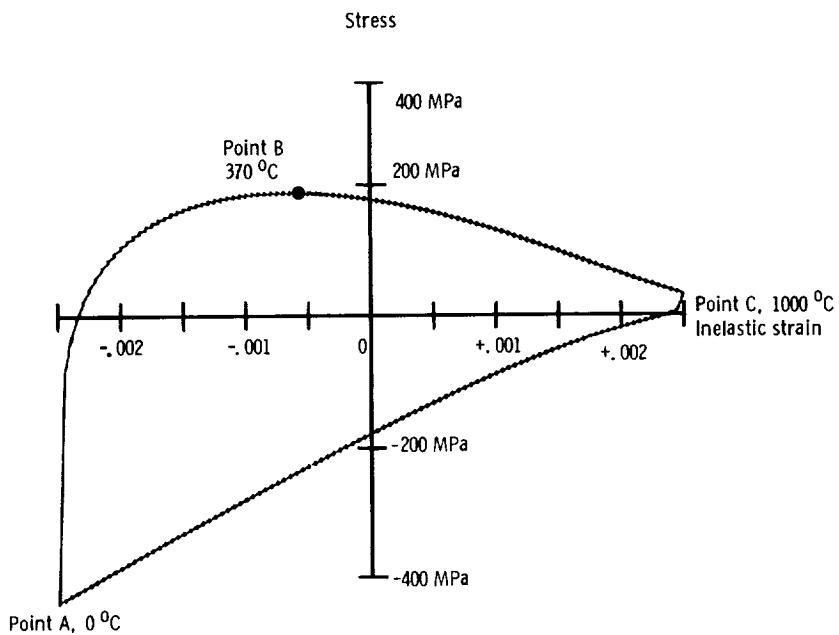


Figure 37. - TMF hysteresis loop, in-phase, inelastic strain range = 0.005, max temperature of 1000 °C, min temperature of 0 °C, inelastic strain rate = 0.0001 sec⁻¹.

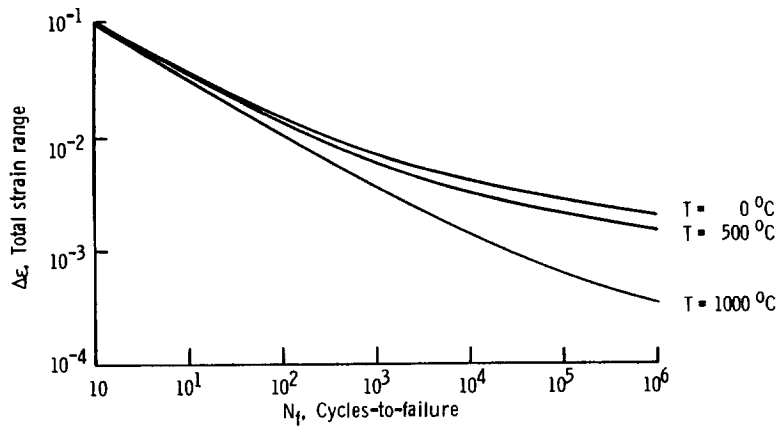


Figure 38. - Total strain range versus cyclic life curves for minimum, average, and maximum temperatures of TMF cycle. Low inelastic strain rate of 0.0001 sec⁻¹.

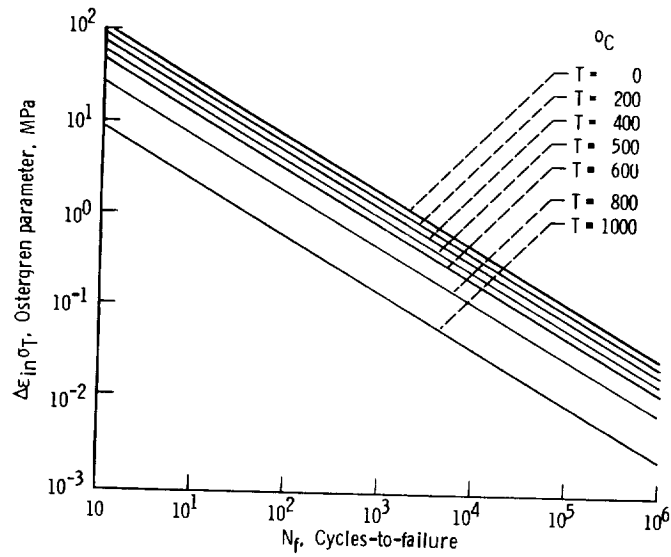


Figure 39. - Isothermal failure criterion using Ostergren's time-dependent product form. Low inelastic strain rate of 0.0001 sec^{-1} .

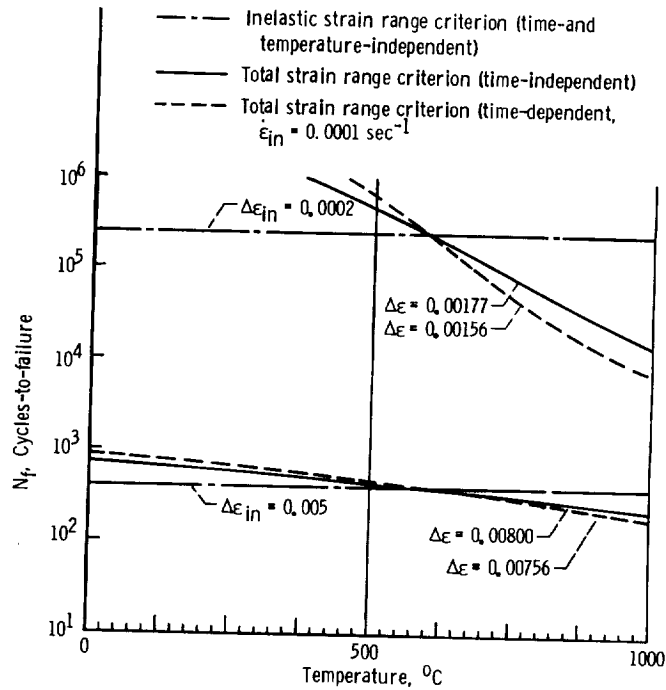


Figure 40. - Predictions of TMF cyclic lifetime based upon isothermal inelastic strain range and total strain range criteria. Predictions shown as function of temperature for two different TMF strain ranges (0.0002 and 0.005 inelastic ranges). Corresponding total strain ranges of TMF cycle are indicated. Time-dependent and time-independent behavior shown.

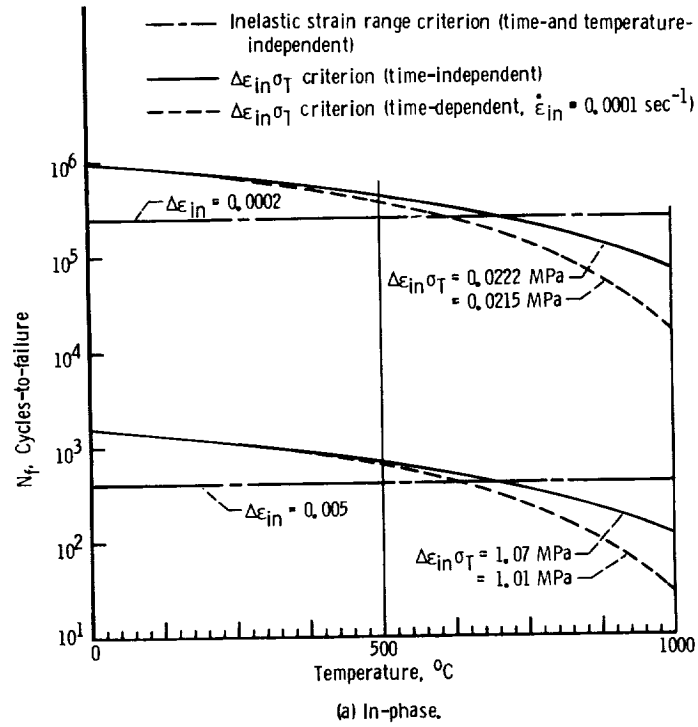
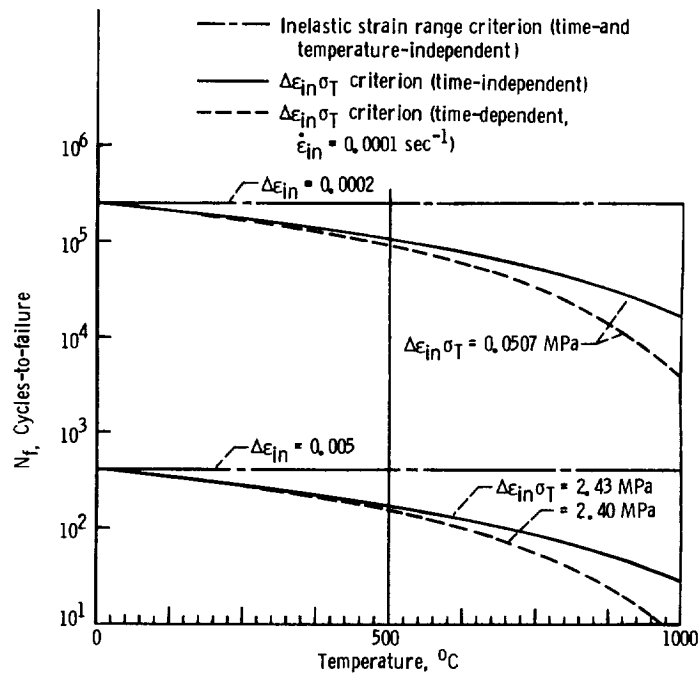
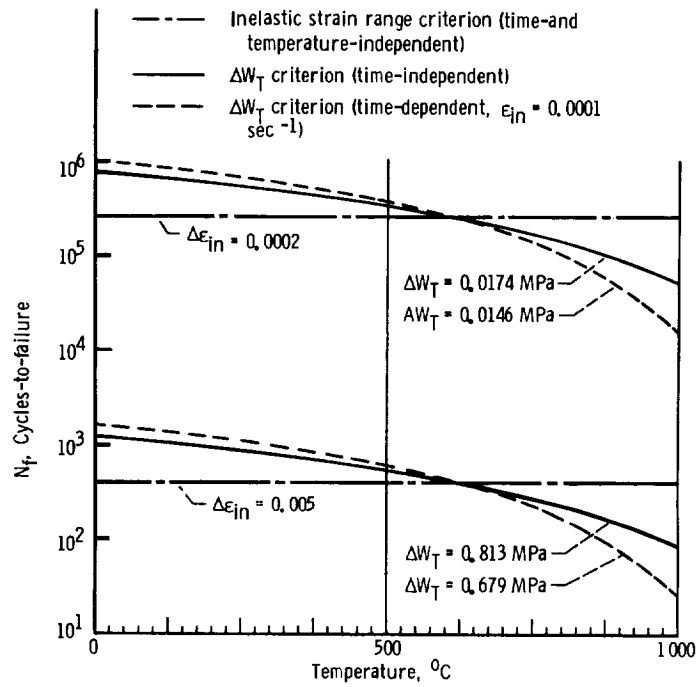


Figure 41. - Predictions of TMF life based upon isothermal failure criterion of Ostergren ($\Delta\epsilon_{in}\sigma_T$). Predictions shown as function of temperature for two different TMF strain ranges (0.0002 and 0.005 inelastic ranges). Corresponding values of Ostergren's parameter are indicated. Time-dependent and time-independent behavior shown.



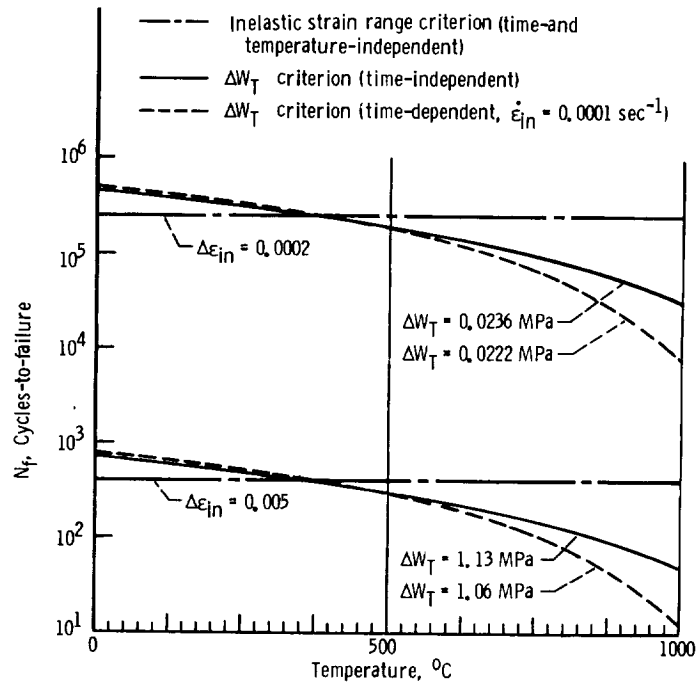
(b) Out-of-phase.

Figure 41. - Concluded.



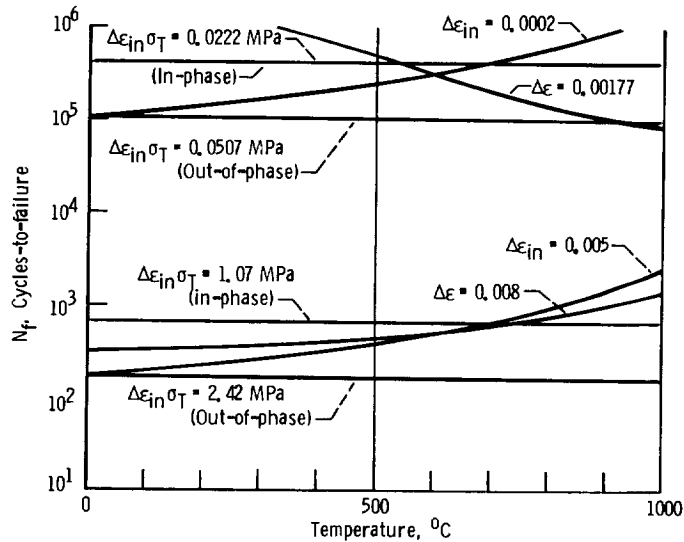
(a) In-phase.

Figure 42. - Predictions of TMF life based upon isothermal failure criterion of Ostergren (ΔW_T). Predictions shown as function of temperature for two different TMF strain ranges (0.0002 and 0.005 inelastic ranges). Corresponding values of Ostergren's parameter (tensile hysteresis energy) are indicated. Time-dependent and time-independent behavior shown.



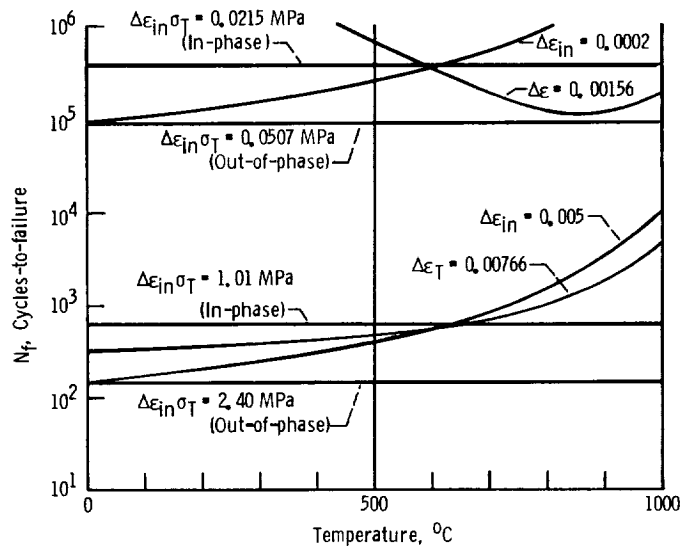
(b) Out-of-phase.

Figure 42. - Concluded.



(a) Time-independent behavior shown ($\dot{\epsilon}_{in} = 1.0 \text{ sec}^{-1}$)

Figure 43. - Predictions of TMF life based upon Isothermal failure criteria of Manson-Coffin, total strain range, and Ostergren ($\Delta\epsilon_{in}\sigma_T$). Ostergren criterion assumed to be temperature-independent. Predictions made for two strain ranges ($\Delta\epsilon_{in} = 0.0002$ and 0.005).



(b) Time-dependent behavior shown ($\dot{\epsilon}_{in} = 0,0001 \text{ sec}^{-1}$).

Figure 43. - Concluded.

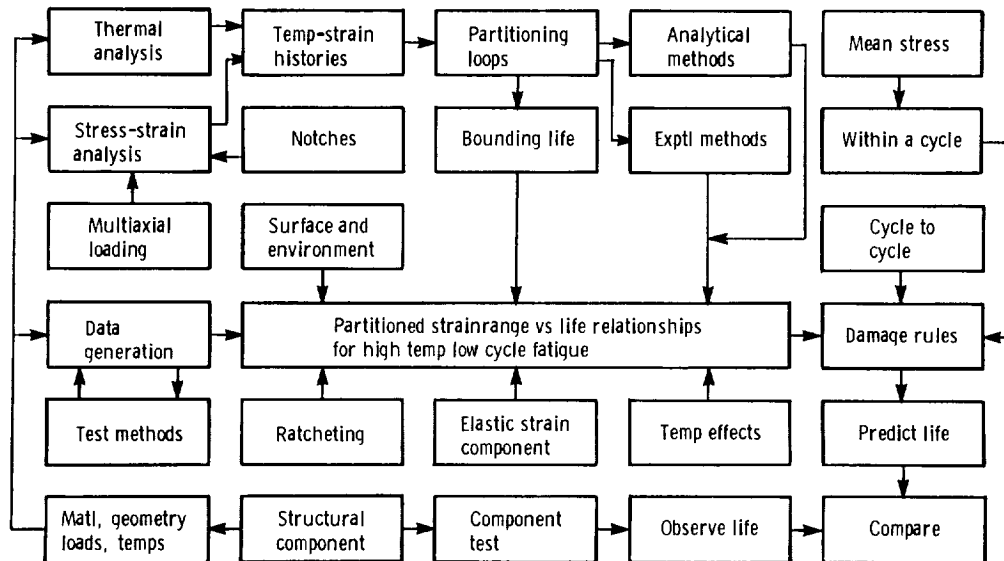


Figure 44. - Schematic flow diagram for structural life prediction (example using strainrange partitioning).

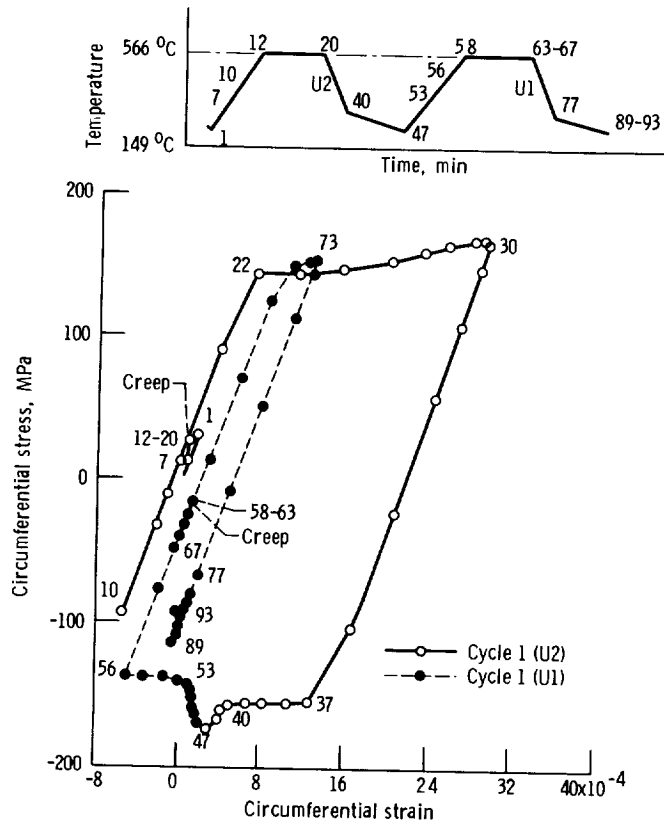


Figure 45. - Stress versus strain in element 249 resulting from thermal fatigue cycle. After Gangadharan, et al (193). Reprinted by permission of the Council of the Institution of Mechanical Engineers.

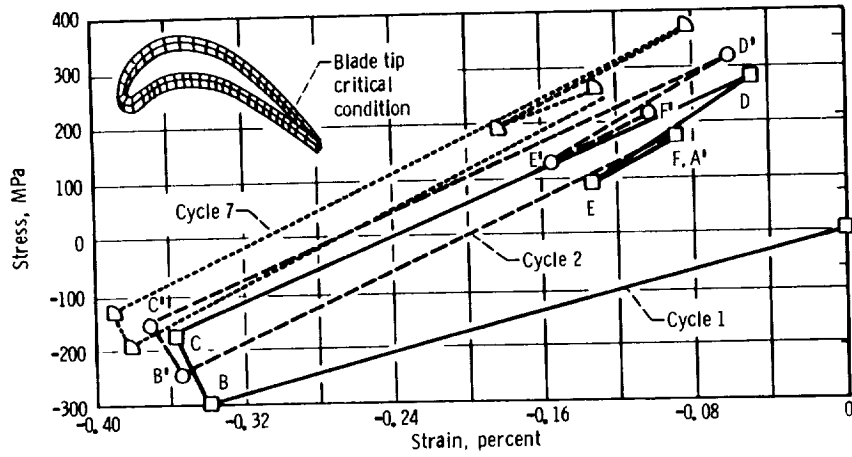


Figure 46. - Inelastic analysis results -- stress-strain response at critical location in blade tip due to thermal fatigue cycling. After Kaufman and Halford (197).

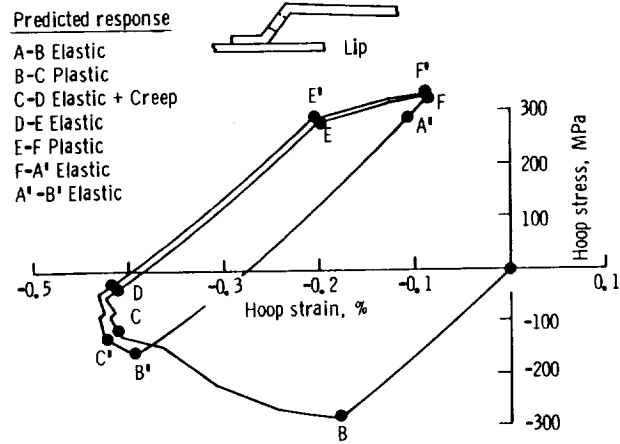


Figure 47. - Predicted lower lip response for first two thermal fatigue loading cycles. After Kaufman and Halford (197).

1

1. Report No. NASA TM-87225	2. Government Accession No.	3. Recipient's Catalog No.	
4. Title and Subtitle Low-Cycle Thermal Fatigue		5. Report Date February 1986	
		6. Performing Organization Code 506-60-12	
7. Author(s) Gary R. Halford		8. Performing Organization Report No. E-2890	
		10. Work Unit No.	
9. Performing Organization Name and Address National Aeronautics and Space Administration Lewis Research Center Cleveland, Ohio 44135		11. Contract or Grant No.	
		13. Type of Report and Period Covered Technical Memorandum	
12. Sponsoring Agency Name and Address National Aeronautics and Space Administration Washington, D.C. 20546		14. Sponsoring Agency Code	
15. Supplementary Notes			
16. Abstract A state-of-the-art review is presented of the field of thermal fatigue. Following a brief historical review, the concept is developed that thermal fatigue can be viewed as processes of unbalanced deformation and cracking. The unbalances refer to dissimilar mechanisms occurring in opposing halves of thermal fatigue loading and unloading cycles. Extensive data summaries are presented and results are interpreted in terms of the unbalanced processes involved. Both crack initiation and crack propagation results are summarized. Testing techniques are reviewed, and considerable discussion is given to a technique for thermal fatigue simulation, known as the bithermal fatigue test. Attention is given to the use of isothermal life prediction methods for the prediction of thermal fatigue lives. Shortcomings of isothermally-based life prediction methods are pointed out. Several examples of analyses and thermal fatigue life predictions of high technology structural components are presented. Finally, numerous "dos" and "don'ts" relative to design against thermal fatigue are presented.			
17. Key Words (Suggested by Author(s)) Fatigue (metal); Low-cycle fatigue; Thermal fatigue; Thermomechanical fatigue; Bi-thermal fatigue; Strain fatigue; Mean stress; Thermal stress; Alloys; Oxidation; Creep-fatigue; Plasticity; Creep; Ratchetting; Crack initiation; Crack propagation; Life prediction;		18. Distribution Statement Unclassified - unlimited STAR Category 39	
19. Security Classif. (of this report) Unclassified	20. Security Classif. (of this page) Unclassified	21. No. of pages	22. Price*

12/26/20

12/26/20